ABSTRACT

Title of dissertation: FLEX CRACKING AND TEMPERATURE-HUMIDITY-BIAS EFFECTS ON RELIABILITY OF MULTILAYER CERAMIC CAPACITORS

Mohammadreza Keimasi, Doctor of Philosophy, 2007

Dissertation directed by: Professor Michael Pecht
Department of Mechanical Engineering

Multilayer ceramic capacitors (MLCCs) are known to be susceptible to cracking when subjected to excessive printed circuit board (PCB) flexure, which is called "flex cracking". The bending of the printed circuit board causes stresses to be transmitted through the solder fillets to the surface mount capacitors. These stresses are the highest at the bottom of the capacitor, where the termination bands end. In order to reduce the amount of stress that is transmitted to the brittle ceramic body of MLCCs through end terminations, a flexible termination system which incorporates a silver-loaded epoxy in end-terminations was developed by some MLCC manufacturers.

With the transition to lead-free materials in the electronics industry there is a concern that MLCCs assembled on PCBs with lead-free solder have different susceptibility to flex cracking than those assembled with eutectic tin-lead solder. In this study, the flex cracking of MLCCs assembled with lead-free solder (Sn3.0Ag0.5Cu) was compared with

those assembled with eutectic tin-lead (Sn37Pb) solder and differences in the results were explained in terms of solder mechanical properties and solder solidification temperature. Tin-silver-copper lead-free solders and eutectic tin-lead solder have different mechanical properties, which affect the stresses that are transmitted to the ceramic body of the capacitor through the solder fillet. The higher solidification temperature for lead-free solder leads to increased residual compressive stresses after the reflow cool-down process for MLCCs assembled with lead-free solder compared with those assembled with tin-lead solder. In this work, the effects of dielectric material, capacitor size, solder assembly process, solder material, and end-termination type on flex cracking of MLCCs were determined for MLCCs from different manufacturers.

Since some flexible- and standard-termination MLCCs are made with precious metal electrodes (silver-palladium), there is a possibility of electrochemical silver migration under bias and humidity. In this study, the effects of temperature-humidity-bias on electrical parameters of flexible-termination MLCCs were characterized and compared with standard-termination MLCCs. In addition, the effect of temperature-humidity-bias on electrical parameters of MLCCs with base metal electrodes was compared to that for precious metal electrode capacitors.

FLEX CRACKING AND TEMPERATURE-HUMIDITY-BIAS EFFECTS ON RELIABILITY OF MULTILAYER CERAMIC CAPACITORS

By

Mohammadreza Keimasi

Thesis submitted to the Faculty of the Graduate School of the
University of Maryland, College Park in partial fulfillment
of the requirements for the degree of
Doctor of Philosophy.
2007

Advisory Committee:

Professor Michael Pecht, Chair

Professor Mohamad Al-Sheikhly

Professor F. Patrick McCluskey

Professor Mohammad Modarres

Professor Peter Sandborn

Dr. Michael H. Azarian

Dedications

To my beloved parents,

my mother (Akram) and my father (Ali),

all beloved members of my family, and

all intimate friends,

who I missed them all during my Ph.D. study at University of Maryland at

United States

Acknowledgments

I would like to specially thank my advisor, Professor Michael Pecht, for his support, guidance, and help during my Ph.D. study at Center for Advanced Life Cycle Engineering (CALCE) at University of Maryland. I specially acknowledge Dr. Michael H. Azarian, for his support, suggestions, and help in all steps of this endeavor. I really enjoyed working with him and his comments and suggestions were very instructive for me. I appreciate his patience and kindness. I would like to thank my advisory committee members for their time, comments, and suggestions for improvements of my Ph.D. dissertation.

I would like to thank all CACLE faculty, lab personnel, and staff for their help and contributions in this work. I would like to thank Dr. Diganta Das and Dr. Sanka Ganesan for their help and support during my study at CALCE. I really appreciate all comments, suggestions, and help from other students in Dr. Pecht group, friends, and roommates.

This work was sponsored by the members of the CALCE Electronic Products and Systems Consortium. I acknowledge Dr. Michael Osterman for his support and suggestions in this work as part of consortium projects. I would like to thank Robert Newman, Ian Fox, Robert Edwards, and other members of the technical staff at Goodrich Engine Control Systems for their sponsorship, support and helpful suggestions. I also wish to thank Guillermo Oviedo at Hewlett-Packard for sponsorship and help in this work.

Table of Contents

List of Figures

List of Tables

1 Introduction to multilayer ceramic capacitors (MLCCs) and their failures

Capacitors are an indispensable component in electronic circuits. The worldwide market in 2004 for tantalum, aluminum, and ceramic capacitors was almost 9 billion dollars per year [1]. Revenues of ceramic capacitor manufacturers reached 5.5 billion dollars in 2004 [2], with a sales growth of 25% per year [3]. However, based on CALCE's analysis of over 150 electronic product failures over a four year period, capacitors are responsible for a larger proportion of failures than any other component or failure site.

MLCCs consist of formulated ceramic dielectric materials which have been fabricated into thin layers, interspersed with metal electrodes which are alternately exposed on opposite edges of the laminated structure (Figure 1). The entire structure is fired at high temperatures, typically around 1000°C, to produce a block which provides the desired capacitance values in a small physical volume. After firing, conductive terminations, typically made of copper or silver, are applied to opposite ends of the chip to make contact with the exposed electrodes. The end terminations are usually overplated with a nickel barrier layer and tin to provide good solderability.

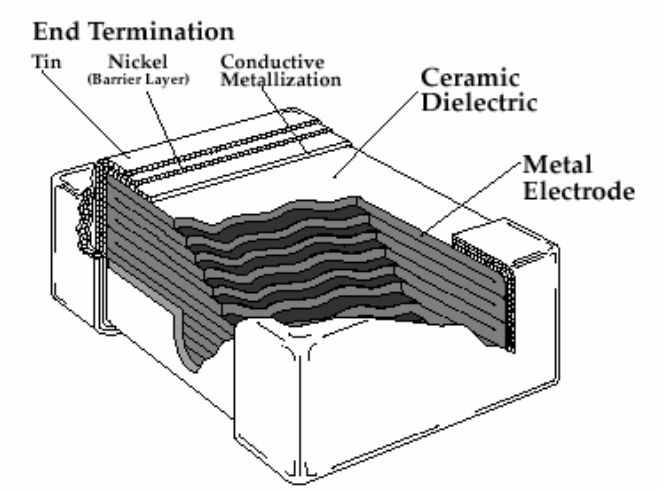

Figure 1. Structure of a standard-termination multilayer ceramic capacitor [4].

CALCE Test Services and Failure Analysis reviewed the last 400 services performed for industrial customers. These services included review of electrical and mechanical design, material characterization, supplier benchmarking, accelerated testing, and root cause failure analysis. Of these 400 services, 40% (159) were identified as analyses of failure during qualification at a customer site. These failures are representative of over 70 companies. They are grouped based on failure site and shown in Figure 2. As it is shown in Figure 2, capacitors' failures are the dominant field failures in electronic products and they include about 30% of failures.

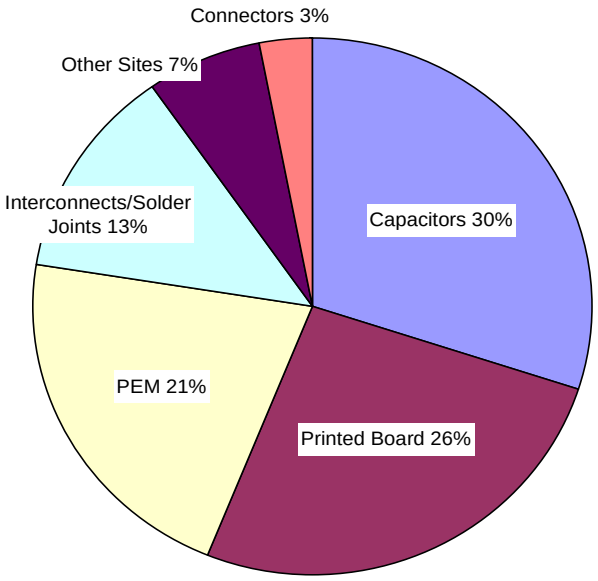

Figure 2. Grouping of field failures of electronic assemblies by failure site.

The overwhelming percentages of MLCCs fail due to the introduction of intrinsic and extrinsic defects. Intrinsic defects are defects introduced as a result of the raw materials or the manufacturing process. The intrinsic defects of MLCCs include firing cracks, knitline cracks (delamination), and voids. The extrinsic defects are defects which occur during assembly or in application field. The extrinsic defects of MLCCs include flex cracks, thermal shock cracks, placement, and handling cracks.

A breakdown of about 40 different MLCC mechanical failures that were analyzed over several years by the CALCE Test Services and Failure Analysis is shown in Figure 3. The largest root causes of failures in MLCCs are defects introduced during capacitor manufacturing processes, including voids and cracks. The second most common cause of failure of MLCCs is cracking due to excessive board flexure, or “flex cracking,” and includes about one quarter of failures. Cracking of MLCCs due to thermal shock in the soldering process or field is the third most common cause of failure.

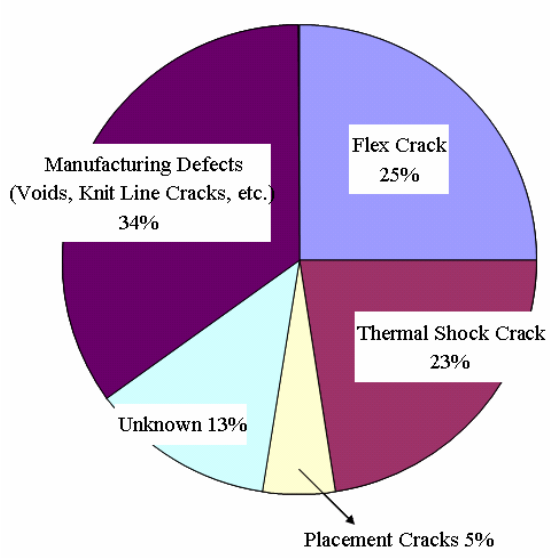

Figure 3. Breakdown of defects in MLCCs.

1.1 Flex cracking failure of multilayer ceramic capacitors

Bending of a printed circuit board (PCB), as shown in Figure 4, will cause forces to be transmitted through the solder fillets to the surface mounted capacitor. When the capacitor is on the convex side of the PCB, these forces are concentrated at the bottom of the capacitor where the termination bands end. Some of the forces are absorbed by the solder and cause elastic and plastic deformation, while the remainders are transmitted to the capacitor. If the stress applied to the capacitor body exceeds its breaking strength, the capacitor will crack.

The ceramic dielectric material is brittle. The forces pulling at the ceramic along the termination edge will lead to a crack if they are of sufficient magnitude. The force at which the capacitor cracks is dependent upon the ceramic material, the solder material and fillet size, the termination materials, and defects within the ceramic structure [5].

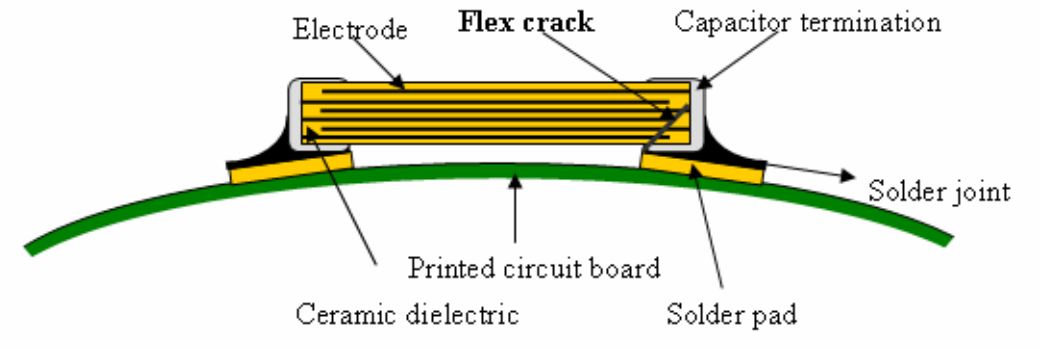

Figure 4. Flex cracking of MLCCs due to printed circuit board bending.

Figure 5 shows a flex crack at one of the MLCC end-terminations. The crack typically starts near the edge of the termination margin, and then extends toward the termination face. Our measurements of the crack angle, as represented in Figure 5, indicate that its value varies between 30 and 70 degrees. The crack may extend into the termination face, thereby separating a corner section. It may also turn toward the top of the capacitor, where it will usually turn out towards the top termination margin's edge. In some cases, this crack can cause the entire end of the capacitor to be separated from the main body of the capacitor. In some cases cracks are visually undetectable at the exterior of the cracked capacitor, and cross-sectioning is necessary to visualize a flex crack.

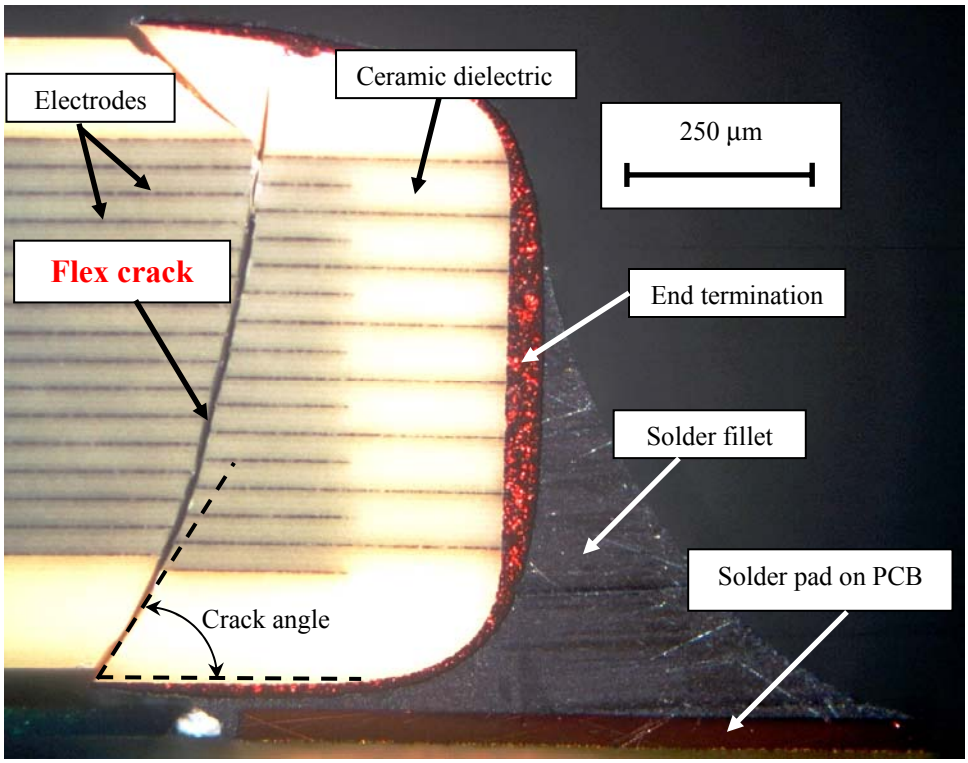

Figure 5. Flex cracking failure of a multilayer ceramic capacitor.

Flex cracking can occur during assembly processes and handling, as a result of excessive flexure of printed circuit boards. Examples of processes causing board flexure include PCB warping during solder reflow, depaneling, handling during processing, testing, assembly, insertion or removal of a board from edge-mount connectors, attachment of a board to other structures (e.g., support plates, heat sinks, and chassis), connection of cables, thermal expansion of a board with respect to a cabinet or chassis, and vibration or shock in the end-use environment.

1.2 Ceramic dielectric types (EIA classifications)

Ceramics used for capacitor dielectrics are mixtures of compounds, almost always including titanium oxides such as barium titanate ($BaTiO_3$) and titanium dioxide (TiO_2) combined with other materials. The electronic industry association (EIA) has designed a classification scheme for MLCCs based on their temperature characteristics [6]. Within this scheme, there are four major classes of ceramic dielectrics, with class I being the least variable with temperature and voltage, and class IV being the most variable.

1.2.1 Class I

Class I dielectrics are typically used in applications requiring the tightest tolerance. Components of this type are temperature compensating ceramic dielectrics, fixed capacitors of a type suited for resonant circuit applications or other applications where high quality factor (Q) and stability of capacitance characteristics are required [6] . Stable temperature-compensating capacitor types (EIA class I) are made with little or no $BaTiO_3$, but are basically TiO_2 or $CaTiO_3$ with additive materials, some of which are magnesium titanate ($MgTiO_3$), strontium titanate ($SrTiO_3$), neodymium titanium oxide ($Nd_2Ti_2O_7$), magnesia (MgO_2), alumina (Al_2O_3), bismuth stannate ($Bi_2Sn_3O_9$), or manganese titanate ($MnTiO_3$). Additive proportions are designed to produce the desired temperature coefficients when mixed and fired in accordance with the manufacturer's proprietary processes [7]. The most popular temperature characteristics for class I are the ultra-stable C0G (also known as NP0, military version BP). As Table 1 shows, the temperature range for this dielectric is -55°C to 125°C and capacitance change over this temperature range is ± 30 ppm.

1.2.2 Class II

Components of this classification are fixed, ceramic dielectric capacitors of a type suited for bypass and decoupling application or for frequency discriminating circuits where quality factor and stability of capacitance characteristics are not of major importance. Class II ceramic dielectrics exhibit a predictable change with time and voltage. EIA class II general-purpose less-stable capacitors use $BaTiO_3$ as a base because of its high dielectric constant, adding stabilizing materials, which can be the same as listed for temperature stable (class I) materials, including TiO_2 and $CaTiO_3$, plus calcium zirconate ($CaZrO_3$), niobium pentoxide (Nb_2O_5), and others [7]. The most popular temperature characteristics for class II are the stable X7R (military BX or BR). As Table 1 shows, the temperature range for this dielectric is -55°C to 125°C and capacitance change over this temperature range is ± 15%.

For X7R dielectrics the barium titanate content is about 90 to 98% [8] [9], while for C0G dielectric the barium titanate content varies from 10 to 50%, supplemented by other titanates, especially neodymium titanium oxide ($Nd_2Ti_2O_7$) [8]. Capacitors with X7R dielectric are more susceptible to flex cracking than C0G dielectric, which has higher fracture toughness [10] [11].

1.2.3 Class III

Components of this type are specifically suited for use in electronic circuits for bypass, decoupling or other applications in which dielectric losses, high insulation

resistance and capacitance stability are not of major consideration. This classification is identical to that of class II, except that it is restricted to those capacitors having different temperature characteristics [6]. These capacitors are also primarily composed of barium titanate but mixed with difference additives, such as calcium zirconate $CaZrO_3$ and barium zirconate $BaZrO_3$ [7]. The most popular temperature characteristics for class III are the general purpose Z5U and Y5V. Table 1 shows the temperature range for Z5U and Y5V dielectrics and capacitance change over their temperature range.

1.2.4 Class IV

This classification is restricted to those components utilizing reduced titanate or barrier layer type construction, while basically fitting the descriptions of class II and class III [6].

Table 1. EIA classification of ceramic dielectric materials based on their temperature characteristics [6] [8].

EIA designation	Class	Temp. range (°C)	Capacitance change with temperature	Max. dielec. constant	Barium titanate content (%)	Other dopants in dielectric	Grain size (μm)
C0G (NP0)	I	-55 to 125	± 30 ppm	100	10-50	$Nd_2Ti_2O_7$, TiO_2, $CaTiO_3$,	1
X7R	II	-55 to 125	± 15%	4,000	90-98	MgO, MnO, Nb_2O_5, CoO	< 1.5
Z5U	III	10 to 85	+22, -56%	14,000	80 - 90	$CaZrO_3$, $BaZrO_3$	3 – 10
Y5V	III	-30 to 85	+22, -82%	18,000	80 - 90	$CaZrO_3$, $BaZrO_3$	3 - 10

1.3 Electrode types (base metal electrodes vs. precious metal electrodes)

There are two kinds of multilayer ceramic capacitors based on electrode materials, precious metal electrode (PME) capacitors, and base metal electrode (BME) capacitors. PME capacitors are divided into two technologies, high-fire and low-fire capacitors.

1.3.1 High-fire capacitors

The high-fire capacitors use ceramic dielectrics normally composed of refractory oxides, which sinter together to make dense bodies only at high temperatures (approximate 1300°C or greater). Because of the chemical stability of the oxides, the

dielectric compositions are compatible with co-fired palladium electrodes. Silver may be added in small quantities (up to 30%), as long as the melting point of the alloy is well above the ceramic sintering temperature. Silver-palladium alloys exhibit a maximum in their electrical resistivity of about four times that of pure palladium in the vicinity of 30% Ag addition. So there is often a trade-off among capacitor equivalent series resistance, electrode thickness, and silver content. High-fire technology is commonly used by Japanese MLCC manufacturers [12].

1.3.2 Low-fire capacitors

In low-fire capacitors several low-melting oxides are added to barium titanate to jointly modify the temperature coefficient of the dielectric constant and lower the firing temperature of the dielectric. Binary oxides containing bismuth became popular modifiers in 1950's, but because bismuth reacts with palladium, only low palladium-content electrodes maybe combined with these dielectrics. To avoid the reaction between bismuth and palladium, palladium-gold (sometimes with platinum added to raise the melting point of the alloy) was used. Further refinements of the technology led to the substitution of the gold with silver. In the last decade, silver alloys with 15 to 35% palladium have been widely used. Low-fire technology is commonly used by U.S. MLCC manufacturers [12].

1.3.3 Co-fire capacitors

Base metal electrode (BME) systems are similar to high-fire systems in that they normally use only very stable oxides in the dielectric composition. The use of nickel electrodes requires that the firing process be carried out in an inert or reducing atmosphere to avoid oxidizing the base metal electrode. It is possible to partially reduce barium titanate, creating oxygen vacancies. These vacancies will migrate under the influence of electric fields, causing degradation of the dielectric. The processing of BME capacitors requires a balancing between reducing the dielectric and oxidizing the electrode. If the nickel is oxidized it will in turn react with and degrade adjacent dielectric material. BME capacitors have been in manufacture for over 20 years [12].

1.4 End-termination types (standard termination vs. flexible termination)

There are two end-termination types for multilayer ceramic capacitors: standard termination and flexible terminations. In standard-terminations MLCCs end-termination is made of three metal layers. For base metal electrodes (BME) MLCCs end-terminations are made of copper and usually plated with nickel and tin layers. For precious metal electrodes (PME) MLCCs end-terminations are made of silver and usually plated with nickel and tin layers.

In order to reduce the amount of stress that is transmitted to the brittle ceramic body of MLCCs through end terminations, a flexible polymer termination system was developed by some manufacturers, including AVX and Syfer, for MLCCs [15]-[19]. AVX produces MLCCs with flexible terminations comprised of a conductive polymer, used in conjunction with base metal electrode (BME) technology and an X7R dielectric.

The conductive polymer coats a copper termination, and is then plated with nickel and tin. Syfer produces MLCCs with flexible terminations and precious metal electrodes (PME). Syfer's FlexiCap™ capacitors use silver loaded polymer in end terminations plated with nickel and tin (Figure 6).

The flexible-termination MLCCs from Syfer are made of precious metal electrodes (silver-palladium) and contain silver-filled polymer in their end terminations. This construction presents a potential risk of silver migration under bias and humidity. However, the sensitivity of these new MLCCs to environmental stresses and DC bias is not well established.

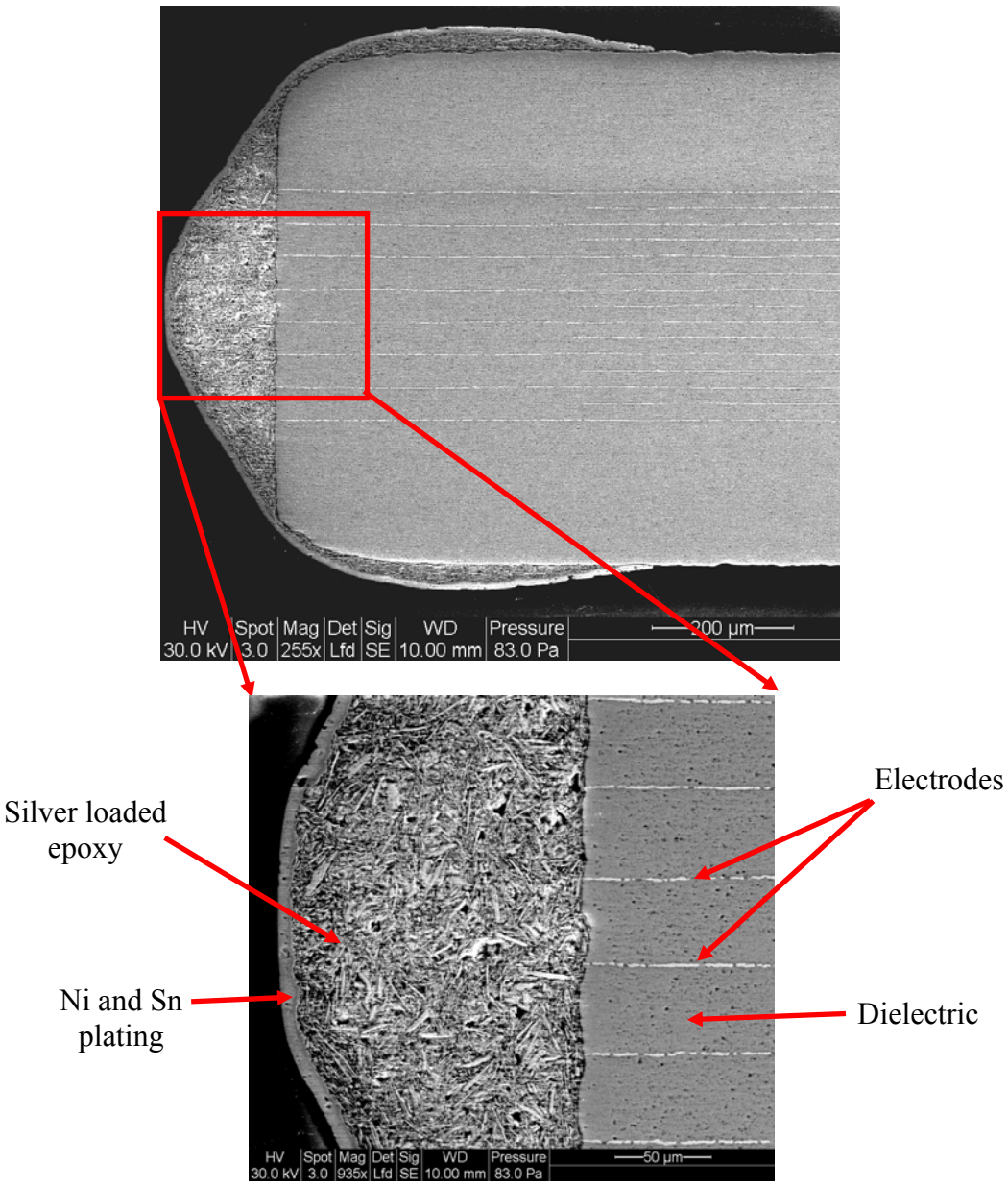

Figure 6. Flexible-termination multilayer ceramic capacitor from Syfer, containing silver loaded epoxy in end-termination to reduce flex cracking.

1.5 Open-mode multilayer ceramic capacitors

Kemet introduced an "open-mode" ceramic capacitor. Open-mode capacitors were designed to greatly reduce the likelihood of a low insulation resistance or short circuit condition in a flex cracking situation. When flexed to failure, an open-mode capacitor may experience a drop in capacitance but a short is unlikely because the crack typically will not cross opposing electrodes.

Figure 7 is a schematic diagram of an open-mode capacitor. The open-mode length is greater than the termination bandwidth length on both sides of these capacitors, within which only one set of electrodes exist. Therefore, flex cracks, which start from an end termination at a cute angle only cross electrodes originating from the same termination and don't cause shorting between opposing electrodes. Since there is no current leakage associated with a typical open-mode flex cracking there is no localized heating and, therefore, no chance for a catastrophic and potentially costly failure event [20].

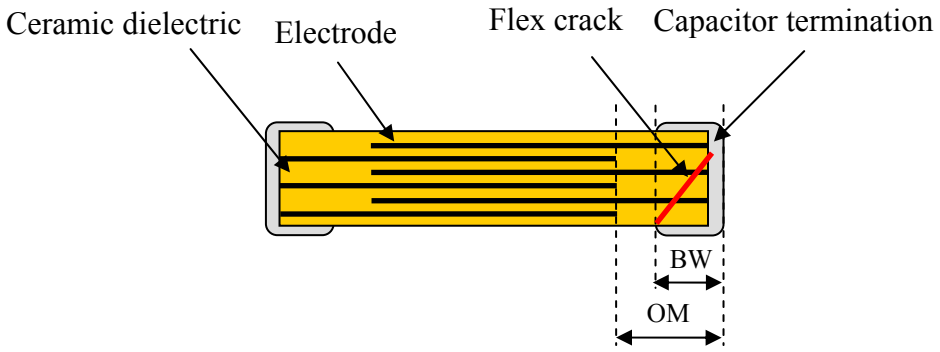

Figure 7. The open-mode ceramic capacitor: The open-mode dimension (OM) exceeds the termination bandwidth dimensions (BW).

1.6 Manufacturing process of MLCCs

There are two basic process techniques for manufacturing of multilayer ceramic capacitors used in the in the industry: first, dry sheet fabrication technique and second, wet build-up fabrication technique. Dry sheet fabrication is more common than wet build-up. Process flow for dry sheet and wet build-up manufacturing of MLCCs are given in Figure 8. The dry sheet manufacturing steps of MLCCs are shown schematically in Figure 9.

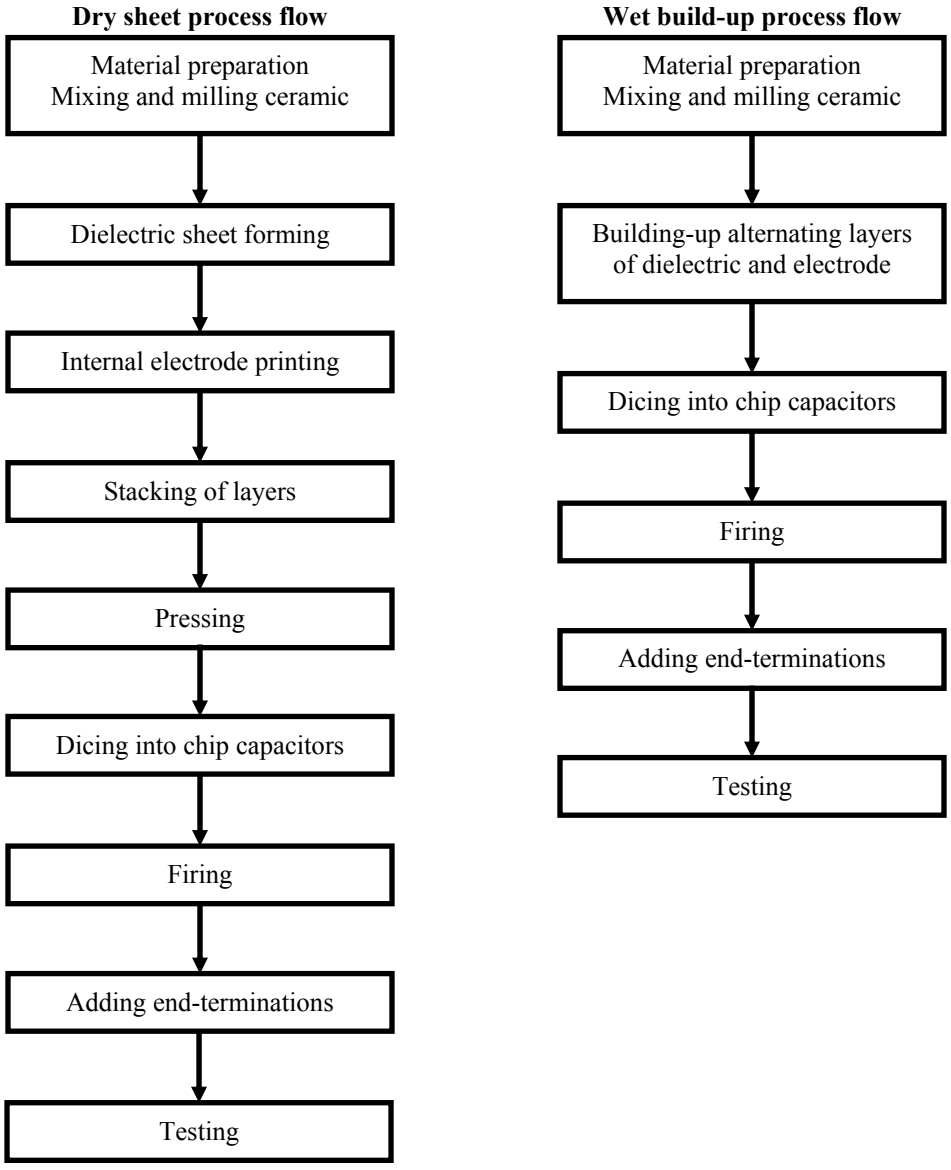

Figure 8. Process flows for manufacturing of MLCCs: dry sheet vs. wet build-up [13] [14].

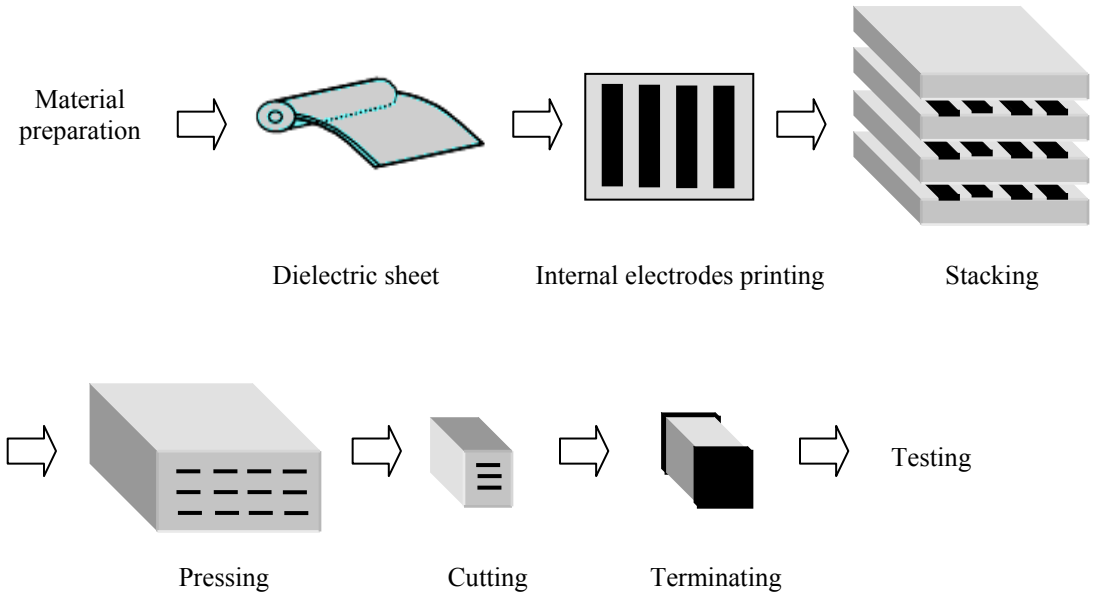

Figure 9. Manufacturing process of MLCCs (dry sheet process).

1.7 Manufacturing defects in MLCCs

Failures due to manufacturing defects make up about one third of multilayer ceramic capacitor failures (See Figure 3). Manufacturing defects of MLCCs include firing cracks, knitline cracks, and voids. If a defective capacitor is used in a field application, a conductive medium, often atmospheric moisture, can penetrate into defect of the capacitor and cause leakage current of the capacitor to increase. This may also lead to the shorting of the opposing electrodes of the capacitor due to electrochemical silver migration through an existing path between internal electrodes in the presence of a DC bias. The characteristics of different manufacturing defects including firing cracks, knitline cracks, and voids are discussed in the following.

1.7.1 Firing cracks

Firing cracks are caused by rapid cooling during the manufacturing of the capacitor. Ceramic capacitors are fired at high temperatures, typically around 1000°C, to produce a block. Rapid cooling after firing process can cause a crack inside the capacitor body due to thermal shock, called firing crack. They often originate at an electrode edge, but not always and propagate perpendicular to the electrodes.

1.7.2 Knitline cracks

Non-optimized pressing or sintering causes insufficient binding strength between internal electrodes and dielectric materials and trapping of air or foreign material into the capacitor lead to delamination between internal electrodes or Knitline cracks. Knitline cracks or delaminations extend parallel to the electrodes.

1.7.3 Voids

Voids are caused by existence of organic and inorganic contaminations in the ceramic dielectric and non-optimized burnout process. Bridging two or more electrodes they can become a short leakage current path and a latent electrical defect. Large voids can also lead to a measurable reduction in capacitance.

1.8 Example of a manufacturing process introduced defects in MLCCs

In the stacking step of the manufacturing process of MLCCs, decided number of layers is stacked after printing. In order to make a monolithic block of dielectric sheet and

internal electrodes, mold is pressed down from top, as shown in Figure 10. A film is used to press on the dielectric. A thick paper is used as a cushion to absorb the shock upon stacking. If the thick paper is misaligned, as it is shown in Figure 11, when the film moves after stacking, the film and the thick paper will rub against each other, thereby causing a small particle of the paper to fall, and stick onto the surface of the dielectric sheet. Then, after the firing process, the substance disappears, thereby leaving void inside dielectric. Therefore moisture and contaminants can ingress in the space between internal electrodes through this path, and in the presence of DC voltage silver electrodes can migrate through this path and cause reduction in insulation resistance of capacitor (increase in leakage current), which eventually causes the capacitor to fail.

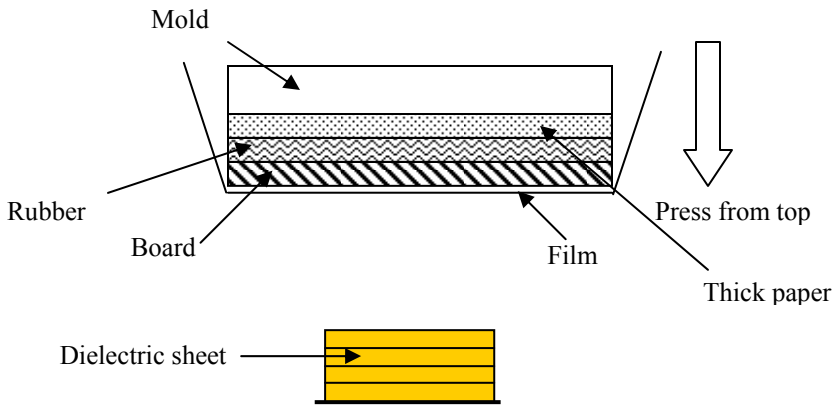

Figure 10. Pressing of dielectric sheet in manufacturing process of multilayer ceramic capacitors.

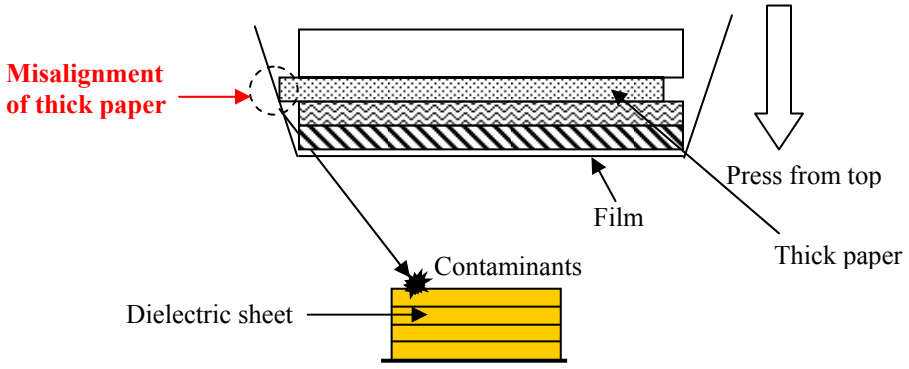

Figure 11. Misalignment of thick paper and rubbing between the film and paper when moving the film can cause paper particles (fibers) to contaminate dielectric sheet.

1.9 Electrochemical silver migration failure in MLCCs

MLCCs made of precious electrodes (Ag-Pd) are prone to electrochemical migration failure. Silver migration failure of multilayer ceramic capacitors is divided into three steps. Step one is the formation of a microscopic path between internal electrodes. This path can be a crack or void which occurs during manufacturing, assembly, or in the

application field during life of the ceramic capacitors. Step two involves penetration or existence of moisture and contaminants, such as ions, into the path. The final step is the silver migration of the electrode materials along the path by an electrochemical process. As a consequence of this, the leakage current of the ceramic capacitor increases and causes the capacitor to fail. It has been hypothesized that at high voltages this path would be vaporized by high current passing through it, for this reason this failure is called "low-voltage" failure of multilayer ceramic capacitors [21] [22].

Zhan, et al. [23] showed the reduction of surface insulation resistance or increase in leakage current in printed circuit boards caused by electrochemical migration (ECM), which is the growth of conductive metal filaments (dendrites) through an electrolyte solution by applying a D.C. voltage bias [24]. They also expressed that intermittent failures are experienced when a dendrite grows, causes an electrical short, and then burns out due to high current densities. They explained that electrochemical migration occurs by a sequence of events including, path formation, electrodissolution, ion transport, electrodiposition, and filament growth.

1.10 Literature Survey

In this section previous works on flex cracking issues of multilayer ceramic capacitors and effects of temperature-humidity-bias on multilayer ceramic capacitors are reviewed. Finally, previous works on failure analysis techniques used for detection of defects inside multilayer ceramic capacitors are presented.

1.10.1 Flex cracking failure of MLCCs

Prymak and Berganthal [5] conducted flex tests on different size multilayer ceramic capacitors. They used a 3-point bend configuration with one capacitor mounted in the middle of each board. In-situ measurement of capacitance was used as means of detecting the occurrence of flex cracking. They showed that for some capacitors, a capacitance drop observed during testing recovered after removal of flexure. This suggested that in-situ monitoring of capacitance during bend testing was necessary. Their results also showed that the larger the capacitor, the more susceptible was to flex cracking. Their experiments were repeated for capacitors from production batches spanning a 25-week period. Their results remained consistent, which led them to believe that the materials and manufacturing processes were consistent.

Berganthal [25] assessed the dependence of several different parameters to flex cracking of ceramic capacitors. Solder fillet size was found to impact bending strength, with larger fillets causing a reduction in strength. Pad size had a similar effect, with narrower pads increasing the bending strength. This is in agreement with Kemet, which recommends that wave solder pads be narrower than reflow solder pads. Chip length was also found to affect bending strength, with larger chip capacitors being more susceptible to flex cracking. Dielectric materials were found to impact bending strength based on their fracture toughness; the C0G dielectric is superior to the X7R dielectric, and X7R is better than Z5U and Y5V dielectrics. The printed circuit board thickness also impacts bending strength. Thicker PCBs are more rigid and transmit more stress to a capacitor at a given deflection. Therefore, thicker PCBs result in flex cracking at lower deflections than thinner boards of the same materials. The PCB material affects the bending strength

primarily through the Young's modulus. Some data indicates that higher capacitor thicknesses increase bending strength, but there appears to be some confusion about this parameter. Some capacitors have thicker cover layers around the active layers. These parts may have higher bending strength than those with thinner cover layers. These results may also arise if a capacitor has cracked prior to an observable drop in its capacitance. Finally, capacitors with wider termination bands typically have greater bending strength. The wider band has the same effect as reducing the capacitor length.

Prymak [26] investigated reverse flex testing of multilayer ceramic capacitors. In a typical flex test, the capacitor is on the convex side of the PCB, but in a reverse flex test the capacitor is on the concave side of the board. In each instance the capacitor failed during the withdrawal of the ram and relaxation of flexure. During flexure, the solder fillets deform to relieve the stress applied to them. When the board flexure is rapidly reduced, the deformed fillets cause tensile stresses to be applied to the capacitor, and failure occurs with a similar characteristic crack to that observed with normal flex testing. The author mentioned that it is unlikely that reverse flex testing provides additional chip-related information beyond that obtained with normal flex testing.

Prymak [27] baked capacitors in a humidity chamber after flex testing to detect "hidden" cracks as low insulation resistance (IR). He showed that, of the capacitors specified as "cracked" by a sudden capacitance change during flex testing, 80% were found to be IR rejects when exposed to humidity. The reduction in IR is due to penetration of moisture into the existing cracks, possibly accompanied by capillary condensation. Destructive physical analysis (DPA) revealed internal cracking in the remaining 20%.

Al-Saffar, et al. [28] investigated the flexure strength, or modulus of rupture (MOR), of multilayer ceramic capacitors using three point bend tests. Their samples included blanks (dielectric material without electrodes) and MLCCs with X7R and Z5U (an EIA class III dielectric [6]) dielectrics containing different numbers of electrodes and ink laydown concentrations (electrode material, which is screened onto the dried ceramic dielectric during manufacturing of multilayer ceramic capacitors). It was found that for blanks, MOR decreased as the specimen thickness increased, and the X7R dielectric had higher flexure strength than the Z5U dielectric. For X7R capacitors, the MOR increased with the number of electrodes, while for Z5U capacitors, the MOR was independent of the number of electrodes and all values were less than values obtained for X7R capacitors. The difference between the two sets of data was believed to be predominantly due to the effect of the metal electrodes. In the Z5U capacitors, noble metals, such as palladium, are used. For X7R capacitors, cheaper alloys typically based on silver-palladium with a high silver content (67% Ag, 33% Pd by weight) are used. The modulus of elasticity (E) for the Pd electrode is about 110 GPa, and that for the Ag-Pd electrode is about 84 GPa. The modulus of elasticity for the ceramic matrix is of the order of 100 GPa in each case. The authors' interpretation was that since $E_{metal} < E_{ceramic}$ in the case of the X7R capacitors, the electrodes should be more plastic and thus provide increasing support as the number of electrodes increases. In contrast, for the Z5U components $E_{metal} > E_{ceramic}$ and so the metal does not provide any 'plastic support'. Thus, with an increasing number of electrodes, there is no increase in flexure strength. Electron microscopy showed major differences in the mode of fracture of Z5U and X7R MLCCs. In their study, for as-fired X7R capacitors without terminations the MOR increased with

the ink laydown concentration to a plateau level (~140 MPa), but in capacitors which had been terminated and annealed, the flexure strength was uniformly higher than capacitors without terminations and independent of ink laydown concentration.

Maxwell [29] compared flexure strength of similarly sized multilayer ceramic and film capacitors. Ceramic capacitors are brittle and crack due to excessive PCB bending. Multilayer film capacitors are made with polymer films, are not brittle under normal conditions, and are more flexible when stressed on a bending PCB. He concluded that surface mount film capacitors did not exhibit failure or degradation when tested at or beyond deflection values that cracked ceramic capacitors of similar size and capacitance value.

Syfer Technology Limited [30], a manufacturer of ceramic capacitors, reported that when capacitors are broken, the problem usually manifests itself at a very late stage of board assembly. Syfer's observation is likely due to the fact that capacitance drops resulting from flexure are frequently not detectable after removal of the bending stress. Another factor that can lead to this phenomenon is the growth of the small cracks introduced by flexure as the board is exposed to additional thermal and mechanical stresses during assembly. An immediate change in any key capacitor parameter is rare. A decline in the insulation resistance of a cracked capacitor requires penetration of a conductive medium, often atmospheric moisture, into the crack structure and this takes time. Hence detection usually occurs late, such as in the field. Typically 60% of damaged parts due to flex cracking do exhibit a detectable change in insulation resistance but only a small minority of these parts is pre-identified as potential failures by a user. Cracks are visible at the exterior of less than 2% of affected parts, and immediate detection of

change of the capacitance is a feature of about 10% of cracked capacitors. They conducted experiments to study the effects of different parameters on flex cracking of ceramic capacitors. Their results showed that the only significant difference in strength, across a broad matrix of capacitor design and build parameters, lies between barium titanate based capacitors (the material used in X7R and Y5V dielectrics) and neodymium titanium oxide based capacitors (the basis for their C0G dielectric). The C0G dielectrics failed at deflections which were twice those of the X7R and Y5V dielectrics. Most ceramic formulations within a given dielectric category were found to have similar bend strengths. Their results indicated that small capacitors are not stronger than large capacitors and thin capacitors are not weaker than thick capacitors. It was shown that large solder joints do have a negative effect on bend strength. A minor difference was observed for flexure strength of parts soldered with Sn36Pb2Ag versus Sn40Pb alloys; however, the performance of a 'soft' solder, In50Pb, was much better. Average deflection at failure was more than double for this soft solder. They also studied the effects of solder pad geometry on flex performance. Pad widths narrower than the chip width were found to increase bend strength.

Nies and Maxwell [31] studied factors in board flexure testing of surface mount ceramic capacitors. They studied the effects of PCB material, board thickness, and solder material on flexure strength of ceramic capacitors. They used boards with different constructions (6, 7, and 8 ply) and different elastic moduli. They concluded that multilayer ceramic capacitors withstand large deflections when the board is thin and compliant, since less stress is transferred to the capacitor. On the other hand, only a relatively small load is needed to deflect thin boards, so flexible boards are not

appropriate for boards experiencing high loads. In contrast, thicker, less flexible boards may cause fewer failures for a given load, but would cause more failures at a given deflection. Therefore, information on either load or deflection alone is not sufficient to generalize results obtained using a specific board in order to establish the allowable range of conditions to minimize the risk of cracking. The authors also studied the effect of solder material on flex strength of ceramic capacitors. Four solder compositions: Sn37Pb, Sn40Pb, Sn36Pb2Ag, and Sn4Ag were used in their experiments. They used both high-fire (> 1300°C) capacitors with palladium electrodes and low-fire (< 1200°C) capacitors with silver-palladium electrodes. Even though silver-doped solders showed somewhat better performance, their standard deviations were large enough to make the statistical significance of this difference questionable.

Long, et al. [32] conducted experiments with both eutectic tin-lead (Sn37Pb) and lead-free solders (Sn3.0Ag0.5Cu) to compare effects of solder material on flex cracking of multilayer ceramic capacitors with X7R dielectric manufactured by Kemet. Their results were mixed, because in some case sizes lead-free solder performed better and for others the eutectic tin-lead solder performed better. Their results for 1812 size capacitors with X7R dielectric showed that lead-free solder gave better flex performance. For 0603 capacitors with X7R dielectric, lead-free and tin-lead solders produced very similar results. For 0805 size capacitors, although the capacitors assembled with lead-free solder performed better, the difference between the two solders at 100 ppm failure rate was less than 0.3 mm of deflection. For 1206 size capacitors, the tin-lead soldered parts performed better at low deflections, whereas above 2.6 mm of deflection the lead-free soldered parts performed better. Based on their investigation of the solder joints, they found that tin-lead

solder had better wetting over the whole pad area, while lead-free solder wetting was limited to part of the solder pad. The reduced wetting with the lead-free solders reduces the effective pad width. The authors hypothesized that this affects the flex performance of ceramic capacitors.

Blattau, et al. [33]-[36] used elastic-plastic finite element analysis (FEA) to study the effects lead-free solders on flex cracking of MLCC. In these studies, the displacement of the PCB was related to the tensile stress in the capacitor using an FEA model. Their results indicated that changing to lead-free solders could lead to an increased risk of flex cracking failures of MLCCs.

Franken, et al. [37] used finite element analysis to study the effects of wave soldering and bending loads on failure probability of MLCCs. They showed that, after soldering process, the bottom cover layer (PCB side) of an MLCC is under compression and the top cover layer is in tension (The cover layer is the layer of ceramic that surrounds the electrode and dielectric stack.). The tensile stress direction was parallel to the electrodes and attained the maximum value the termination edge. In addition, they showed that bending of the PCB generates tensile stresses in the bottom cover layer and compressive stresses in the top cover layer. The stresses due to PCB bending are offset by stresses due to the soldering process.

1.10.2 Effects of temperature-humidity-bias on MLCCs

Cracks and other flaws not only can be sources of mechanical failure, but also can lead to electrical degradation of multilayer ceramic capacitors. Sato, et al. [21] described a three-step mechanism for low-voltage failure of multilayer ceramic capacitors. Step one

is the formation of a microscopic path between internal electrodes. This path can be a crack or void which occurs during manufacturing or in the application field during life of the ceramic capacitors. Step two involves penetration or existence of moisture and contaminants, such as chlorine ions, into the path. The final step is the migration of the electrode materials, such as silver, along the path by an electrochemical process. As a consequence of this, the leakage current of the ceramic capacitor increases and causes the capacitor to fail. It has been hypothesized that at high voltages this path would be vaporized by high current passing through it. When the voltage is lowered, the electrochemical process takes place again [22].

Freiman and Gonzalez [38] demonstrated that the existence of a crack connecting two inner electrodes in a multilayer ceramic capacitor is a necessary but not a sufficient condition for producing high leakage currents. They showed that a conducting medium, such as a salt solution must exist in the crack to cause an electrical short failure in the ceramic capacitor.

Ling and Jackson [39] correlated the normal voltage failures in MLCCs to silver migration using the temperature-humidity-bias (THB) test. THB failures increased after some of the MLC lots had undergone a barrel plating operation, indicating moisture penetration and ionic contaminants as the likely cause of accelerating the failure rate. In cross sections of failed MLC, they observed large holes and internal cracks connecting electrodes of opposite polarity, with silver inclusions along the length of the cracks. These observations suggested that silver migration was the cause of electrically short-circuit paths. This conclusion was supported by model experiments in which silver from

exposed electrodes migrated large distances (700 μm) under THB conditions (85°C/85% relative humidity, and two-times rated voltage).

Munikoti and Dhar [40] presented a method of screening out potential low-voltage failures in manufactured lots of multilayer ceramic capacitors. This is performed in few hours (about 6 hours) without affecting good devices. MLCCs are frequently used in low dc voltage applications, where voltages are less than a tenth of their rated voltage. Under these conditions, failures in the form of sudden increase in the leakage current id observed. It is generally accepted that these failures are tied to extrinsic defects in capacitor dielectric such as voids, cracks, and porosity. These failures are seen even in lots that have successfully passed the standard life test of 2000 hours duration.

The best known and accepted screening method for low-voltage failures is the temperature-humidity-bias (THB) test carried out under 85°C, 85% relative humidity (RH), 1.5 Vdc for a minimum period of 168 hours. This test is conducted in addition to the 1000-4000 hours of life test under 125°C and twice the rated voltage stress, to assess the lot mean time to failure (MTTF). These long tests are unsuitable for lot-to-lot reliability evaluation [40].

The technique, described by Munikoti and Dhar [40] [41], eliminates all the potential failures in capacitor lots, using a highly accelerated life test (HALT). In this technique, the 50-V rated capacitors are subjected to accelerated test at 140°C and 400 Vdc, instead of standard 125°C and 100 Vdc accepted in industry. This screen is based on the concept that low-voltage failures are caused by extrinsic defects in MLCCs and these defects can be eliminated in a very short time using high voltage and temperature acceleration. This HALT test is demonstrated to have the capability of eliminating the 85°C, 85% RH test.

Rawal and Chan [42] showed that two types of failure, called the avalanche breakdown (ABD) and thermal runaway (TRA), have been observed in various dielectrics under high temperature and high voltage stresses. The avalanche breakdown is an abrupt burst of current which results in an immediate breakdown. The thermal runaway is a much more gradual increase of leakage current which leads to self-heating and its subsequent failure. High voltages normally favor the avalanche breakdown type of failure, and high temperatures normally favor the thermal runaway type of failure. The two types of failure modes may coexist depending on the test conditions and the type of the ceramic studied. In general, imperfections in ceramics may be classified into (i) intrinsic which include electronic disorders, dislocations, grain boundaries, etc., and (ii) extrinsic such as porosity, delamination, cracks, etc. From various experiments in these two groups, it was shown that avalanche breakdown type failure is attributed to extrinsic flaws and thermal runaway type failure is caused by intrinsic characteristics of the ceramic.

Chen, et al. [42] investigated water-induced electrical degradation of barium titanate ceramics. They showed that water has quite different effects on barium titanate ceramics in the presence and in the absence of bias. Barium titanate without bias is very stable against water. When electricity is present, electrolysis of water occurs and the resistance of barium titanate is decreased by orders of magnitude, and the dielectric loss is increased. It is proposed that barium titanate is reduced by atomic hydrogen generated by electrolysis of water at ambient temperature, and electrons are formed in barium titanate ceramics, which results in electrical resistance degradation and dielectric loss.

Donahoe, et al. [45]-[46] demonstrated a new time dependent degradation phenomena in barium titanate MLCCs with base metal electrodes in humid environment without DC bias and showed that precious metal electrode capacitors are not susceptible to this type of degradation. MLCCs were exposed to around 2600 hours of autoclave conditions (121ºC, 100% RH, 205 KPa pressure) with periodic capacitance monitoring. After autoclave exposure, MLCCs were baked at 125ºC to determine if the MLCCs could be de-aged. It was shown that the degradation is not reversible, while known aging of MLCCs is a reversible phenomenon.

1.10.3 Techniques for detection of defects in MLCCs

Defects in multilayer ceramic capacitors are not always detectable by electrical or functional testing. These defects can occur during manufacturing of MLCCs, assembly, handling, testing, and etc. This behavior would be indicative of a "walking-wounded" in field applications, because a crack or defect exists. If a defected capacitor is used in a field application a conductive medium, often atmospheric moisture and ionic contaminants, can penetrate through the crack or defect into the capacitor and cause leakage current of the capacitor to increase. This may also lead to the shorting of the opposing electrodes of the capacitor, ultimately causing catastrophic failure in applications such as those involving high power, in which the short circuit may initiate a fire. There is a need for a technique, especially a non-destructive technique, for screening of multilayer ceramic capacitors. In this section, previous works on different techniques used for detection of defects in MLCCs are reviewed.

Condra, et al. [47] implemented scanning laser acoustic microscopy (SLAM) as screening for incoming multilayer ceramic capacitors. They observed that the failures observed in environmental testing were correlated well with earlier scanning laser acoustic microscopy testing on capacitors prior to assembly.

Weiler [48] presented analysis of multilayer chip capacitor cross sectioning, testing in less than 5 kppm internal H_2O environment and 85°C/85% humidity with known good and known bad capacitors, methanol test, delamination and crack formation, tunneling voids, metal migration under DC bias and moisture, scanning laser acoustic microscopy (SLAM) test, thermal stress of solder fillets on end terminations of ceramic capacitors using ANSYS, and DC bias voltage effect on metal migration shorts.

Chittick et al. [49] [50] implemented a screening technique for chip capacitors known as the "methanol test" that can detect the structural defects that are likely to give rise to low voltage failure. The technique is rapid and nondestructive, and is particularly suited to on-line production testing of chips as well as being suitable for goods inward inspection by the customer.

Methanol is an electrically conductive liquid. Capillary action and low viscosity allow methanol to wick inside cracks which are exposed to an external surface. Methanol penetrates between adjacent electrodes, thereby establishing a conductive film that causes a measurable increase in leakage current. Methanol testing can not be applied for cracks that do not emerge at an outside surface of the capacitor body. Special care is necessary to apply this technique to MLCCs mounted on printed circuit boards, in order to avoid creation of an electrical leakage path underneath the capacitor which could be interpreted as a crack.

Erdahl and Ume [51] developed a laser ultrasonic and interferometric measurement system in identifying flex cracks in MLCCs. Their technique provided a non-contact, non-destructive, and online approach for inspection of MLCCs. A pulsed infrared laser excites a specimen into vibration through laser-generated ultrasound, and the vibration displacement is measured using an interferometer. Differentiation between acceptable and unacceptable devices was achieved using signal-processing techniques that compared waveforms between two devices, where one of the waveforms is a reference waveform from a good MLCC.

Ousten, et al. [52] [53] used the residual piezoelectricity for in ceramic capacitors. Piezoelectricity provides an impedance signature at resonance allowing detection of defects. In this paper, they concluded that impedance spectroscopy measurements are probably one of the best ways to analyze passive components. They have shown that the use of the piezoelectric response on impedance for type II and relaxor ceramic capacitors is a powerful technique for detection of micro-defects. The sensitivity allows detecting defects of less than 1 mm, without exceeding two times of the rated voltage as bias voltage, under the only condition to have a defect-free response for reference.

Bechou et al. [54] also focused on a technique based on the principle of electromechanical resonances existing in piezoelectric materials under a DC bias. Based on the correlation between the impedance measurement of the chip under a sufficient voltage allows them to highlight some conclusions concerning the behavior, the nature of the defects and the long-term reliability of ceramic chip capacitors. This method has the advantage of being non-destructive, rapid, efficient and low cost.

Boser [55] used impedance measurements as a function of frequency on ceramic capacitors with X7R and Z5U dielectrics and showed electromechanical resonances which are caused by the piezoelectric nature of the barium titanate-based dielectric materials.

Love and Ewell [56] applied acoustic microscopy for detection of delamination inside MLCCs. This tool is sensitive to erratic electrode stacking, ceramic margins, termination quality, and other defects. In addition, some preliminary work has been done investigating the ability of acoustic microscope to evaluate chips for dielectric voids. Chan and Rawal [57] evaluated an ac-voltage-induced acoustic emission test technique for screening physical flaws, particularly delamination, in multilayer ceramic capacitors.

Spiiggs and Cronshagen [58] devised and applied a radiographic method for the detection of delaminations in small ceramic chip capacitors. Their results indicated that this nondestructive technique is suitable for sampling or 100% screening of lots. The radiograph provides an integrated image of internal structure rather than a view of just of one plane as in cross sectioning.

1.11 Focus of the present study

With the transition to lead-free materials in the electronics industry there is a concern that multilayer ceramic capacitors assembled on printed circuit boards with lead-free solder have different susceptibility to flex cracking than those assembled with eutectic tin-lead solder. In the present study, the main focus is to investigate differences in flex cracking of MLCCs assembled with lead-free solder as compared with eutectic tin-lead solder, through a systematic examination of factors which had not been studied

previously in this context and explain the difference in flex cracking susceptibility of MLCCs assembled with lead-free and tin-lead solders.

Tin-silver-copper lead-free solders and eutectic tin-lead solder have different mechanical properties, which affect the amount of the stresses that is transmitted to the ceramic body of the capacitor through the solder fillet. In addition, solidification temperature for Sn3.0Ag0.5Cu lead-free solder is about 34° higher than for eutectic tin-lead (Sn37Pb) solder. The higher solidification temperature for lead-free solder causes the amount of residual compressive stresses after reflow cool-down process for MLCCs assembled with lead-free solder to be higher than those assembled with tin-lead solder.

In this study, the effects of different parameters on flex cracking of multilayer ceramic capacitors were investigated. The effects of dielectric material, capacitor size, solder assembly process, solder material, and end-termination type on flex cracking of multilayer ceramic capacitors were determined for MLCCs from different manufacturers. Flex cracking of standard- and flexible-termination MLCCs mounted on PCBs with two different solder materials, lead-free solder and eutectic tin-lead solder, was investigated and compared. Capacitors from several manufacturers were included in order to incorporate variations in materials and manufacturing processes, which provide insight into the range of behavior possible from commercially available components. Two capacitor sizes and two commonly used dielectric materials were considered in experimental design of flex testing of MLCCs. Flex cracking of convective reflow-soldered MLCCs was compared with wave-soldered MLCCs for both flexible and standard terminations.

Destructive and non-destructive failure analysis techniques were used to confirm cracking of MLCCs, which were identified as failures in flex tests. The tested capacitors were potted and cross-sectioned, and then environmental scanning electron microscopy (E-SEM) and optical microscopy were used to characterize the cracks inside capacitors. Non-destructive techniques, such as impedance spectroscopy and X-ray radiography, were also applied to detect cracks inside capacitor body.

Since some flexible-termination and standard-termination MLCCs are made with precious metal electrodes (silver-palladium), there is a possibility of electrochemical silver migration under bias and humidity. In addition, the polymer buffer layers in flexible-termination MLCCs are loaded with silver for electrical conduction, which is another potential source for silver migration.

In this study, effects of temperature-humidity-bias (THB) on electrical parameters of multilayer ceramic capacitors with both flexible and standard terminations were investigated. There is no published data available of temperature-humidity-bias testing for the new technology flexible-termination MLCCs. Users of this new technology have the concern that long term exposure to moisture cause failure or electrical degradation in flexible-termination MLCCs. In addition, temperature-humidity-bias effects on electrical parameters of MLCCs made of precious metal electrode (Ag-Pd) are compared with MLCCs made of base metal electrodes (Ni).

In manufacturers' qualification testing of MLCCs in temperature-humidity-bias conditions and previous work on testing of MLCCs in THB conditions, electrical parameters of MLCCs has not been measured in-situ during THB testing. They usually measured electrical parameters periodically during testing at room temperature or only

before and after completion of the THB testing. In this situation, intermittent failures that occur during testing are not captured and the failed MLCCs, which are recovered at room temperature-humidity conditions, are not captured as failures too. In-situ measurement of different electrical parameters (capacitance, dissipation factor, and insulation resistance) of MLCCs during THB testing was implemented in the present study. This helps to capture intermittent failures of MLCCs during testing and finding effects of temperature-humidity-bias on each electrical parameter separately. It is possible that an MLCC exhibit out of specification value for one of the electrical parameters, while other electrical parameters are still within the specification limits.

2 Flex cracking of multilayer ceramic capacitors with standard and flexible terminations

In this section, experimental results on flex testing of assembled multilayer ceramic capacitors with standard and flexible terminations are presented. With the transition to lead-free materials in the electronics industry there is a concern that multilayer ceramic capacitors assembled on printed circuit boards with lead-free solder have different susceptibility to flex cracking than those assembled with eutectic tin-lead solder. In the present study, the main focus is to investigate the differences in flex cracking of MLCCs assembled with lead-free solder as compared with eutectic tin-lead solder.

There is some new legislation worldwide on the use of hazardous material such as lead in electronic industry. In such legislation, the use of hazardous materials such as lead is often limited in order to improve the ease of recycling. The European Parliament and the Council of the European Union passed some directives to minimize the risks that the production, use, treatment, and disposal of waste electrical and electronic equipment have on human health and the environment. Directive on the restriction of hazardous substances (ROHS) in electrical and electronic equipment [59] and directive on waste electrical and electronic equipment (WEEE) [60] were proposed for several years. They identify lead as a material not allowed in electrical and electronic equipment to be put on the market after July 1, 2006 [61].

In this section, the effects of different parameters on flex cracking of multilayer ceramic capacitors are investigated. The effects of dielectric material, capacitor size, solder assembly process, solder material, and end-termination type on flex cracking of multilayer ceramic capacitors are determined for MLCCs from different manufacturers.

Flex cracking of standard- and flexible-termination MLCCs assembled on PCBs with two lead-free and eutectic tin-lead solders are investigated and compared. Flex cracking of two capacitor sizes and two commonly used dielectric materials are compared. Flex cracking of convective reflow-soldered MLCCs are compared with wave-soldered MLCCs for both flexible and standard terminations.

The difference in results of MLCCs assembled with lead-free and tin-lead solder is explained in terms of solder mechanical properties using finite element analysis, and solders solidification temperature. In addition, effects of isothermal high temperature aging on flex cracking of MLCCs assembled with tin-lead and lead-free solders are presented. The results of isothermal high temperature aging on flex cracking of MLCCs are explained and related to difference in susceptibility of flex cracking of MLCCs assembled with tin-lead and lead-free solders.

Finally, destructive and non-destructive failure analysis techniques were used to confirm cracking of MLCCs, which were identified as failures in flex tests. The solder fillet geometrical parameters for MLCCs assembled with lead-free and tin-lead solder are compared. Material analysis and constructional analysis of tested MLCCs are presented.

2.1 Experimental procedure

In order to study flex cracking of multilayer ceramic capacitors, printed circuit boards were designed and built using high glass transition temperature (T_g = 170°C) FR4 material (glass fiber reinforced epoxy resin matrix). On each board, 24 capacitors were assembled. There were two board designs (similar to each other but with different pad sizes) for 0805 capacitors and 1812 capacitors. The solder pads on these boards were

plated with immersion tin. The layout of the test board for 1812 size MLCCs is shown in Figure 12. A lead-free solder (Sn3.0Ag0.5Cu) and eutectic tin-lead solder (Sn37Pb), were used to assemble capacitors on the boards using convective solder reflow. The temperature profiles of the reflow process for these two different solder materials were different. The peak reflow temperature for eutectic tin-lead solder was between 210 and 230°C, while for Sn3.0Ag0.5Cu lead-free solder it was between 235 and 255°C.

After assembling capacitors, boards were subjected to deflection based on IPC/JEDEC standard 9702 [62] using the 4-point bend test shown in Figure 13. Vertical displacement of load rams versus time on an MTS hydraulic tester during a flex test is shown in Figure 14. The ram displacement was increased in 0.2 mm steps at a rate of 4 mm/s and then held at that position for 10 seconds to allow capacitance measurement of all 24 capacitors assembled on the board at each step. Figure 5 contains a photograph that was taken during actual bend testing at the maximum ram displacement of 10 mm. After the ram reached its maximum displacement for 10 seconds, it was brought back to zero displacement in one step at a rate of 4 mm/s.

In order to measure PCB strain during flex testing, strain gauges were mounted on each board. Since the net vertical force between the two load rams of the 4-point bend test is zero, the radius of curvature between the load rams, where the capacitors were mounted, is theoretically constant.

The capacitance of each capacitor was monitored in-situ throughout the flex test in order to detect the occurrence of flex cracking. A multiplexing switch was used to scan all the capacitors mounted on the board and measure each capacitor using a LCR meter. Capacitance is expected to drop upon cracking of a capacitor if a crack passes through the

electrodes of the capacitor. Recovery after the end of the flex test for some capacitors necessitates in-situ monitoring of capacitance. In addition, after each capacitance measurement, the strain on board was measured to determine the strain level that caused a capacitor to crack. A software program in Labview was developed to control the LCR meter, switch, and digital multimeter.

Strain was measured for each column individually on one board, with strain gauges placed in the locations shown in the center line of the board in Figure 12. From these measurements it was found that strain varied by a maximum of about 12% from the average, although this difference remained below 10% for nearly all deflection levels. Analysis of variance (ANOVA) for strain-to-failure data from each of the three columns of capacitors on a PCB revealed that these three distributions belong to the same population.

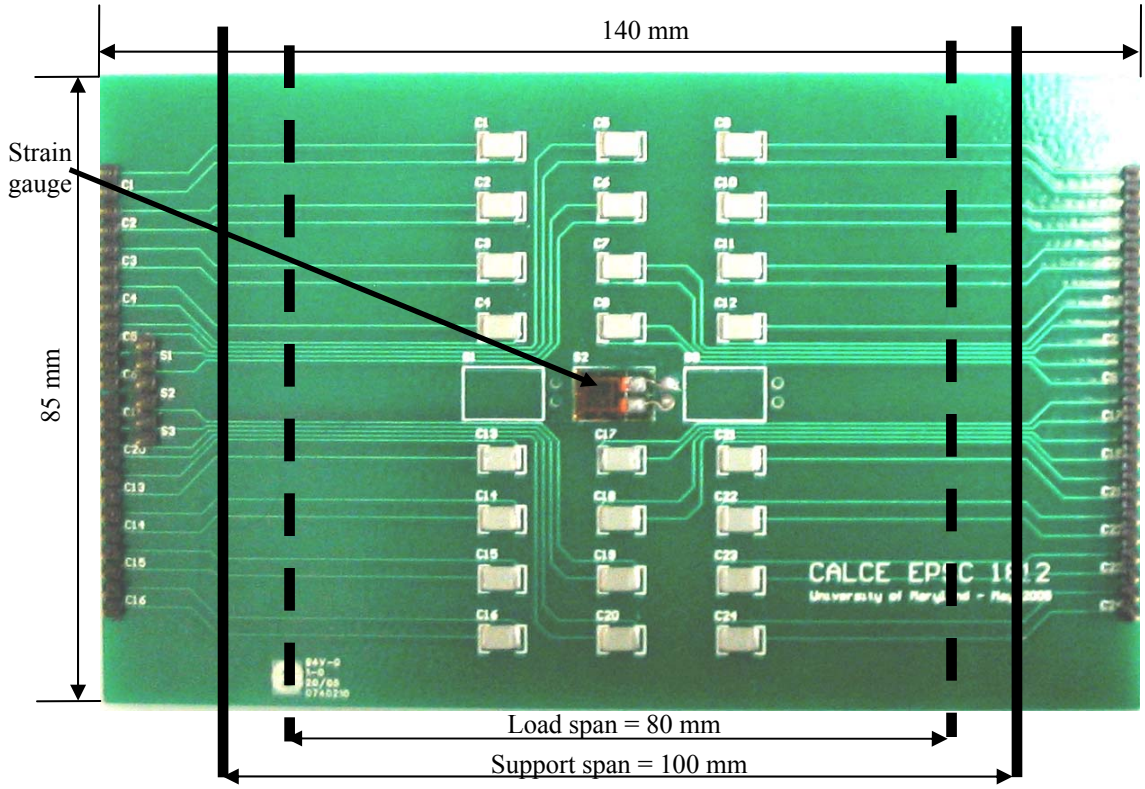

Figure 12. Test board for flex cracking test of 1812 size MLCCs. The thickness of boards is 1.57 mm.

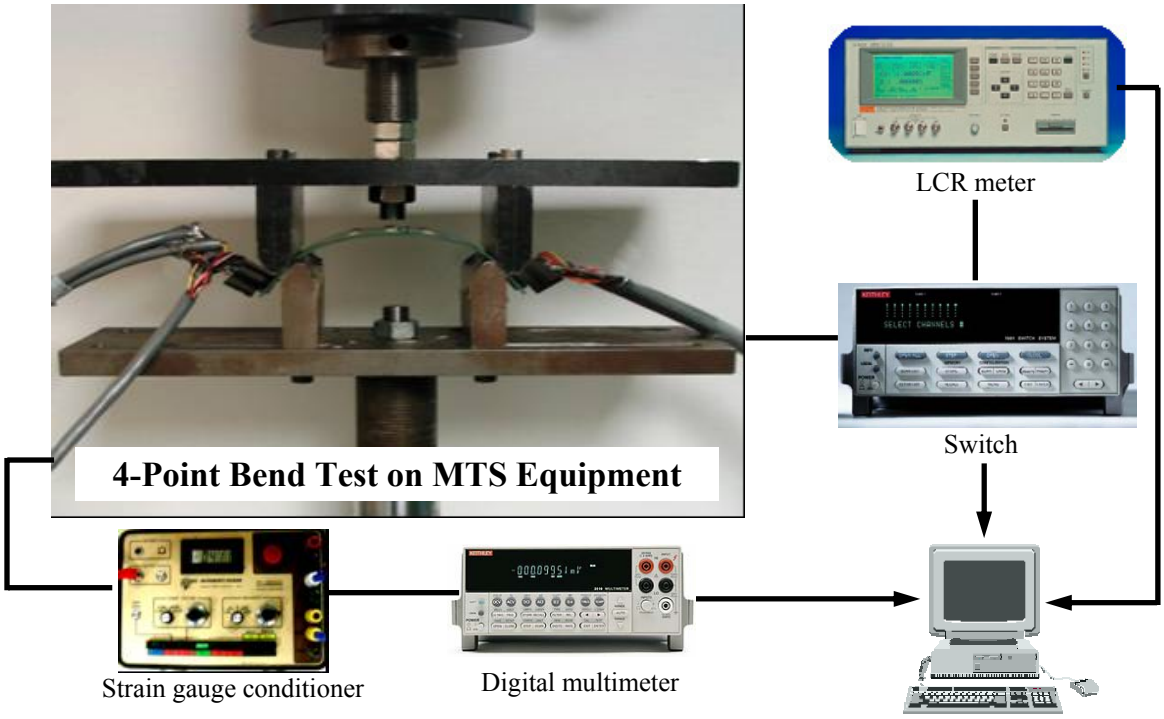

Figure 13. Schematic of experimental setup for flex testing of MLCCs.

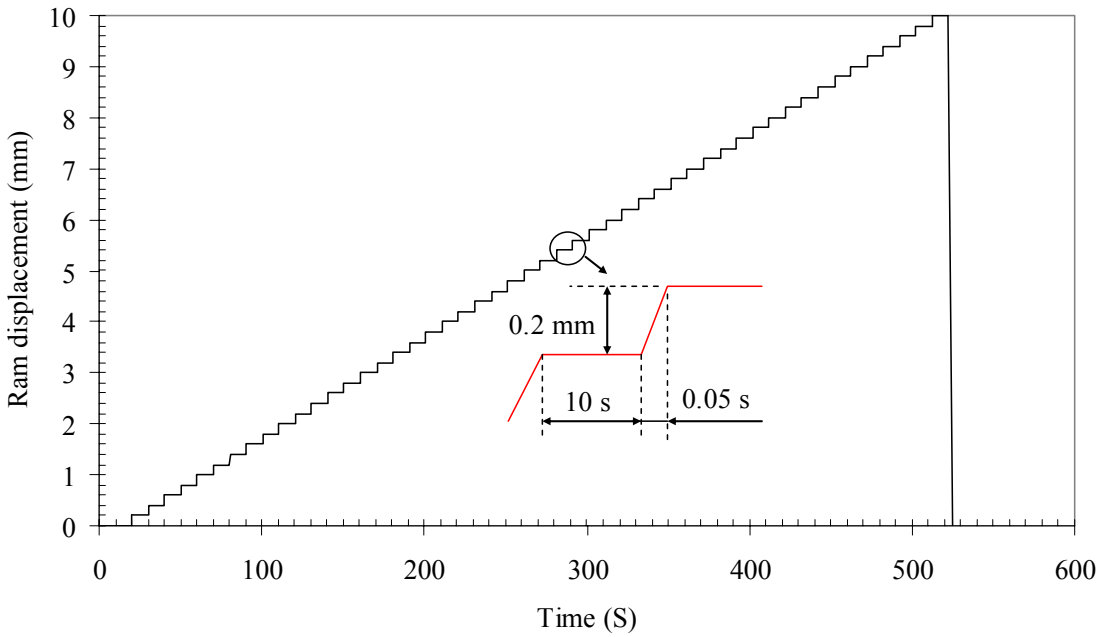

Figure 14. Vertical load ram displacement versus time during flex testing of MLCCs.

2.2 Experimental design for flex test of MLCCs

The experiment addressed six parameters, which affect flex cracking of MLCCs: solder material, solder assembly process, dielectric material, capacitor size, end-termination type, and manufacturer. The sample matrix for standard-termination and flexible-termination MLCCs assembled with convective reflow soldering are presented separately. Finally, sample matrix for MLCCs assembled with wave soldering is presented.

2.2.1 Experimental design for flex test of standard-termination MLCCs

In order to study the effect of solder material on flex cracking of MLCCs, two solder materials were used to assemble the capacitors on PCBs, eutectic tin-lead solder (Sn37Pb) and a lead-free solder (Sn3.0Ag0.5Cu). Two capacitor sizes were selected, 0805 and 1812, to allow comparison of susceptibility to flex cracking of a larger size capacitor (1812) with a smaller size capacitor (0805). Finally, two dielectrics were considered, C0G and X7R, in order to compare flex cracking of two commonly used dielectric materials with different mechanical properties.

The sample matrix for the flex tests of standard-termination MLCCs assembled on PCBs with convective reflow soldering is shown in Table 2. Capacitors from four manufacturers, AVX, Kemet, Vishay, and TDK were studied. All capacitors used in this study were obtained from authorized distributors and they are standard production parts. Initially, 1812 capacitors from Kemet, with two different dielectrics (X7R, and C0G) were tested using both solder materials (lead-free and tin-lead). As shown in Table 2, 4 boards with 24 capacitors on each board were tested for each case. In addition, capacitors

from Kemet and AVX with size 0805 and dielectric X7R were tested using both solder materials.

In order to compare flex cracking of ceramic capacitors from different manufacturers, capacitors with size 1812 and dielectric X7R from the three other manufacturers (AVX, Vishay, and TDK) were tested using both solder materials. The larger capacitor size was selected, because it is more susceptible to flex cracking.

Some parameters affecting flex cracking of MLCCs were kept constant in our experiments to the extent possible. These parameters include the pad size for each capacitor size and their distance from each other, PCB thickness, and PCB material. The capacitors which have been selected for testing have a capacitance of 0.1 μF except capacitors with C0G dielectric from Kemet and X7R capacitors from TDK. For capacitors with C0G dielectric, a value of capacitance has been chosen to keep the thickness of the capacitors the same as that for 1812 size capacitors with X7R dielectric selected for testing (see Table 2). For capacitors from TDK, a higher capacitance value was chosen because smaller capacitance value from this manufacturer was not available.

Table 2. Sample matrix for flex testing of standard-termination MLCCs assembled on PCBs with convective reflow soldering.

Solder	Size	Dielectric	C (μF)	Manufacturer	# of boards	# of capacitors
Sn37Pb	1812	C0G	0.0068	Kemet	4	96
Sn3.0Ag0.5Cu	1812	C0G	0.0068	Kemet	4	96
Sn37Pb	1812	X7R	0.1	Kemet	4	96
Sn3.0Ag0.5Cu	1812	X7R	0.1	Kemet	4	84
Sn37Pb	1812	X7R	0.1	AVX	2	46
Sn3.0Ag0.5Cu	1812	X7R	0.1	AVX	2	48
Sn37Pb	1812	X7R	0.1	Vishay	2	47
Sn3.0Ag0.5Cu	1812	X7R	0.1	Vishay	2	48
Sn37Pb	1812	X7R	1.5	TDK	2	48
Sn3.0Ag0.5Cu	1812	X7R	1.5	TDK	2	48
Sn37Pb	0805	X7R	0.1	Kemet	2	48
Sn3.0Ag0.5Cu	0805	X7R	0.1	Kemet	2	48
Sn37Pb	0805	X7R	0.1	AVX	2	48
Sn3.0Ag0.5Cu	0805	X7R	0.1	AVX	2	48

2.2.2 Experimental design for flex test of flexible-termination MLCCs

Four-point bend tests will be conducted to study flex cracking of MLCCs with flexible termination assembled on PCBs with two different solders; eutectic tin-lead (Sn37Pb) and lead-free (Sn3.0Ag0.5Cu). Table 3 shows the sample matrix for flex tests of flexible-termination MLCCs assembled on boards with convective reflow soldering. Flexible-termination MLCCs from two manufacturers (AVX and Syfer) with size of 1812 and flexible-termination MLCCs with size of 0805 from AVX were considered. For each

case, 48 capacitors will be tested. AVX's flexible-termination MLCCs are made of base metal electrodes (nickel), while Syfer's flexible-termination MLCCs are made of precious metal electrodes (silver-palladium).

Based on these experimental results, flex cracking susceptibility of flexible-termination MLCCs assembled on PCBs with lead-free solder will be compared with those assembled with eutectic tin-lead solder. In addition, flex cracking susceptibility of flexible- and standard-termination MLCCs will be compared.

Table 3. Sample matrix for flex test of flexible-termination MLCCs assembled on PCBs with convective reflow soldering.

Solder	Size	Dielectric	C (μF)	Manuf.	# of boards	# of capacitors
Sn37Pb	1812	X7R	0.22	AVX	2	48
Sn3.0Ag0.5Cu	1812	X7R	0.22	AVX	2	48
Sn37Pb	1812	X7R	0.1	Syfer	2	48
Sn3.0Ag0.5Cu	1812	X7R	0.1	Syfer	2	48
Sn37Pb	0805	X7R	0.1	AVX	2	48
Sn3.0Ag0.5Cu	0805	X7R	0.1	AVX	2	48

2.2.3 Experimental design for flex test of wave-soldered MLCCs

Four-point bend tests will be conducted to study flex cracking of MLCCs assembled on PCBs with wave soldering using eutectic tin-lead solder. Table 4 shows the sample matrix for flexible- and standard-termination MLCCs assembled on PCBs with wave soldering. Flexible- and standard-termination MLCCs from AVX were considered in these experiments. Manufacturers of MLCCs recommend wave soldering of MLCCs for

sizes smaller than 1206. Therefore, only MLCCs with size of 0805 were considered in flex test of wave-soldered parts. Based on these experimental results, flex cracking susceptibility of wave-soldered flexible- and standard-termination MLCCs will be compared with those assembled with convective reflow soldering.

Table 4. Sample matrix for flex test of flexible- and standard- termination MLCCs assembled on PCBs with wave soldering.

Solder	Size	Dielectric	End termination	Manufacturer	# of boards	# of capacitors
Sn37Pb	0805	X7R	Flexible	AVX	2	48
Sn37Pb	0805	X7R	Standard	AVX	2	48

2.3 Experimental results

This section presents plots of cumulative percent failure as a function of PCB strain for capacitors assembled using two different solder materials. The results are compared to examine the effects of solder material, solder assembly process, capacitor size, dielectric material, end-termination type, and manufacturer.

The capacitance of each capacitor was measured during board bending to detect crack formation. Figure 15 and Figure 16 show capacitance change and strain on the board as a function of time during flex testing. In Figure 15, capacitance drops upon the occurrence of the flex crack and recovers after removal of the strain. This behavior would be indicative of a “walking-wounded” in field applications, because a crack exists. If a cracked capacitor is used in a field application a conductive medium, often atmospheric moisture, can penetrate through the crack into the capacitor and cause leakage current of

the capacitor to increase. This may also lead to the shorting of the opposing electrodes of the capacitor, ultimately causing catastrophic failure in applications such as those involving high power, in which the short circuit may initiate a fire. In Figure 16 capacitance drops upon the occurrence of the flex crack and does not recover. Cross-sections and optical microscopy of tested capacitors verified conclusions of in-situ measurements of capacitance. The failure criterion for flex cracking was chosen to be a 10% drop in capacitance relative to the nominal value of capacitance according to the manufacturer's datasheet for the part, indicating the point at which the capacitance fell out of specification. In practice, the high rate of crack growth for these brittle components meant that the final results were almost insensitive to whether capacitance drop was calculated relative to the nominal value or to the initial measured value.

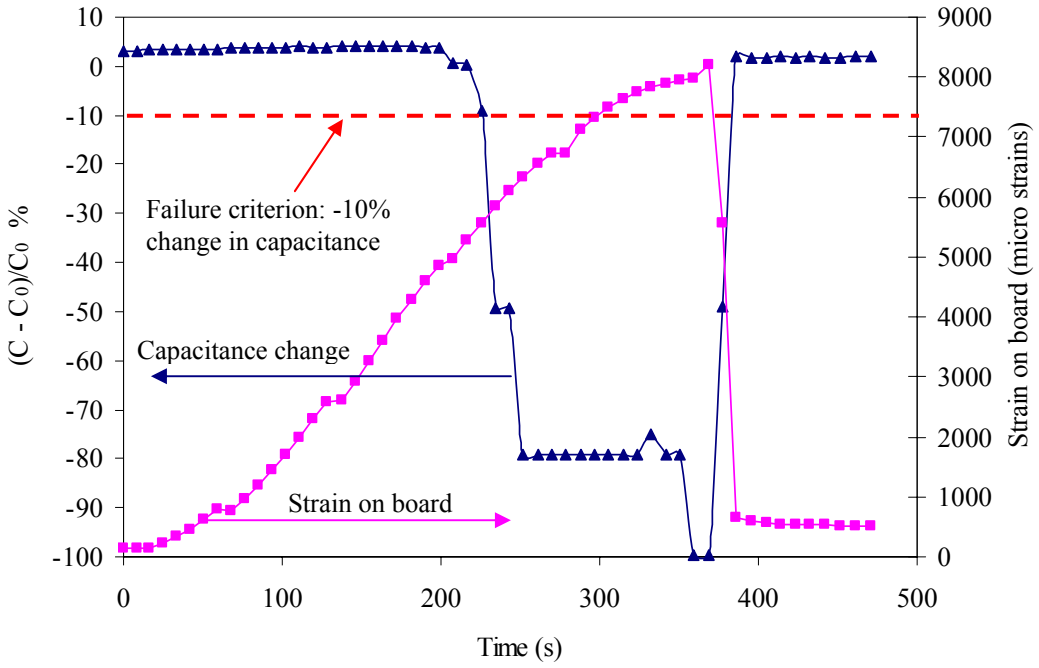

Figure 15. Capacitance change and strain on board as a function of time during flex testing of MLCCs. The capacitance drops due to flex cracking and recovers after removal of the strain. C_0 is the nominal capacitance of the capacitor, which is equal to 0.1 µF for the capacitor shown here.

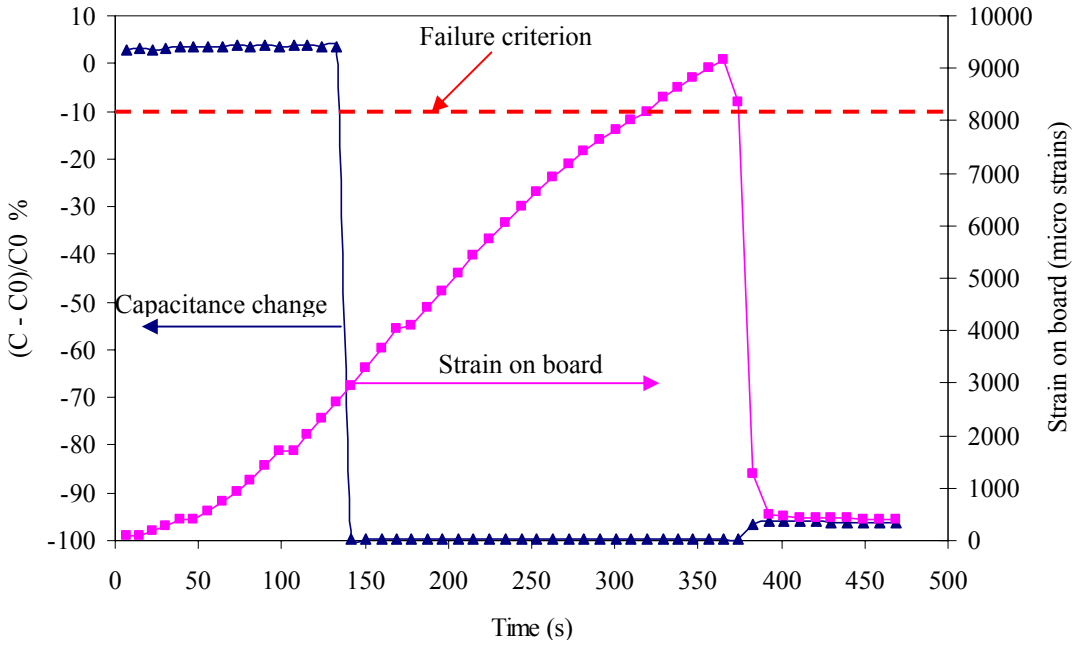

Figure 16. Capacitance change and strain on board as a function of time during flex testing of MLCCs. The capacitance drops due to flex cracking and does not recover after removal of the strain.

2.3.1 Comparison of the effects of the solder material on flex cracking of MLCCs

Flex cracking of MLCCs mounted on boards with eutectic tin-lead solder and Sn3.0Ag0.5Cu lead-free solder was studied. Figure 17 compares the effects of Sn37Pb and Sn3.0Ag0.5Cu solders on the flex cracking of capacitors with 1812 size and X7R dielectric from Kemet. MLCCs mounted on boards with lead-free solder showed less susceptibility to flex cracking than capacitors mounted with eutectic tin-lead solder, and this was true for capacitors from the other two manufacturers. A similar trend to that observed for 1812 size capacitors was also observed for 0805 size capacitors (Figure 18).

Figure 19 and Figure 20 compare flex cracking susceptibility of capacitors with 1812 size and X7R dielectric from the three different manufacturers mounted on boards with tin-lead and lead-free solders, respectively. The results from three manufacturers are comparable with each other in the case of tin-lead solder, while among capacitors mounted on boards with lead-free solder, capacitors from Kemet showed higher susceptibility to flex cracking compared to capacitors from AVX and Vishay. The differences observed with lead-free solder among capacitors from different manufacturers may be related to solder fillet variations or to their response to the higher solidus temperature for lead-free solder, which will be discussed later.

For 0805 size capacitors and X7R dielectric from two different manufacturers also exhibited the same trend that was observed for 1812 size capacitors. Figure 21 compares flex cracking susceptibility of capacitors with 0805 size and X7R dielectric from the two different manufacturers (AVX and Kemet) mounted on boards with tin-lead solders. The results from two manufacturers are comparable with each other in the case of tin-lead solder, while among capacitors mounted on boards with lead-free solder, capacitors from Kemet showed higher susceptibility to flex cracking compared to capacitors from AVX. For 0805 size capacitors from Kemet mounted on boards with lead-free solder, 8 out of 48 samples showed failure during flex testing, while in the same situation for capacitors from AVX showed no failure out of 48 samples (see Table 5).

Table 5 provides the strain on board which causes one percent and ten percent failure for standard-termination MLCCs. Although the strain on board for 1812 size X7R capacitors showed a big difference between tin-lead and lead-free solder for ten percent failure, the differences are less at one percent failure (see Table 5).

The Weibull 3-parameter distribution was used to generate the curves that are fit to the flex test data. The probability density function (PDF) for the Weibull 3-parameter distribution is

$$f(t) = \beta\eta^{-\beta}(t-\gamma)^{\beta-1} e^{-\left(\frac{t-\gamma}{\eta}\right)^{\beta}},$$

and the cumulative distribution function (CFD) is

$$Q(t) = 1 - e^{-\left(\frac{t-\gamma}{\eta}\right)^{\beta}},$$

where β is the shape parameter, η is the scale parameter, and γ is the location parameter.

Table 6 lists the Weibull parameters for these distributions. It is clear that scale parameters for MLCCs assembled with lead-free solder are much larger than those for MLCCs assembled with tin-lead solder, which confirms that MLCCs assembled with tin-lead solder are more susceptible to flex cracking.

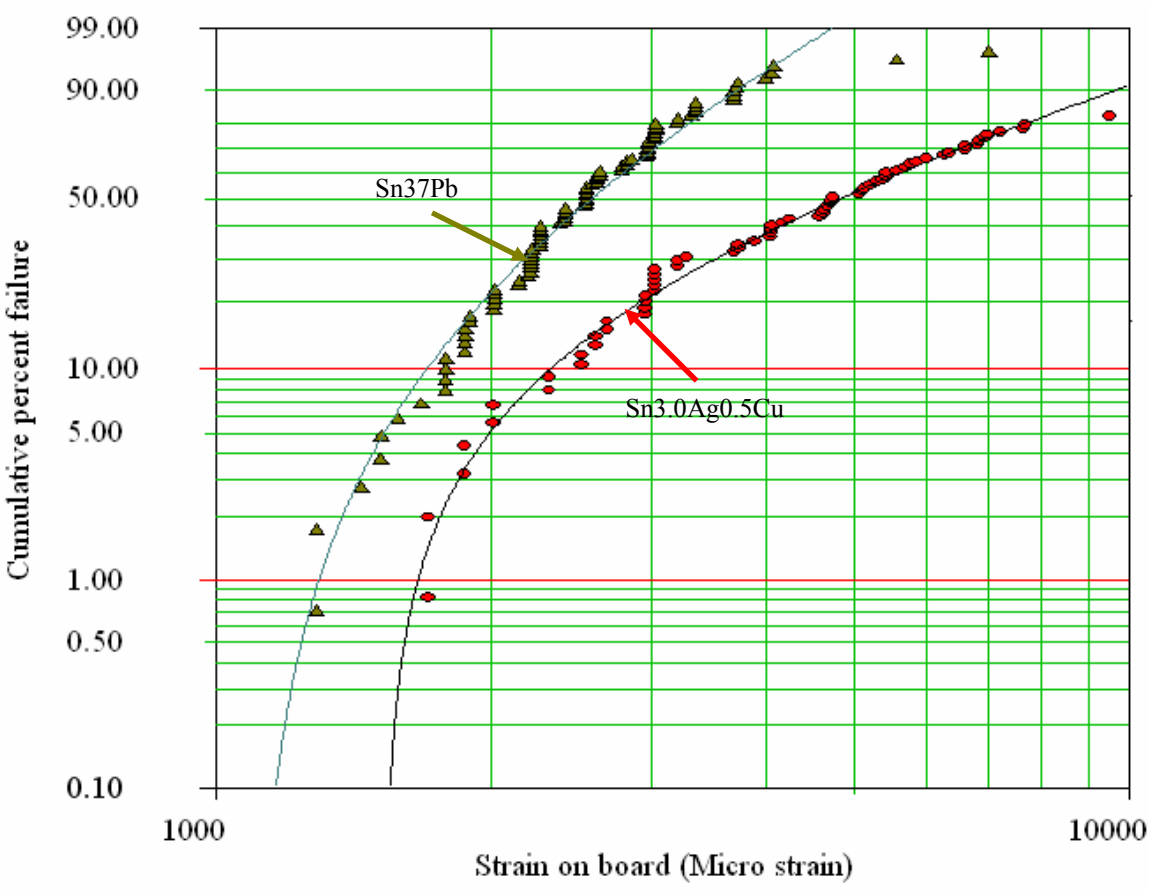

Figure 17. Comparison of cumulative percent failure as a function of strain on board for 1812 size, X7R capacitors from Kemet assembled with Sn37Pb and Sn3.0Ag0.5Cu solders.

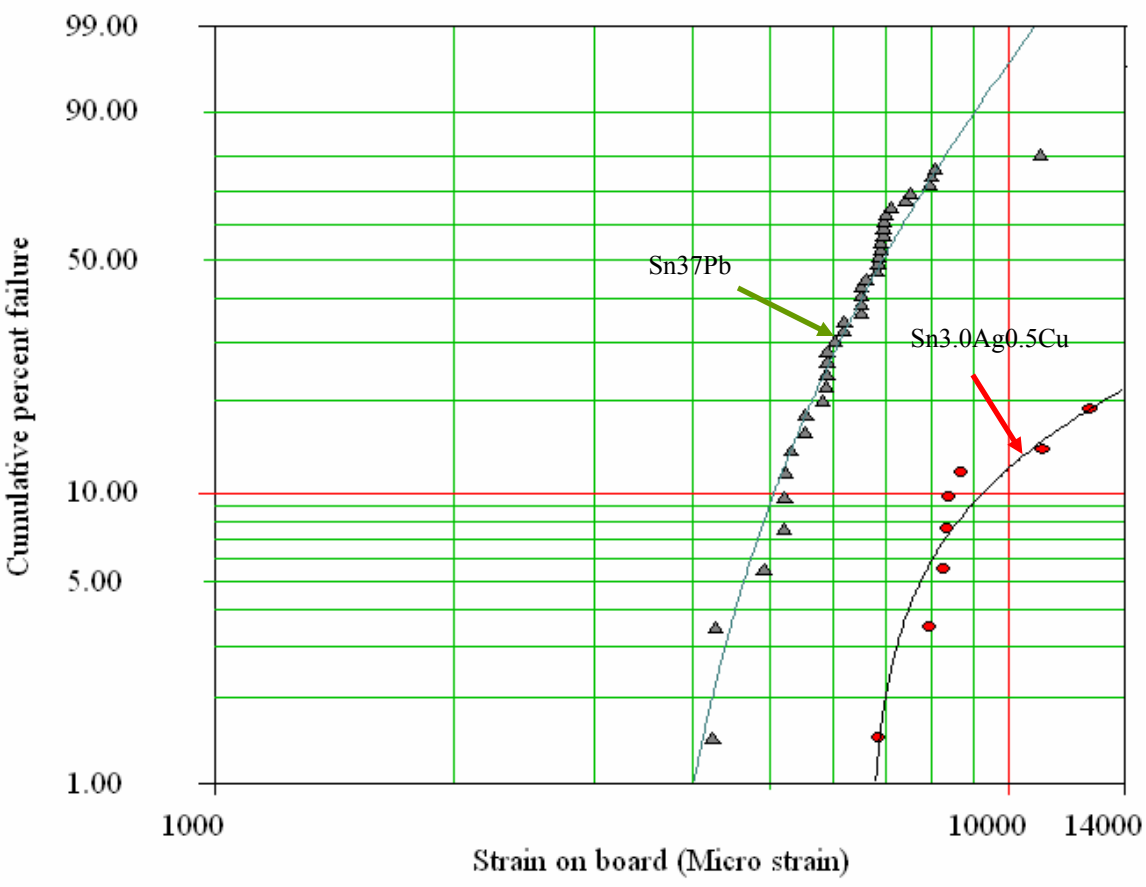

Figure 18. Comparison of cumulative percent failure as a function of strain on board for 0805 size, X7R capacitors from Kemet assembled with Sn37Pb and Sn3.0Ag0.5Cu solders.

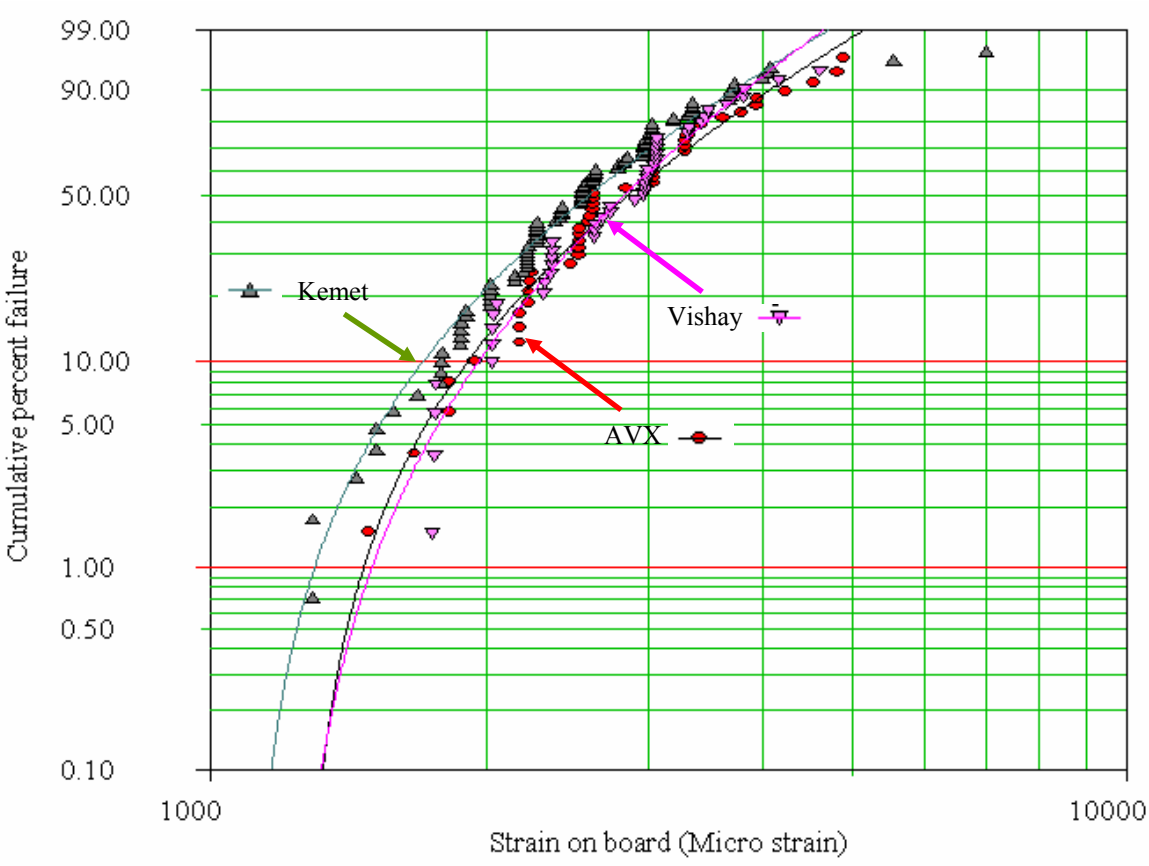

Figure 19. Comparison of cumulative percent failure as a function of strain on board for 1812 size, X7R capacitors from different manufacturers (Kemet, AVX, and Vishay) mounted on boards with Sn37Pb solder.

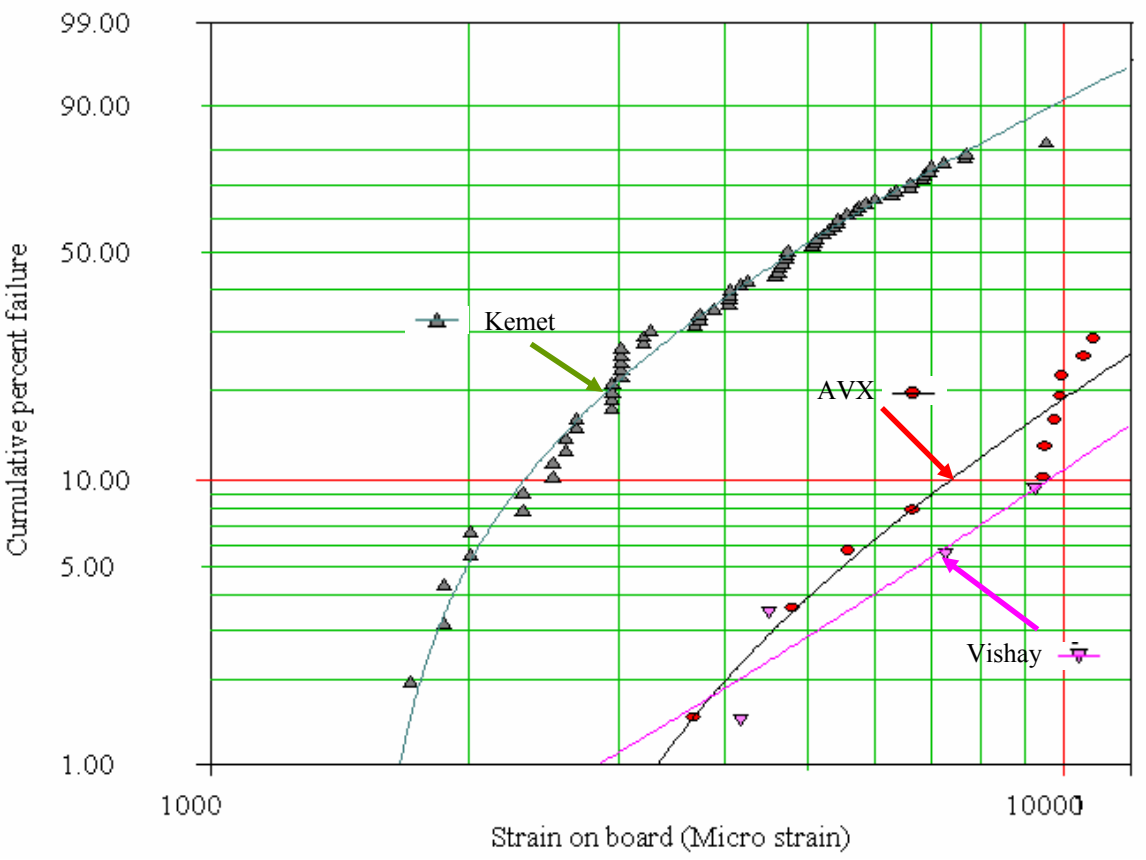

Figure 20. Comparison of cumulative percent failure as a function of strain on board for 1812 size, X7R capacitors from different manufacturers (Kemet, AVX, and Vishay) mounted on boards with Sn3.0Ag0.5Cu lead-free solder.

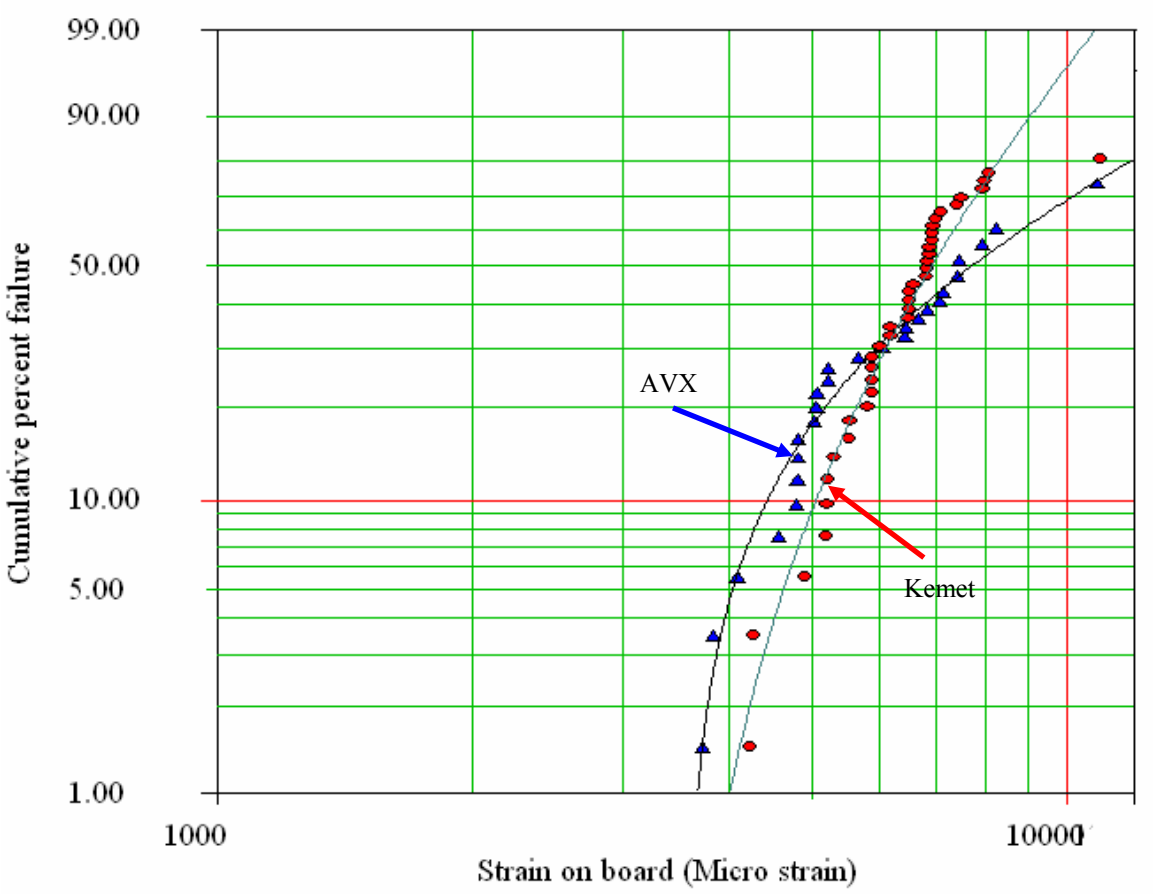

Figure 21. Comparison of cumulative percent failure as a function of strain on board for 0805 size, X7R capacitors from different manufacturers (Kemet, and AVX) mounted on boards with Sn37Pb solder.

Table 5. The strain on board at 1 and 10% failure due to flex cracking of MLCCs. Within the last two columns, the bold and underlined numbers indicate the lowest and the highest values, respectively, of strain on board at that percent of failure among MLCCs with X7R dielectric and 1812 size.

Solder	**Size**	**Diele.**	**Solder assembly process**	**Manuf.**	**Strain on board at 1% failure (Micro strain)**	**Strain on board at 10% failure (Micro strain)**
Sn37Pb	1812	C0G	Reflow	Kemet	No failure	No failure
Sn3.0Ag0.5Cu	1812	C0G	Reflow	Kemet	No failure	No failure
Sn37Pb	1812	X7R	Reflow	Kemet	**1,300**	**1,700**
Sn3.0Ag0.5Cu	1812	X7R	Reflow	Kemet	1,700	2,300
Sn37Pb	1812	X7R	Reflow	AVX	1,500	1,900
Sn3.0Ag0.5Cu	1812	X7R	Reflow	AVX	3,300	7,400
Sn37Pb	1812	X7R	Reflow	Vishay	1,500	2,000
Sn3.0Ag0.5Cu	1812	X7R	Reflow	Vishay	2,800	<u>9,600</u>
Sn37Pb	1812	X7R	Reflow	TDK	1,600	1,900
Sn3.0Ag0.5Cu	1812	X7R	Reflow	TDK	<u>3,600</u>	5,600
Sn37Pb	0805	X7R	Reflow	Kemet	4,000	5,100
Sn3.0Ag0.5Cu	0805	X7R	Reflow	Kemet	6,800	9,300
Sn37Pb	0805	X7R	Reflow	AVX	3,700	4,400
Sn3.0Ag0.5Cu	0805	X7R	Reflow	AVX	No failure	No failure
Sn37Pb	0805	X7R	Wave	AVX	4,000	4,500

Table 6. Weibull distribution parameters for flex test results on standard-termination MLCCs with X7R dielectric.

Solder	Size	Solder assembly process	Manuf.	Shape parameter (β)	Scale parameter (η)	Location parameter (γ)
Sn37Pb	1812	Reflow	Kemet	2.1	1,765	1,096
Sn3.0Ag0.5Cu	1812	Reflow	Kemet	1.3	4,337	1,528
Sn37Pb	1812	Reflow	AVX	2.1	1,898	1,253
Sn3.0Ag0.5Cu	1812	Reflow	AVX	1.7	20,597	2,052
Sn37Pb	1812	Reflow	Vishay	2.5	1,874	1,203
Sn3.0Ag0.5Cu	1812	Reflow	Vishay	2.2	28,812	-584
Sn37Pb	1812	Reflow	TDK	1.0	3,063	1,620
Sn3.0Ag0.5Cu	1812	Reflow	TDK	1.3	13,390	3,159
Sn37Pb	0805	Reflow	Kemet	2.6	4,200	3,280
Sn3.0Ag0.5Cu	0805	Reflow	Kemet	0.8	40,863	6,640
Sn37Pb	0805	Reflow	AVX	1.2	5,655	3,542
Sn37Pb	0805	Wave	AVX	1.2	3,643	3,927

2.3.2 Comparison of the effects of the dielectric material on flex cracking of MLCCs

Flex testing of 1812 capacitors with C0G dielectric mounted on boards with eutectic tin-lead and Sn3.0Ag0.5Cu lead-free solder was conducted to compare with X7R dielectric. 96 capacitors with C0G dielectric were tested for each solder material. None of the capacitors with C0G dielectric showed evidence of flex cracking up to the maximum strain level on board of about 13,000 micro-strains (The value of the strain given in micro-strains should be multiplied by 10^{-6} to get strain). In contrast, in the case of X7R

capacitors from the same manufacturer assembled with tin-lead solder, 94 out of 96 capacitors failed. Our results are in agreement with previous results that capacitors with X7R dielectric are known to be more susceptible to flex cracking than those with C0G dielectric , which has higher fracture toughness [10] [11].

2.3.3 Comparison of the effects of the capacitor size on flex cracking of MLCCs

In order to study the effect of capacitor size on flex cracking of MLCCs, flex tests of two different capacitor sizes (0805 and 1812) from Kemet were conducted. Figure 22 compares the cumulative percent failure of 1812 and 0805 capacitors with X7R dielectric assembled on boards with eutectic tin-lead solder. Smaller capacitors (0805) showed better resistance to cracking compared to larger capacitors (1812) for tin-lead solder. A similar trend was observed for MLCCs assembled with lead-free solder. Our results are in agreement with previous literature [5] that smaller capacitors are less susceptible to flex cracking. Strain on board at 10% failure was 5,100 micro-strains for 0805 size capacitors from Kemet assembled with tin-lead solder. In comparison, for 1812 size capacitors from the same manufacturer the strain on board at 10% failure was 1,700 micro-strains (see Table 5).

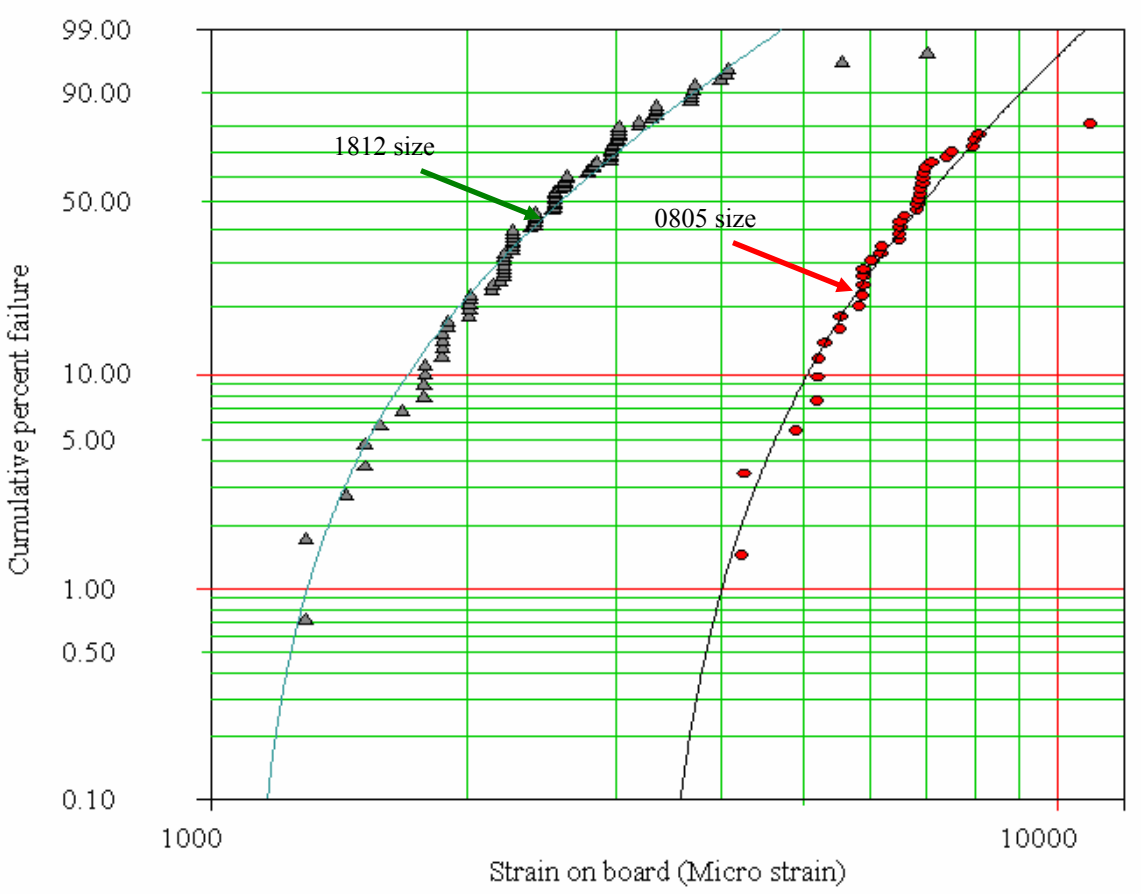

Figure 22. Comparison of cumulative percent failure as a function of strain on board for capacitors of size 1812 and 0805 with X7R dielectric from Kemet mounted on boards with Sn37Pb solder.

2.3.4 Comparison of the effects of the solder assembly process on flex cracking of MLCCs

Flex testing of MLCCs assembled with convective reflow soldering and wave soldering was conducted to study the effects of the solder assembly process on flex cracking of MLCCs. Manufacturers of MLCCs recommend wave soldering of MLCCs for sizes smaller than 1206. Therefore, only MLCCs with size of 0805 were considered in

the flex test of wave-soldered parts. Figure 23 compares cumulative percent failure as a function of strain on board for capacitors assembled with convective reflow soldering and wave soldering. Capacitors are size 0805 with X7R dielectric from AVX and assembled with Sn37Pb solder. MLCCs assembled with convective reflow soldering showed comparable results with MLCCs assembled with wave soldering.

Table 7 shows the strain on board at 10% failure due to flex cracking and 95% confidence bounds of strain at 10% failure for standard-termination MLCCs assembled with reflow and wave soldering. The strain at 10% failure was selected as a metric for comparing the effects of solder assembly process, although the conclusions are valid over a wide range of cumulative percent failure. The MLCCs assembled with convective reflow soldering and wave soldering showed very similar results in flex testing and the analysis shows that the 95% confidence intervals for reflow and wave soldering overlap.

Table 7. The strain on board at 10% failure due to flex cracking and 95% confidence bounds of strain at 10% failure for standard-termination MLCCs assembled with reflow and wave soldering.

Solder material	Solder assembly process	Upper bound of strain at 10% failure at 95% confidence level	Strain on board at 10% failure (Micro strain)	Lower bound of strain at 10% failure at 95% confidence level
Sn37Pb	Reflow	5200	4400	4000
Sn37Pb	Wave	5100	4500	4200

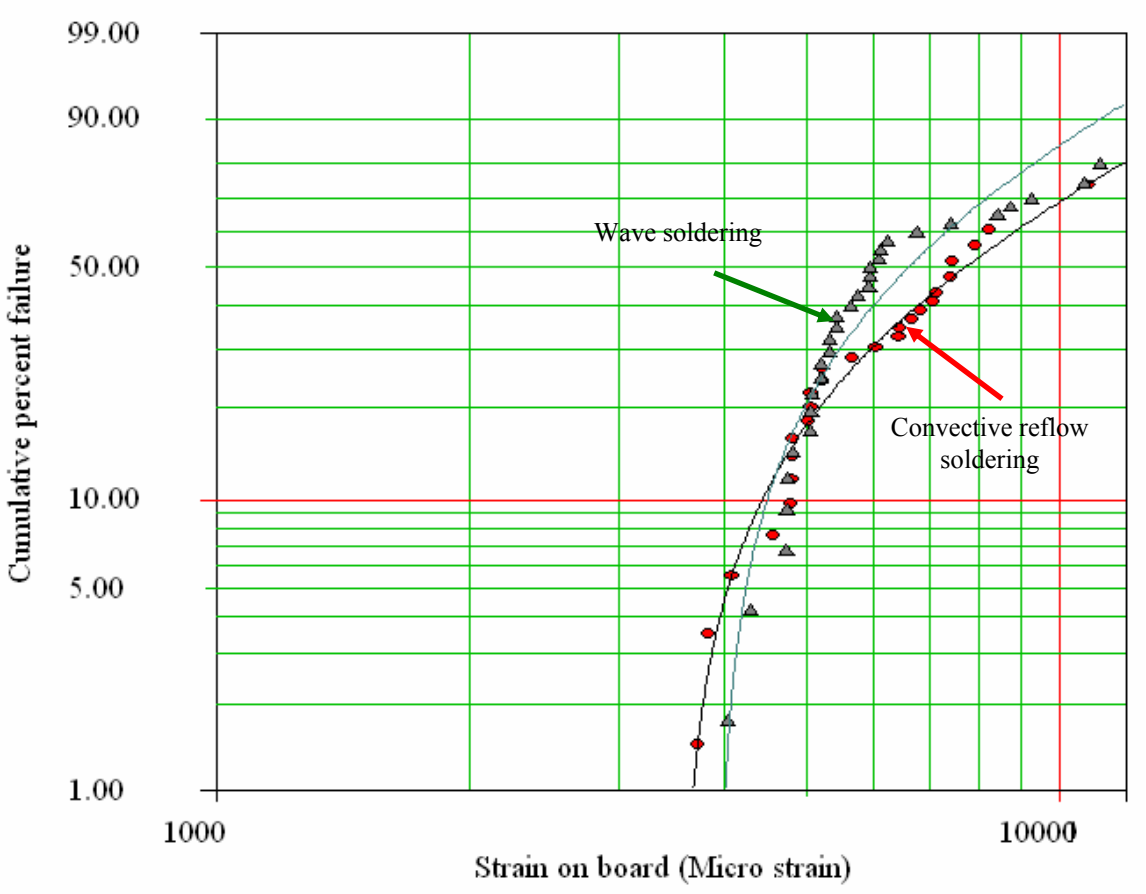

Figure 23. Comparison of cumulative percent failure as a function of strain on board for capacitors assembled with convective reflow soldering and wave soldering. Capacitors are size 0805 with X7R dielectric from AVX and assembled with Sn37Pb solder.

2.3.5 Flex test results of the flexible-termination MLCCs

Flex test results of flexible-termination MLCCs mounted on boards with eutectic tin-lead and lead-free solders are summarized in Table 8. Flexible-termination MLCCs were tested up to a maximum board strain level of 12,000 micro strain (load ram displacement of 10 mm). This was similar to the maximum level of board strain to which standard-

termination MLCCs were tested. In general, flexible-termination MLCCs are much less susceptible to flex cracking than standard-termination MLCCs.

For flexible-termination MLCCs assembled with lead-free solder, no failures out of 48 samples were observed in flex testing. In contrast, for 1812 size MLCCs assembled with tin-lead solder some failures were observed during flex testing of boards, although it was still much less than what was observed for standard-termination MLCCs. For 1812 size flexible-termination MLCCs from AVX assembled with tin-lead solder, two out of 48 samples failed in flex testing and for 1812 size flexible-termination MLCCs from Syfer only one failure out of 48 samples was observed. The strain on board at failure for each of these failures is given in Table 8. For 0805 size flexible-termination MLCCs, no failure out of 48 samples was observed for both reflow-soldered and wave-soldered samples.

Table 8. Flex test results of the flexible-termination MLCCs.

Solder	**Soldering process**	**Size**	**Manuf.**	**# of samples**	**# of failures**	**Strain at failure (Micro strain)**
Sn37Pb	Reflow	1812	AVX	48	2	4,900 and 8,100
Sn3.0Ag0.5Cu	Reflow	1812	AVX	48	0	-
Sn37Pb	Reflow	1812	Syfer	48	1	7,700
Sn3.0Ag0.5Cu	Reflow	1812	Syfer	48	0	-
Sn37Pb	Reflow	0805	AVX	48	0	-
Sn3.0Ag0.5Cu	Reflow	0805	AVX	48	0	-
Sn37Pb	Wave	0805	AVX	48	0	-

2.4 Isothermal aging effects on flex cracking of assembled multilayer ceramic capacitors

It was shown in the experiments that MLCCs assembled with lead-free solder (Sn3.0Ag0.5Cu) are less susceptible to flex cracking compared to MLCCs assembled with eutectic tin-lead solder. Lead-free solder solidifies at a higher temperature than tin-lead solder. Therefore, after solder assembly lead-free solder exerts more compressive stress on MLCCs than tin-lead solder. Consequently, capacitors assembled with lead-free solder should require a larger applied bending stress to crack than those assembled with tin-lead solder. The motivation behind the isothermal aging of MLCCs followed by flex testing was to reduce the amount of the compressive stress in MLCCs through stress relaxation, especially in the case of lead-free solder, in order to investigate its effect on flex cracking.

2.4.1 Experimental procedure of the flex testing of aged assembled MLCCs

In the experiment, 24 capacitors were assembled on each board, some boards with lead-free solder (Sn3.0Ag0.5Cu) and others with eutectic tin-lead solder (Sn37Pb) using convective solder reflow (see Table 9). The temperature profiles of the reflow process for these two different solder materials were different. The peak reflow temperature for eutectic tin-lead solder was approximately 220°C, while for Sn3.0Ag0.5Cu lead-free solder it was approximately 245°C.

As shown in the flow chart for the experimental procedure (Figure 24), some boards were aged for 200 hours at either 100 or 150°C. The reason for choosing 150°C was that

it was high enough to cause high amount of creep in solder alloy and relaxing compressive residual stress inside the capacitors, and 150°C is still below the melting temperatures of both eutectic tin-lead and tin-silver-copper lead-free solders. Also, 150°C was below the glass transition temperature of FR4 PCB (T_g = 170°C). In addition, another temperature (100°C) was chosen to enable comparison between two aging temperatures. The difference between the two aging conditions was chosen to be 50°C to make it more likely that we would observe the effects of different aging temperatures.

The boards were then subjected to deflection at room temperature based on IPC/JEDEC standard 9702 [62] using a four-point bend test to compare susceptibility to flex cracking of capacitors which were aged at high-temperature with those which were not. In order to ensure that capacitors retained electrical functionality, capacitance and dissipation factor were measured before and after aging. In order to measure PCB strain during flex testing, strain gauges were mounted on each board. Further details regarding the experimental procedure and apparatus used for four-point bend testing were explained in section 2.1.

The capacitance of each capacitor was monitored in-situ throughout the flex test in order to detect the occurrence of flex cracking. Capacitance is expected to drop if a crack passes through the electrodes of the capacitor. In-situ monitoring of capacitance was necessary since some cracked capacitors exhibit recovery after completion of the flex test. Along with each capacitance measurement the strain on board was measured to determine the strain level that caused failure. Optical microscopy of cross-sectioned capacitors was used to verify conclusions of in-situ capacitance measurements.

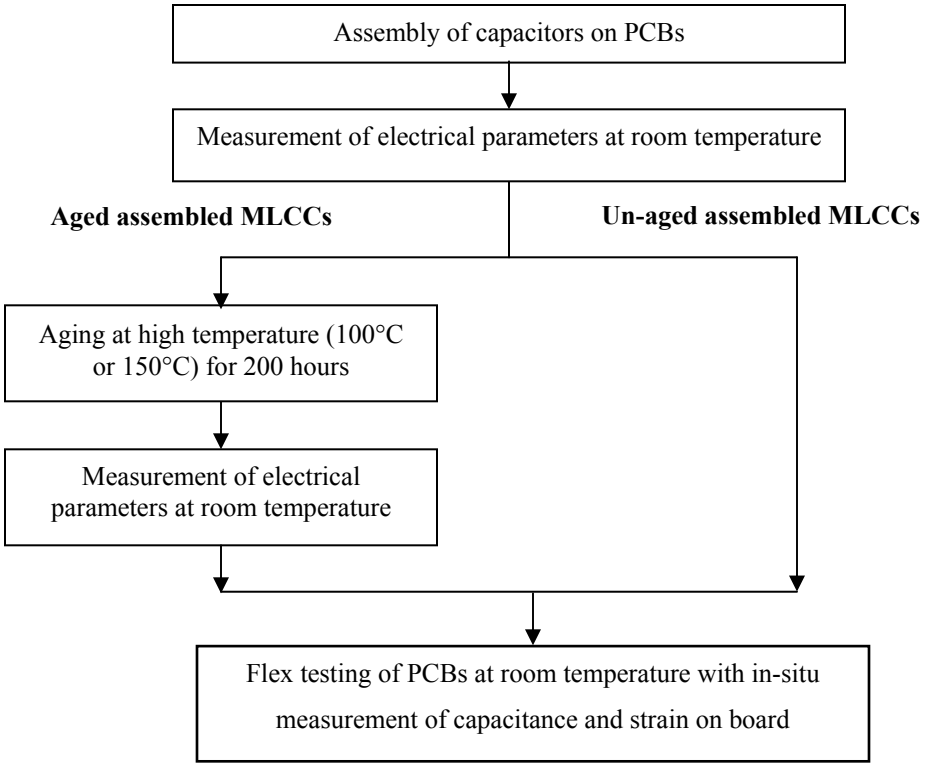

Figure 24. Flow chart of experimental procedure of the flex testing of aged and un-aged assembled MLCCs.

2.4.2 Experimental design of the flex testing of aged assembled MLCCs

The capacitors were assembled on the PCBs using eutectic tin-lead solder (Sn37Pb) and a lead-free solder (Sn3.0Ag0.5Cu), to compare the effect of assembly with lead-free solder to eutectic tin-lead solder. MLCCs with both standard and flexible terminations were considered, as presented in the sample matrix shown in Table 9. MLCCs from two manufacturers, AVX and Syfer, were studied. Some boards were aged at one of two elevated temperatures, 150°C and 100°C, for 200 hours. In addition, boards which were not aged were tested to compare flex cracking susceptibility with those that were aged. All capacitors had a capacitance of 0.1 μF and a rated voltage of 100 volts and contained

X7R dielectric. They were of 1812 size, which means that their length was 0.18 in (4.6 mm) and their width was 0.12 in (3 mm). The thickness of the capacitors was 0.03 in (0.8 mm). The number of capacitors tested in each condition is shown in Table 9.

Table 9. Sample matrix for flex testing of MLCCs at different aging conditions.

Aging condition	Solder material	End termination	Manufacturer	# of boards	# of capacitors
150°C, 200 hours	Sn37Pb	Flexible	Syfer	1	24
	Sn3.0Ag0.5Cu	Flexible	Syfer	1	24
	Sn37Pb	Standard	AVX	1	24
	Sn3.0Ag0.5Cu	Standard	AVX	1	24
100°C, 200 hours	Sn37Pb	Flexible	Syfer	1	24
	Sn3.0Ag0.5Cu	Flexible	Syfer	1	24
	Sn37Pb	Standard	AVX	1	24
	Sn3.0Ag0.5Cu	Standard	AVX	1	24
Un-aged	Sn37Pb	Flexible	Syfer	2	48
	Sn3.0Ag0.5Cu	Flexible	Syfer	2	48
	Sn37Pb	Standard	AVX	2	48
	Sn3.0Ag0.5Cu	Standard	AVX	2	48

2.4.3 Experimental results of the flex testing of aged assembled MLCCs

In this section, flex testing results are presented to examine the effects of isothermal aging, solder material, and end termination construction. The failure criterion for flex cracking was chosen to be a 10% drop in capacitance relative to the nominal value of capacitance according to the manufacturer's datasheet.

2.4.3.1 Flex test results for aged assembled standard-termination MLCCs

Flex cracking results for standard-termination MLCCs assembled on boards with eutectic tin-lead solder and Sn3.0Ag0.5Cu lead-free solders are presented in Figure 25 and Figure 26, respectively. These plots also enable comparison of un-aged capacitors with those aged at 100°C and 150°C. MLCCs mounted on boards with lead-free solder showed less susceptibility to flex cracking than capacitors mounted with eutectic tin-lead solder. For MLCCs assembled with tin-lead solder, isothermal aging, even at 150°C, had little influence on flex cracking. In the case of lead-free solder, after aging at 150°C the susceptibility to flex cracking increased compared to un-aged MLCCs. Consequently, results for boards assembled with tin-lead and lead-free solder are significantly closer to each other after aging at 150°C.

Table 10 lists the Weibull parameters for these distributions. It is clear that scale parameters for MLCCs assembled with lead-free solder are much larger than those for MLCCs assembled with tin-lead solder, which confirms that MLCCs assembled with tin-lead solder are more susceptible to flex cracking. In addition, for lead-free solder after aging at 150°C the scale parameter decreased considerably, approaching the values for tin-lead solder.

Table 11 shows the strain on board at 10% failure due to flex cracking of MLCCs with standard terminations and the 95% confidence bounds of strain at 10% failure. This parameter was selected as a metric for comparing the effects of solder alloy and aging, although the conclusions are valid over a wide range of cumulative percent failure. For MLCCs assembled with tin-lead solder, un-aged and aged capacitors showed very similar

results in flex testing and our analysis shows that the 95% confidence intervals for different aging conditions overlap.

In the case of assembly with lead-free solder, capacitors aged at 150°C showed the lowest strain at 10% failure in flex testing, whereas the strain at 10% failure appears to be highest for capacitors aged at 100°C. However, Table 11 shows that 95% confidence intervals of strain at 10% failure for un-aged and 100°C-aged capacitors overlap, whereas the 95% confidence interval for capacitors aged at 150°C does not overlap with that of the un-aged and 100°C-aged capacitors. This confirms that, to a level of 95% confidence, the true value of strain at 10% failure for MLCCs aged at 150°C is lower than that for un-aged and 100°C-aged capacitors in lead-free assemblies.

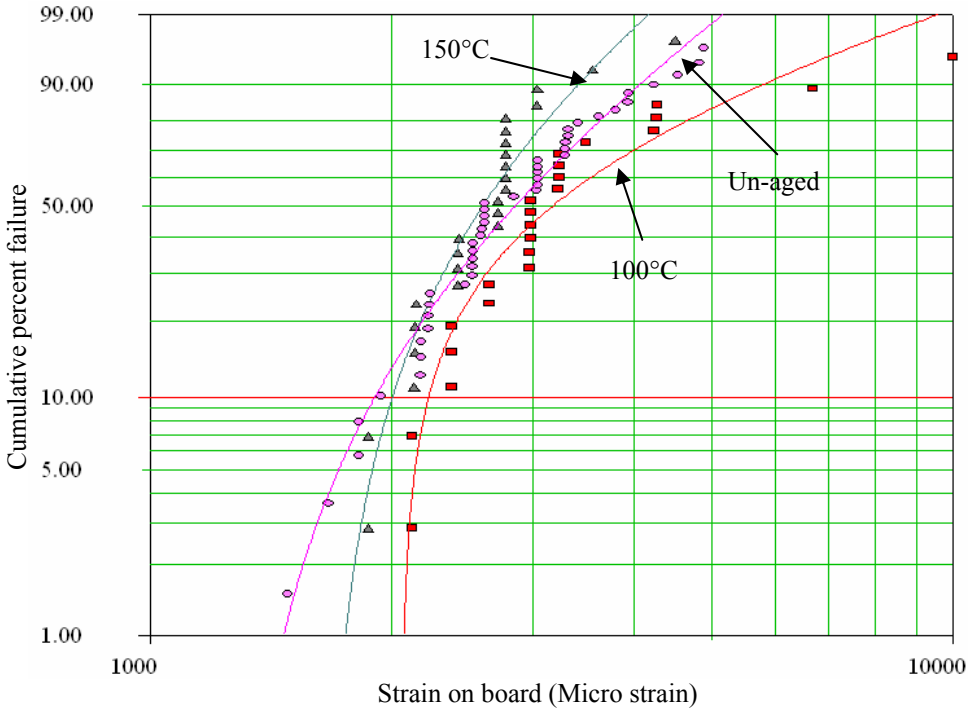

Figure 25. Cumulative percent failure due to flex cracking as a function of strain on board for MLCCs assembled with tin-lead solder, tested without aging or after aging at either 100°C or 150°C.

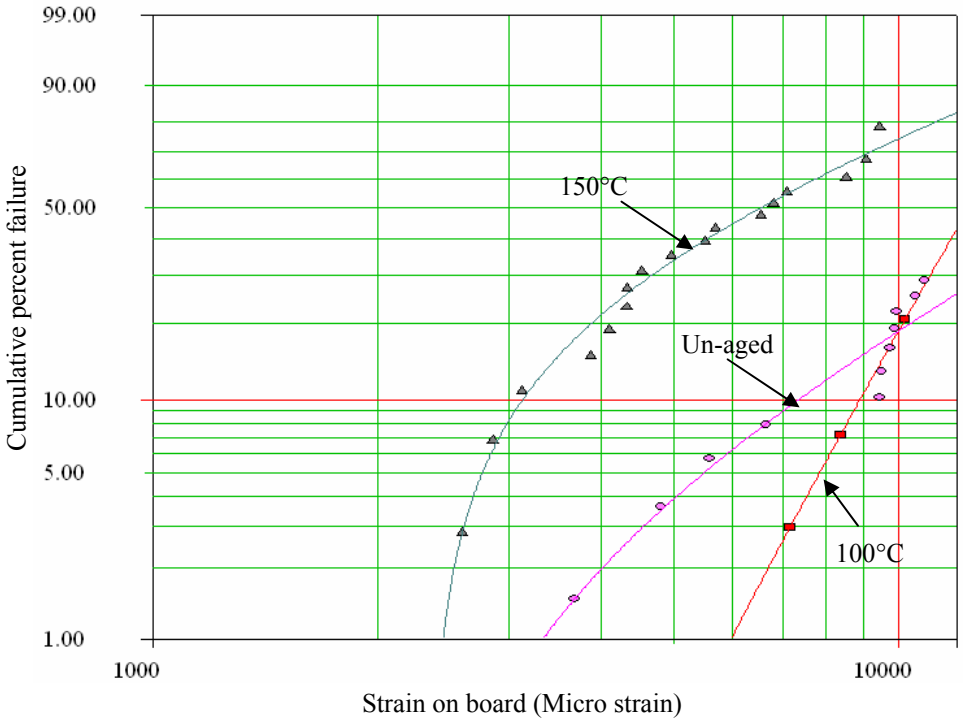

Figure 26. Cumulative percent failure due to flex cracking as a function of strain on board for MLCCs assembled with lead-free solder, tested without aging or after aging at either 100°C or 150°C.

Table 10. Weibull distribution parameters for flex test results on MLCCs with standard terminations.

Solder material	**Aging condition**	**Shape parameter (β)**	**Scale parameter (η)**	**Location parameter (γ)**
Sn37Pb	150°C, 200 hours	1.9	1148	1646
	100°C, 200 hours	1.0	1612	2057
	Un-aged	2.1	1898	1253
Sn3.0Ag0.5Cu	150°C, 200 hours	1.1	5803	2359
	100°C, 200 hours	5.0	12204	1121
	Un-aged	1.7	20597	2052

Table 11. The strain on board at 10% failure due to flex cracking of MLCCs with standard terminations and 95% confidence bounds of strain at 10% failure.

Solder material	Aging condition	Upper bound of strain at 10% failure at 95% confidence level	Strain on board at 10% failure (με)	Lower bound of strain at 10% failure at 95% confidence level
Sn37Pb	150°C, 200 hours	2210	2000	1870
	100°C, 200 hours	2480	2220	2120
	Un-aged	2140	1910	1730
Sn3.0Ag0.5Cu	150°C, 200 hours	4270	3140	2680
	100°C, 200 hours	10940	8890	7270
	Un-aged	10470	7350	5390

Aging at high temperature may cause material properties of capacitors, solder, and boards to change. However, any changes in board and capacitor material properties should happen similarly in both tin-lead and lead-free assemblies. Therefore, the difference in aging affects on tin-lead and lead-free assemblies were related to another factor, such as dissimilar stress relaxation of solders.

After aging assemblies at high temperature for 200 hours, they were cooled down to room temperature. This cooling process generates residual compressive stress inside the capacitor body. In order to calculate residual compressive stress inside capacitor body, thermal contraction of the PCB and capacitor during the cool-down process is taken into account as follows:

$$\sigma_{Compressive} = E\,\Delta CTE\,\Delta T = E_{Capacitor}\,(CTE_{Board} - CTE_{Capacitor})\,(T_{aging} - T_{Room}),$$

where $\sigma_{Compressive}$ is residual compressive stress inside the capacitor body, $E_{Capacitor}$ is the elastic modulus of the capacitor body, CTE_{Board} and $CTE_{Capacitor}$ are coefficients of thermal expansion for the board and capacitor, respectively, and ΔT is the temperature change from aging temperature (T_{aging}) to room temperature (T_{Room}). Table 14 and Table 15 include thermo-mechanical properties of materials used in above equation. The compressive residual stress, for both tin-lead and lead-free solders, is calculated to be 89 MPa after aging at 150°C and 54 MPa after aging at 100°C.

This calculation indicates the upper limit for the compressive stresses, based on the differential expansion between the board and the dielectric of the capacitor. The actual compressive stresses which develop due to reflow may be lower because some stress relaxation may occur during and after cool-down (to a greater extent in the eutectic

solder), and the solder and end termination may deform and thus reduce the stresses transmitted to the dielectric.

2.4.3.2 Flex test results for aged assembled flexible-termination MLCCs

Flex cracking results of flexible-termination MLCCs mounted on boards with eutectic tin-lead and lead-free solders are summarized in Table 12. In general, flexible-termination MLCCs are much less susceptible to flex cracking than standard-termination MLCCs. For flexible-termination MLCCs assembled with lead-free solder, no failures were observed in flex testing for boards with any aging condition. In contrast, for MLCCs assembled with tin-lead solder some failures were observed during flex testing of boards aged at different temperatures. In the case of MLCCs aged at 150°C, the cumulative percent failure was four times higher in comparison with un-aged MLCCs, although it was still much less than what was observed for standard-termination MLCCs.

Table 12. Number of failures due to flex cracking and the strain on board at failure for MLCCs with flexible terminations.

Aging condition	Solder materials	End termination	# of capacitors	# of failures	Strain on board at failure (με)
150°C, 200 hours	Sn37Pb	Flexible	24	2	7,500 and 7,800
	Sn3.0Ag0.5Cu	Flexible	24	0	No failure
100°C, 200 hours	Sn37Pb	Flexible	24	1	8,300
	Sn3.0Ag0.5Cu	Flexible	24	0	No failure
Un-aged	Sn37Pb	Flexible	48	1	7,700
	Sn3.0Ag0.5Cu	Flexible	48	0	No failure

2.5 Discussion on the flex test results

Experimental results showed that MLCCs assembled with lead-free solder are less susceptible to flex cracking compared to MLCCs assembled with eutectic tin-lead solder. There are three factors which have been considered to explain this difference: solder fillet geometry, solder solidification temperature, and mechanical properties of the solder materials.

2.5.1 Solder fillet geometry analysis of assembled MLCCs

In order to investigate the solder fillet geometries, four parameters were measured for cross-sectioned MLCCs: the maximum height of the solder fillet, solder wetting angle at the top of the fillet, stand-off height of the capacitor body above the solder pad surface,

and capacitor misalignment in longitudinal direction relative to solder pads. Figure 27 gives the definition of solder height, solder wet angle, stand-off height, and misalignment, which were measured for cross-sectioned MLCCs. As shown in Table 13, based on the mean values and standard deviations for solder height, stand-off height, and solder wetting angle, the differences in solder fillet parameters for tin-lead and lead-free solders were not statistically significant. After comparing solder fillet geometrical parameters for MLCCs assembled with eutectic tin-lead solder and lead-free solder, it appears that the capacitor misalignment is almost 3-times bigger for MLCCs assembled with lead-free solder than those assembled with eutectic tin-lead solder, except for MLCCs from AVX (see Table 13).

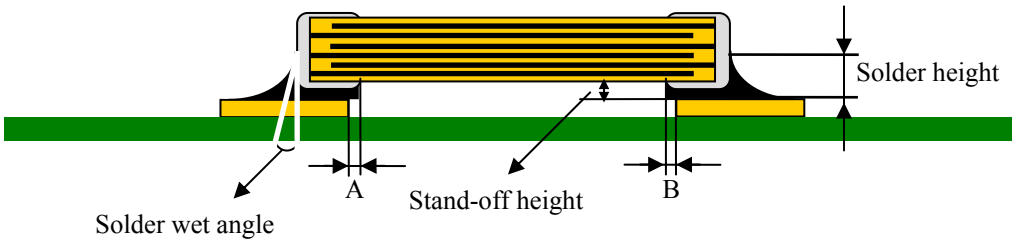

Misalignment = (A-B) / 2

Figure 27. Definition of solder fillet geometrical parameters.

Table 13. Solder fillet geometry analysis of assembled MLCCs on PCBs with X7R dielectric. Values for each parameter are the average of number of samples analyzed for each type of capacitor and values in parentheses are standard deviations.

Solder	Size	Manf.	No. of caps cross-sectioned	Solder height (μm)	Solder wetting angle (degree)	Standoff height (μm)	Capacitor misalign-ment (μm)
Sn37Pb	1812	Kemet	9	569 (75)	9 (3)	59 (13)	22 (19)
Lead-free	1812	Kemet	9	538 (122)	7 (3)	53 (15)	65 (66)
Sn37Pb	1812	Vishay	6	494 (99)	7 (1)	40 (12)	16 (15)
Lead-free	1812	Vishay	6	451 (105)	7 (3)	52 (12)	42 (28)
Sn37Pb	1812	AVX	3	593 (12)	10 (2)	32 (6)	58 (46)
Lead-free	1812	AVX	3	610 (51)	8 (2)	37 (13)	10 (11)
Sn37Pb	0805	Kemet	6	532 (74)	11 (5)	51 (6)	19 (8)
Lead-free	0805	Kemet	6	608 (45)	9 (3)	56 (9)	67 (61)

2.5.2 Finite element analysis of compressive residual stress inside MLCCs after solder assembly process

The second factor which was examined to explain the difference between flex cracking susceptibility of MLCCs assembled with tin-lead and lead-free solders is solder solidification temperature. During the solder reflow process, the printed circuit board and capacitors expand and contract as a result of temperature changes. The coefficient of thermal expansion (CTE) for a barium titanate-based ceramic capacitor was measured to be 9.0 ± 0.6 ppm/°C for the temperature range of 25°C to 200°C. For an FR4 PCB in the plane of the board, the CTE below the glass transition temperature is around 15 ppm/°C,

and the corresponding value above the glass transition temperature is around 20 ppm/°C [63]. Therefore, the FR4 board expands more than the capacitors during the heating phase of the reflow process, especially when the temperature is higher than the glass transition temperature. During solder reflow cool-down, the board and capacitors contract. Before the solder completely solidifies, the amount of stress that is transmitted to the capacitor body is negligible. Below the solidification temperature of the solder when the last remaining liquid has solidified, stresses are transmitted through the solder material to the capacitor body.

The eutectic temperature for tin-silver-copper lead-free solder is 217°C, while the corresponding value for tin-lead solder is 183°C [63]. Therefore, during the cool-down process, the near-eutectic lead-free solder completes solidification at 47°C above the glass transition temperature of the FR4 board (Tg = 170°C), while eutectic tin-lead solder is completely solidified at about 13°C above the glass transition temperature. As a result of this difference, lead-free solder transmits more residual compressive stress to the capacitors than tin-lead solder.

Finite element analysis (FEA) was implemented to calculate residual stress inside the capacitor after the solder reflow cool-down process. A two-dimensional finite element model in ANSYS® was constructed, incorporating half of the capacitor and half of the PCB using two-fold symmetry. Figure 28 shows the geometry of the assembled capacitor used in the FEA model. Table 14 and Table 15 include thermo-mechanical properties of materials used in FEA models. The temperature of the assembly was decreased from the solder solidification temperature to room temperature (25°C). It was assumed that the capacitor at the solidification temperature was in a stress-free condition. Figure 29 shows

the stress distribution after the reflow cool-down process for an MLCC assembled on the PCB with lead-free solder. It was found that the bottom of the capacitor is under compression and the top of the capacitor is in tension, which is in agreement with previously reported results in the literature [37].

The maximum residual compressive stress in the longitudinal direction was calculated to be 75 MPa for a capacitor assembled with tin-lead solder and 92 MPa for a capacitor assembled with lead-free solder. The reason for the different levels of compressive stress originates in the fact that the solidification temperature for the lead-free solder is 217°C, while the corresponding value for the tin-lead solder is 183°C.

This calculation indicates the upper limit for the compressive stresses. The actual compressive stresses which develop due to reflow may be lower because some stress relaxation may occur during and after cool-down (to a greater extent in the eutectic solder). Nevertheless, the calculation does serve to illustrate that there is a difference in the residual compressive stress between the eutectic and lead-free assemblies.

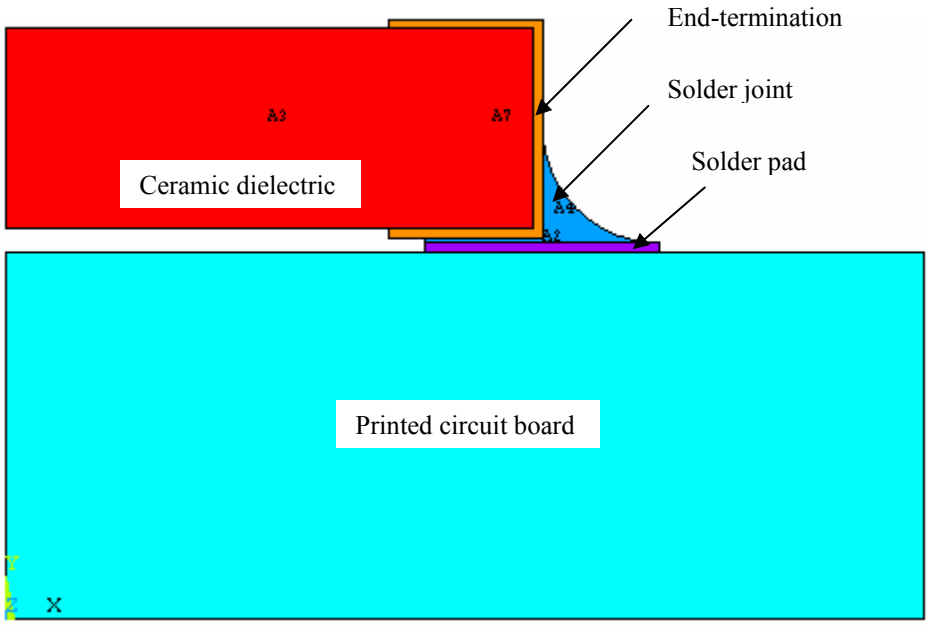

Figure 28. Geometry of the capacitor assembled on a PCB as used in the FEA model. The figure is truncated on the right hand side of the PCB in order to show a magnified view near the capacitor.

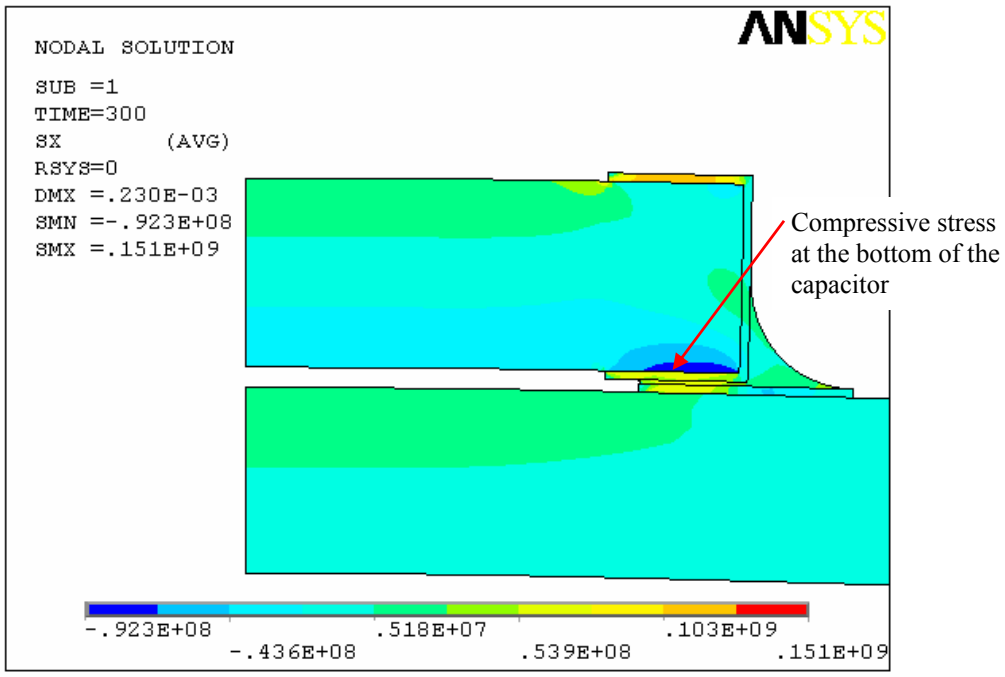

Figure 29. Stress distribution after the solder reflow cool-down process for an MLCC assembled on the PCB with lead-free solder.

Hunt and Dusek [69] showed that the creep rate for both lead-free and tin-lead solders increases with temperature. The secondary creep rate increases by a factor of approximately 100 between 20 and 80°C for lead-free solder. Therefore, aging at elevated temperature causes the solder alloy to creep and reduces the amount of residual compressive stress in MLCCs, especially in the case of lead-free solder when aging is performed at higher temperatures (e.g., 150°C). As a result of the reduction of compressive stresses, a higher cumulative percent failure was obtained during flex testing of MLCCs assembled with lead-free solder and aged at 150°C in comparison to un-aged samples.

Table 14. Thermo-mechanical properties of materials used in finite element analysis.

Material	Elastic modulus (E: GPa)	Poisson ratio (υ)	Reference for elastic modulus and Poisson ratio values	Coefficient of thermal expansion (CTE: ppm/°C)	Reference for CTE values
FR4 board	14	0.16	[64]	See Table 15	[63]
Copper pad	117	0.35	[64]	17.6	[68]
Eutectic tin-lead solder	36	0.38	[63] [33]	24.7	[37]
Tin-silver-copper lead-free solder	40	0.35	[65] [33]	22.4	[63]
Capacitor end-termination	73	0.30	[66]	17.6	[68]
X7R dielectric	105	0.34	[67] [66]	9.0	Our measurement

Table 15. Coefficient of thermal expansion (CTE) used for FR4 PCB in finite element analysis [63].

FR4 PCB	**CTE in the plane of PCB (ppm/°C)**	**CTE in vertical direction to PCB (ppm/°C)**
Below glass transition temperature (Tg = 170°C)	15.8	85
Above glass transition temperature	20	400

2.5.3 Finite element analysis of assembled MLCCs under PCB flexure

The last factor which was considered to explain the difference between flex cracking susceptibility of MLCCs assembled with tin-lead and lead-free solders is solder mechanical properties. Finite element analysis (FEA) was conducted of ceramic capacitors under PCB flexure in a four-point bend configuration. A two-dimensional FEA model in ANSYS® was constructed, considering half of the capacitor and half of the PCB using two-fold symmetry. Figure 28 shows the geometry of the assembled capacitor used in the FEA model. A symmetry boundary condition was applied in the vertical centerline of the capacitor and PCB. A vertical displacement was applied to the PCB at the location of the load ram, while zero vertical displacement was applied to the PCB at the location of the support ram (see Figure 12), to represent the four-point bend test. This FEA model was constructed using both eutectic tin-lead and SnAgCu lead-free solder. The plastic stress-strain relation for both solder materials was implemented in the FEA model [70]:

$$\sigma = C_{pl}\varepsilon_{pl}^{\ n},$$

where C_{pl} and n are constants, given in Table 16 for both solder materials.

Table 16. Plastic model constants for eutectic tin-lead and tin-silver-copper lead-free solders calculated for 25°C and tensile loading [70].

Solder alloy	**C_{pl} (MPa)**	**n**
Eutectic tin-lead solder	138	0.243
Tin-silver-copper lead-free solder	112	0.278

Figure 30 shows the first principal stress distribution for an MLCC assembled on the PCB with lead-free solder. The FEA modeling shows that PCB bending applies a tensile stress to the body of the capacitor which is highest along the bottom side. This result is

consistent with the previous studies reported in the literature [36] [37]. The maximum stress location inside the capacitor body was found to be at the bottom of the capacitor near the edge of the termination margin. The location of the maximum stress obtained by the FEA model matches with the location of crack initiation inside the flex tested capacitors, as was shown in Figure 5.

Comparison of the FEA results of MLCCs assembled with lead-free and tin-lead solder showed that the maximum stress inside the capacitor for an MLCC assembled with tin-lead solder is higher than lead-free solder. The first principal stress near the edge of the end-termination for an MLCC assembled with tin-lead solder was calculated to be 313 MPa, while the corresponding value for an MLCC assembled with lead-free was 267 MPa for the applied load ram displacement of 10 mm. This value was the maximum load ram displacement which was applied to the PCBs during flex testing. The higher stress for tin-lead solder is due to higher strain hardening in comparison with tin-silver-copper lead-free solder [70], which causes more stress to be transmitted to the capacitor body.

Flex cracking is the result of tensile stresses inside the capacitor body exceeding the fracture strength of the ceramic. However, as discussed in section 2.5.2, there are residual compressive stresses inside the capacitor body after the solder reflow cool down process, which mitigate the tensile stresses generated by PCB bending. These residual compressive stresses are higher for MLCCs assembled with lead-free solder than for MLCCs assembled with tin-lead solder. Therefore, greater PCB deflection is required for MLCCs assembled with lead-free solder for the tensile stresses to reach the ceramic fracture strength, in order to overcome the higher residual compressive stress. If bending

produces a net tensile stress greater than the fracture strength of the dielectric, a crack will initiate at the bottom of the capacitor at the edge of the end termination.

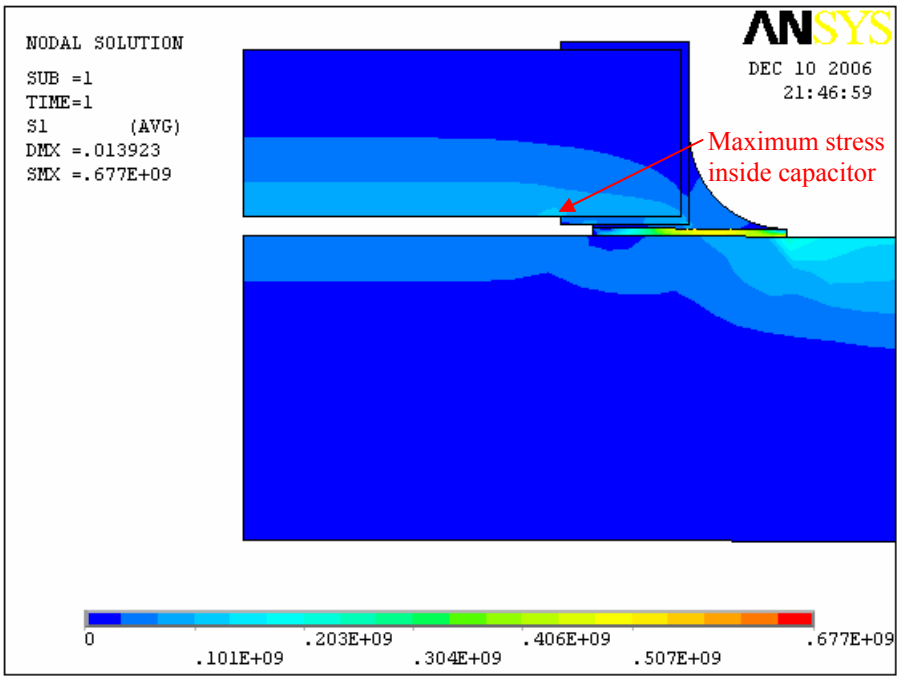

Figure 30. First principal stress distribution for an MLCC assembled on the PCB with lead-free solder. The stress distribution is shown for a PCB deflection of 5 mm at the load ram location (see Figure 12).

2.6 Compositional analysis of MLCCs

Compositional analysis for dielectric, electrodes, and end-terminations of MLCCs was conducted using environmental scanning electron microscopy (E-SEM) combined energy dispersive X-ray spectroscopy (EDX). Figure 31 shows EDX mapping of electrodes and dielectric for an 1812 size MLCC from AVX with X7R dielectric. Electrodes are made of nickel, which mean this MLCC is a base metal electrode (BME)

MLCC and dominant materials in dielectric are barium and titanate. Figure 32 shows EDX mapping of end-termination layers for an 1812 size MLCC from AVX with X7R dielectric. When an MLCC is made of base metal electrodes, end-terminations are made of copper and usually plated with nickel and tin.

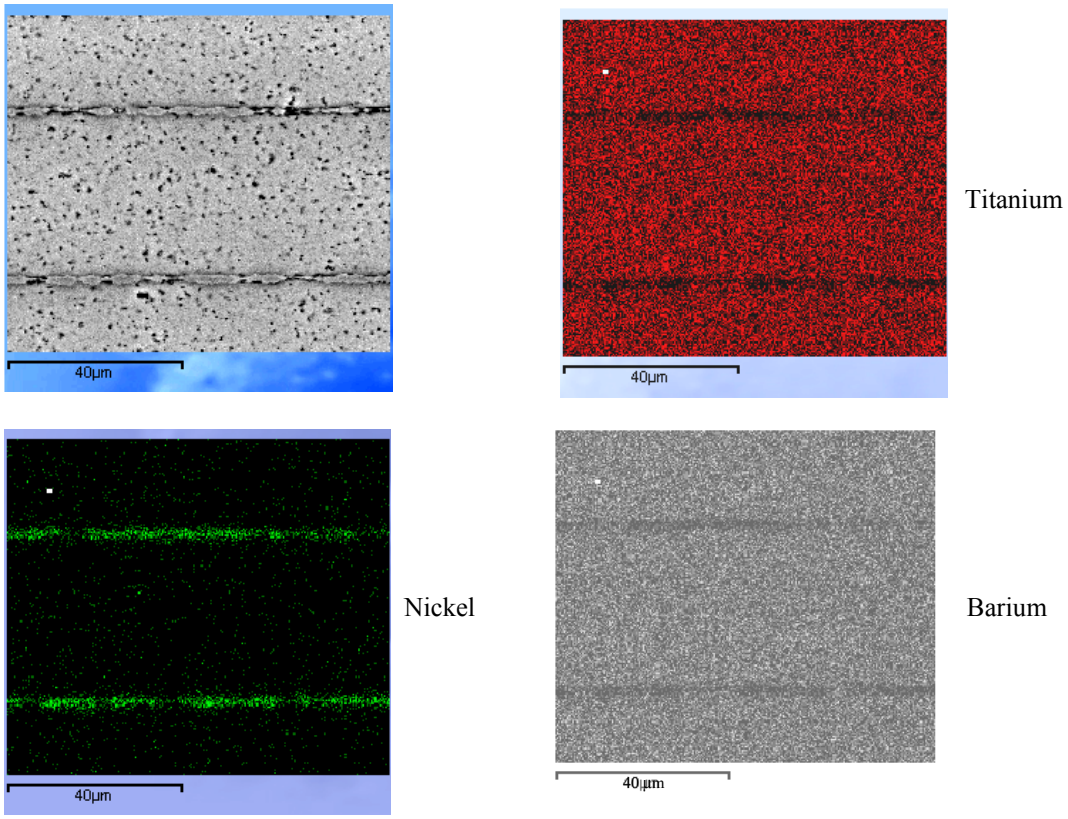

Figure 31. EDX mapping of electrodes and dielectric for an 1812 size standard-termination MLCC from AVX with X7R dielectric.

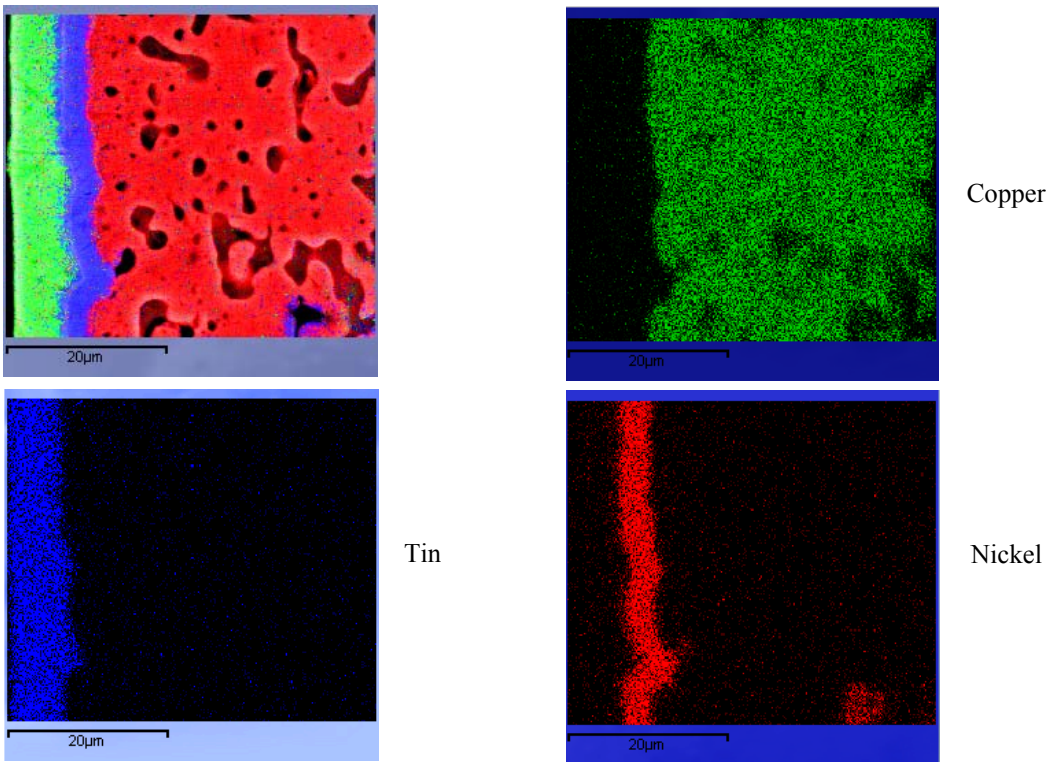

Figure 32. EDX mapping of end-termination layers for an 1812 size standard-termination MLCC from AVX with X7R dielectric.

Table 17 summarizes compositional analysis of MLCCs with standard and flexible terminations from different manufacturers. Standard-termination MLCCs with X7R dielectric from Kemet, AVX, and TDK are made of base metal electrodes (nickel). Standard-termination MLCCs with X7R dielectric from Vishay and MLCC with C0G dielectric from Kemet are made of precious metal electrodes (silver-palladium).

Table 17 also shows the weight percent of barium, titanium, and oxygen for X7R dielectric type. By converting weight percents to atomic percents, it is found that the ratio of barium and titanium to oxygen is 1 to 3. It can be concluded that the dielectric material is barium titanate ($BaTiO_3$).

Flexible-termination MLCCs from Syfer are made of silver-palladium electrodes, indicating a precious metal electrode (PME), while flexible-termination MLCCs from AVX are made of nickel electrodes, indicating a base metal electrode (BME). End-termination of the flexible-termination MLCCs from AVX is made of four layers, copper, silver-loaded epoxy, nickel, and tin. While in the end-termination of the flexible-termination MLCCs from Syfer, no copper layer exist between the epoxy layer and the capacitor body and the silver-loaded epoxy is directly attached to the capacitor body.

Table 17. Summary of compositional analysis of MLCCs.

Manuf.	Electrode type	Electrode materials	End-term. type	End-term. materials	Diele. type	Dielectric materials
Kemet	BME	Ni	Standard	Cu-Ni-Sn	X7R	Barium (55%), Oxygen (25%), Titanium (20%)
AVX	BME	Ni	Standard	Cu-Ni-Sn	X7R	Barium (55%), Oxygen (25%), Titanium (20%)
TDK	BME	Ni	Standard	Cu-Ni-Sn	X7R	Barium (55%), Oxygen (25%), Titanium (20%)
Vishay	PME	Ag-Pd	Standard	Ag-Ni-Sn	X7R	Barium (48%), Oxygen (23%), Titanium (19%), and Bismuth (10%)
Kemet	PME	Ag-Pd	Standard	Ag-Ni-Sn	C0G	Neodymium (34%), Oxygen (28%), Titanium (20%), Barium (10%), Bismuth (5%), lead (2%), and other materials (<1%)
Syfer	PME	Ag-Pd	Flexible	Silver loaded epoxy-Ni-Sn	X7R	Barium (55%), Oxygen (25%), Titanium (20%)
AVX	BME	Ni	Flexible	Cu-Silver loaded epoxy-Ni-Sn	X7R	Barium (55%), Oxygen (25%), Titanium (20%)

2.7 Failure analysis of the flex tested MLCCs

Destructive and non-destructive failure analysis techniques were used to confirm cracking of MLCCs, which were identified as failures in flex tests. These failure analysis

techniques are also applied to confirm that those capacitors, which did not show failure during flex testing, do not contain any crack or defect inside them. Destructive technique that is used include cross-sectioning of tested MLCCs followed by optical microscopy. Non-destructive techniques, such as impedance spectroscopy and X-ray radiography, were also applied to detect cracks in capacitors.

2.7.1 Destructive technique for detection of flex cracks in MLCCs

Destructive technique that is used include cross-sectioning of tested MLCCs followed by optical microscopy. In this destructive technique, the tested assembled capacitors on PCBs were potted in the mixture of resin and hardener. After the potting materials became hard, the potted samples were cross-sectioned close to the capacitor body. Then the cross-section was made flat and smooth by using six different grit sizes of sand papers. The grit size of sand papers, which were used, include: 120, 240, 400, 600, 800, and 1200. The 120-grit size is the coarsest sand paper and 1200-grit size is the finest sand paper that is used. The grinding with sand paper was continued until it was reached the plane of the interest. Finally, alumina powder mixed with water over polishing equipment was used for final fine polishing of the surface. Then using optical microscope, the picture of the cross-sectioned MLCCs was obtained. The optical microscopy pictures were used to detect cracks or defects inside capacitors, conducting compositional and structural analysis of MLCCs, and finding solder fillet geometrical parameters.

Figure 33 shows a flex crack in a cross-sectioned standard-termination MLCC with size 1812 and X7R dielectric manufactured by Kemet. This capacitor showed a capacitance drop during in-situ monitoring when tested in a four-point bend test. For

cracked standard-termination MLCCs, flex cracks were always found inside the capacitor body, passing through the dielectric and electrodes. This can lead to short circuits when standard-termination MLCCs fail in field applications. For all cross-sectioned samples listed in Table 13, it was confirmed that for those MLCCs which showed a capacitance drop during in-situ measurement of flex testing, there was a crack inside the capacitor body. For all those MLCCs which did not exhibit a capacitance drop during in-situ measurement, no crack was found inside the capacitor body as expected.

Figure 34 shows a flex crack in a cross-sectioned standard-termination MLCC with an open mode design and size 1812 and X7R dielectric manufactured by TDK. This capacitor showed a capacitance drop during in-situ monitoring when tested in a four-point bend test. For standard-termination MLCCs with open mode design, flex cracks, which start from an end termination at a cute angle only cross electrodes originating from the same termination and don't cause shorting between opposing electrodes. Since there is no leakage current increase associated with a typical open-mode flex cracking there is no localized heating and, therefore, no chance for a catastrophic failure.

Figure 35 shows a crack in the solder joint of a flexible-termination MLCC manufactured by Syfer and tested in a four point bend test. This capacitor showed capacitance drop during in-situ monitoring when tested in a four point bend test. The capacitance recovered at the end of the test, when board was brought back to no-bend condition. For all failed flexible-termination MLCCs, cracks were found at the interface of the solder joint and end-termination or in the polymer layer of the end-termination, not inside the capacitor body as for standard-termination MLCCs. This causes flexible-termination MLCCs to fail in open mode, preventing catastrophic failures due to shorting

of a cracked capacitor in field applications. In contrast, in failed standard-termination MLCCs flex cracks were inside the capacitor body, allowing them to fail in short mode in field applications.

Figure 36 shows a crack in the solder joint and end-termination of a flexible-termination MLCC manufactured by AVX and tested in a four point bend test. This capacitor showed capacitance drop during in-situ monitoring when tested in a four point bend test. The capacitance recovered at the end of the test, when board was brought back to no-bend condition. For this failed flexible-termination MLCC, crack were found at the interface of the solder joint and end-termination at the bottom of the capacitor and then crack moved into the polymer layer of the end-termination and caused rupture of the polymer layer as shown in Figure 36.

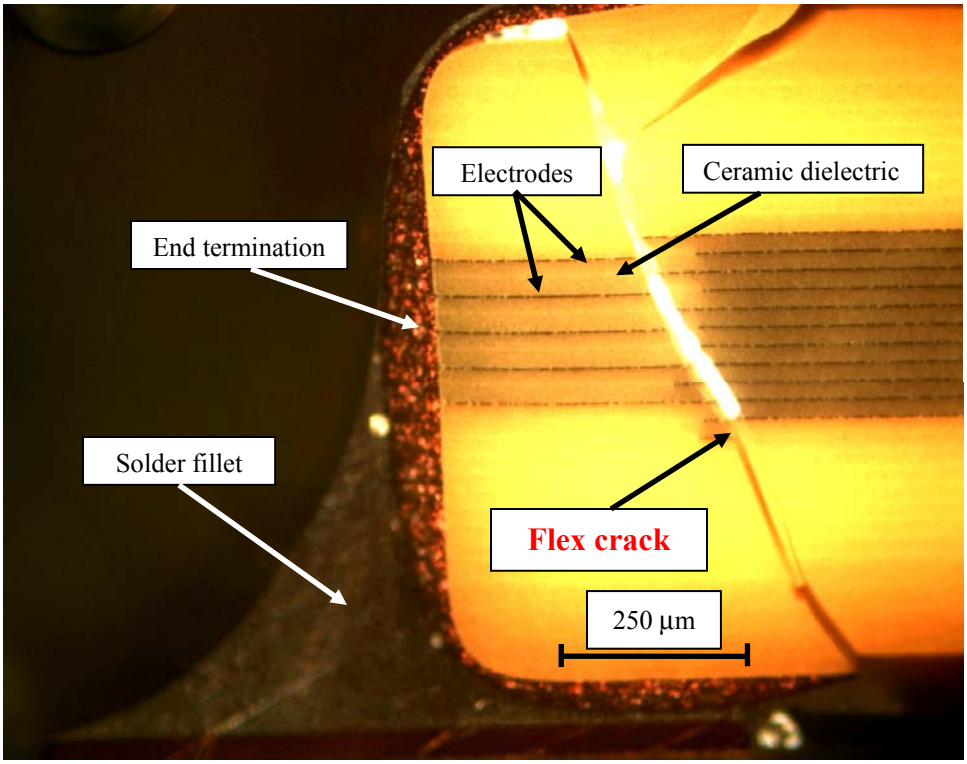

Figure 33. Flex crack in a standard-termination MLCC with size 1812 and X7R dielectric manufactured by Kemet.

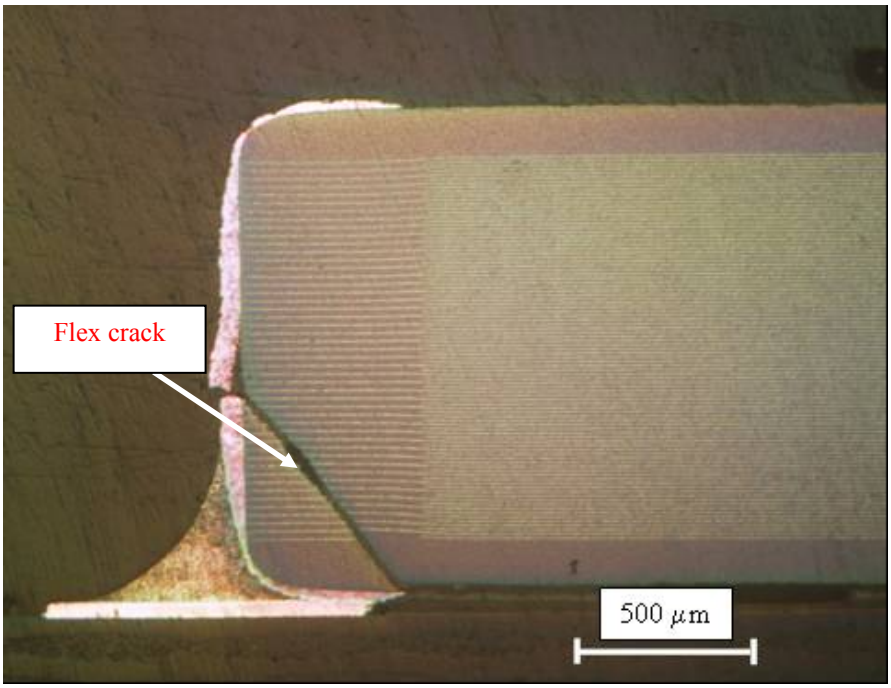

Figure 34. Flex crack in a standard-termination MLCC with an open mode design and size 1812 manufactured by TDK.

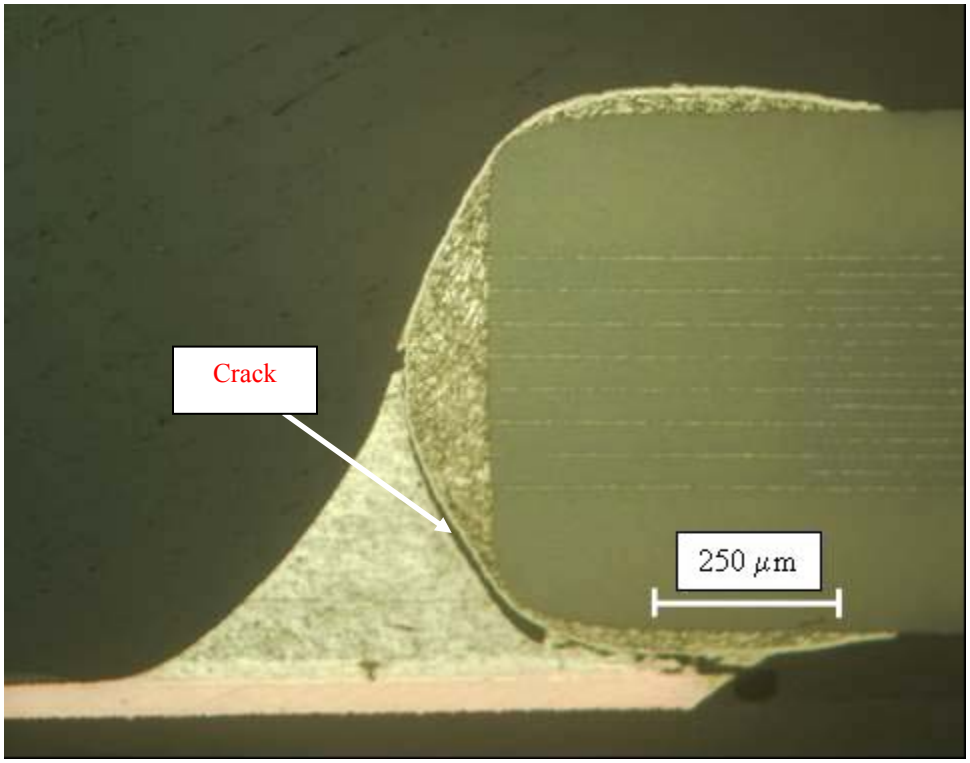

Figure 35. Crack in the solder joint of a flexible-termination MLCC manufactured by Syfer and tested in a four point bend test.

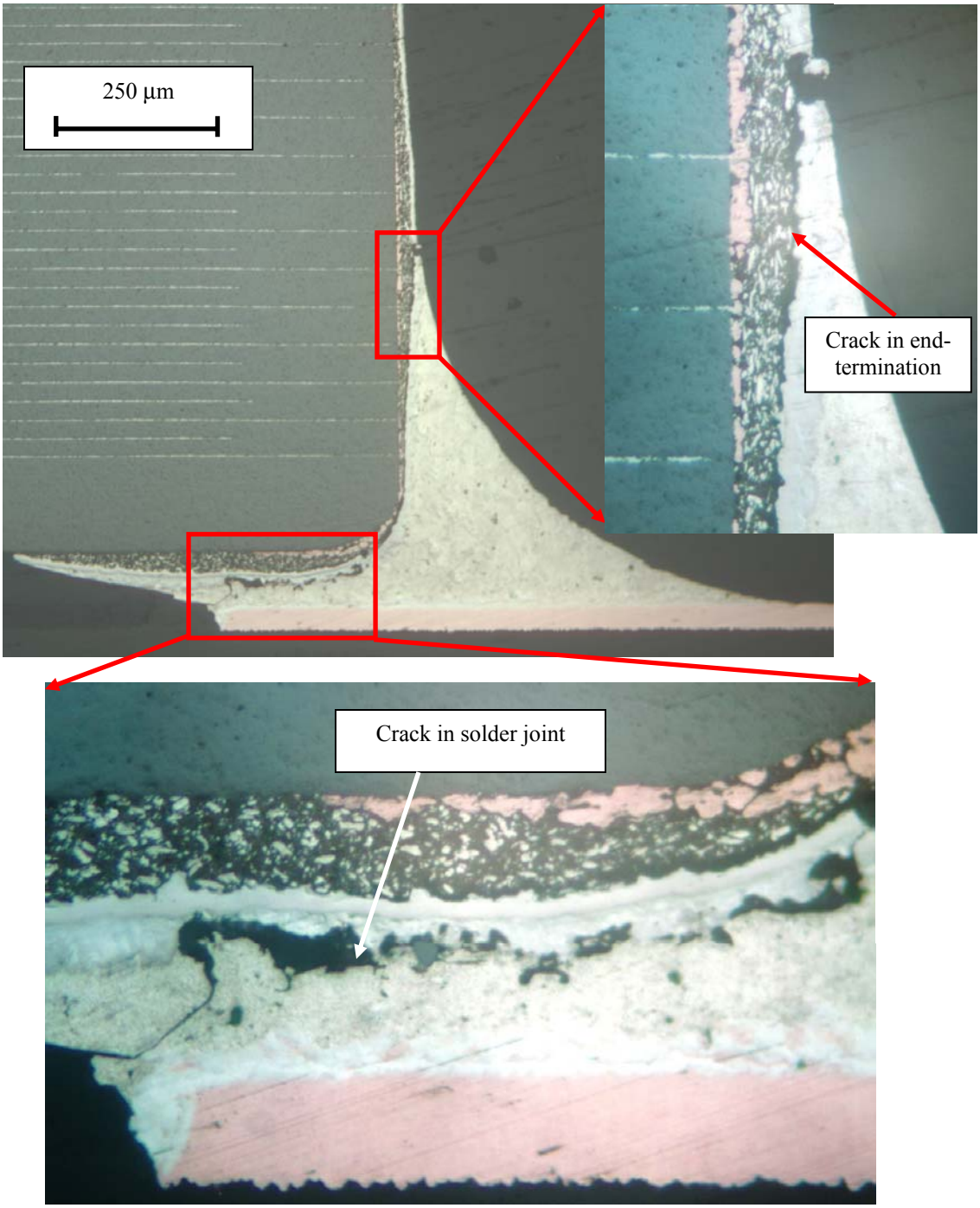

Figure 36. Crack in solder joint and end-termination of a flexible-termination MLCC manufactured by AVX and tested in a four point bend test.

2.7.2 Non-destructive techniques for detection of flex cracks in MLCCs

Defects in multilayer ceramic capacitors are not always detectable by electrical or functional testing. These defects can occur during manufacturing of MLCCs, assembly, handling, testing, and etc. This behavior would be indicative of a "walking-wounded" in field applications, because a crack or defect exists. If a defected capacitor is used in a field application a conductive medium, often atmospheric moisture and ionic contaminants, can penetrate through the crack or defect into the capacitor and cause leakage current of the capacitor to increase. This may also lead to the shorting of the opposing electrodes of the capacitor, ultimately causing catastrophic failure in applications such as those involving high power, in which the short circuit may initiate a fire. There is a need for a technique, especially a non-destructive technique, for screening of multilayer ceramic capacitors.

Non-destructive testing (NDT) for screening of defective MLCCs has been an important objective for users of these components in high reliability applications, as well as for general quality control in mass production. A variety of non-destructive test methods have been reported, including X-ray radiography, scanning acoustic microscopy (SAM), scanning laser acoustic microscopy (SLAM), methanol testing, and impedance spectroscopy. Due to their small inter-layer spacings and large number of interfaces, MLCCs remain a challenge for those seeking an NDT approach to defect detection. In this section, two of non-destructive techniques for detection of flex cracks in MLCCs are applied and their relative merits are discussed.

2.7.2.1 X-ray radiography (two-dimensional and three-dimensional X-ray)

Two-dimensional and three-dimensional (computed tomography scan) X-ray has been applied to detect flex cracks in MLCCs. Figure 37 shows two-dimensional X-ray radiograph of a flex cracked MLCCs. The flex crack is visible at the end-termination of the capacitor. Figure 38 shows three-dimensional X-ray tomography of a flex cracked MLCCs. By using three-dimensional X-ray tomography, different planes inside the capacitor body can be visualized. In Figure 38, the 3-D X-ray picture was cropped by software to be able to visualize the flex crack inside the capacitor body near the edge of the end-termination.

For two-dimensional X-ray radiography, it is difficult to see fine cracks against the projection of the MLCC body; particularly challenging for MLCCs mounted on PCBs with multiple layers and many neighboring components. Three-dimensional X-ray is time-consuming for a large number of samples and it may be difficult to rotate sample if mounted on a PCB with large components near the MLCC.

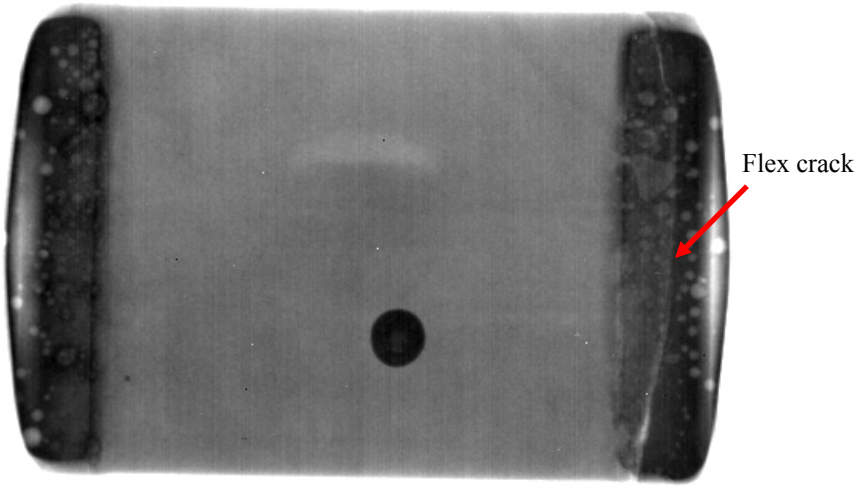

Figure 37. Two-dimensional X-ray radiograph of a flex cracked MLCCs.

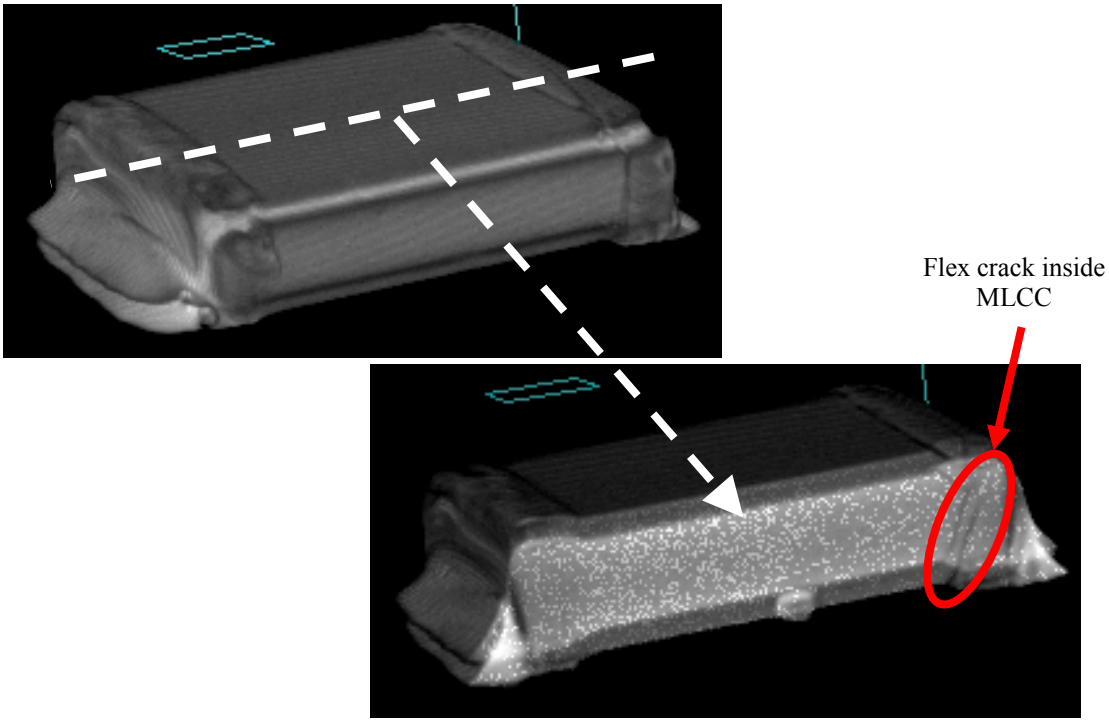

Figure 38. Three-dimensional X-ray tomography of a flex cracked MLCCs.

2.7.2.2 Impedance spectroscopy

Barium titanate ($BaTiO_3$) is used as a dielectric material in multilayer ceramic capacitors. Barium titanate is a piezoelectric material. Due to piezoelectricity of the dielectric material, MLCCs exhibit electromechanical resonances under the influence of a DC bias field. Resonances associated with the length, width, and thickness of the capacitor can be identified using impedance spectroscopy.

Measurements of the capacitor impedance as a function of frequency for good and defective MLCCs under DC bias allow us to detect defects inside MLCCs. Figure 39 compares the impedance spectrum of a cracked MLCC with an MLCC without crack. There are three resonances associated with the length, width, and thickness of the capacitor. MLCCs mounted on a PCB exhibit damping of resonance peaks. The cracked

capacitor exhibits a length resonance with reduced amplitude. Ability to detect defects requires a good reference sample with identical geometry and materials characteristics.

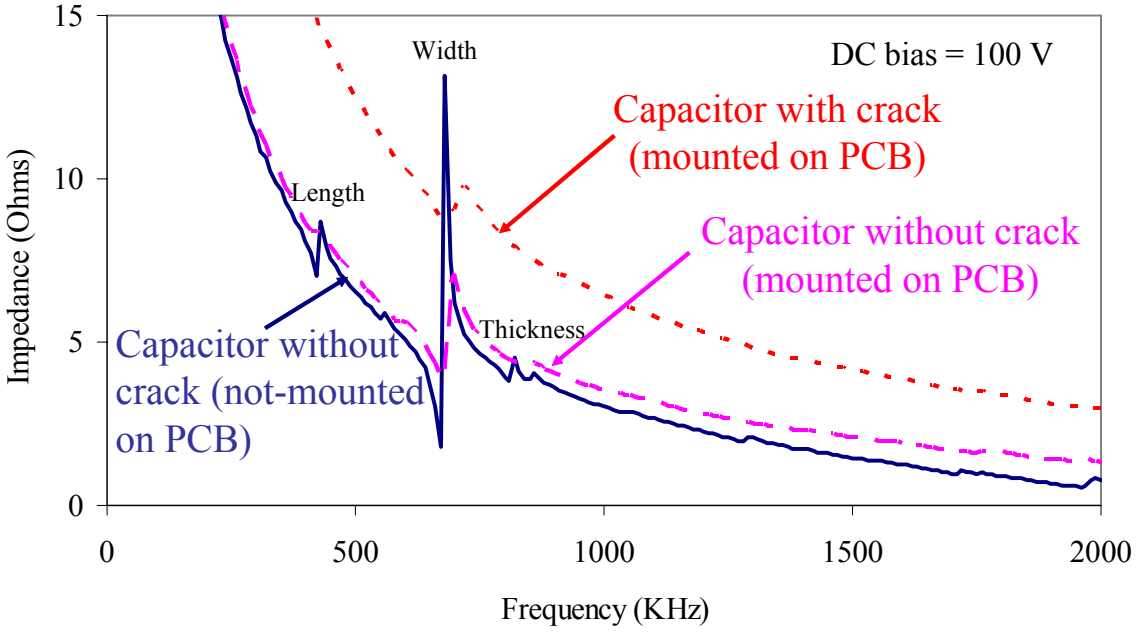

Figure 39. Comparison of the impedance spectrum of a cracked MLCC with an MLCC without crack.

2.8 Conclusions and summary

Experiments were conducted to investigate the effects of different parameters on the flex cracking susceptibility of multilayer ceramic capacitors assembled on PCBs. The design of experiments included MLCCs assembled with lead-free solder (Sn3.0Ag0.5Cu) and eutectic tin-lead solder (Sn37Pb), two different sizes (1812 and 0805), two different dielectric materials (C0G and X7R), two end-termination types (standard termination and flexible termination), two solder assembly processes (convective reflow soldering and wave soldering), and different manufacturers. PCBs were flexed using a four-point bend

test, during which the strain on the board and the capacitance of each MLCC were monitored in order to determine the strain-to-failure. In-situ capacitance measurement provided data on the strain-to-failure. For some failed capacitors, the capacitance recovered after removal of flexure. This behavior could allow an electronic assembly containing a cracked capacitor to pass electrical functional tests, and enter the application environment as a "walking-wounded" part. Eventually, this could lead to a field failure and possibly a fire.

Experimental results showed that MLCCs assembled with lead-free solder are less susceptible to flex cracking compared to MLCCs assembled with eutectic tin-lead solder. This was the trend for all manufacturers included in this study. The discussion provides two factors which make capacitors assembled with lead-free solder less susceptible to flex cracking: the lower tensile stresses which are a result of the differing elastic-plastic mechanical properties of the solder, and the higher residual compressive stresses inside the capacitor body after the solder assembly cool down process, which are a result of the higher solidification temperature for lead-free solder.

Cooling of a capacitor after solder reflow assembly places the capacitor under compressive stress. Because for a higher-melting solder, cooling of assembled capacitors places capacitors under greater compressive stress, a capacitor assembled with a higher-melting solder should require more bending stress to crack. Since the solidus temperature for Sn3.0Ag0.5Cu lead-free solder (about 217°C) is higher than that for eutectic tin-lead solder (183°C), lead-free solder places more residual compressive stresses on a capacitor after assembly than tin-lead solder. Therefore, capacitors assembled with lead-free solder

should require more applied bending stress to crack than those assembled with tin-lead solder.

Finite element analysis (FEA) was conducted of ceramic capacitors under PCB flexure in a four-point bend configuration. Comparison of the FEA results of MLCCs assembled with lead-free and tin-lead solder showed that the maximum stress inside the capacitor for an MLCC assembled with tin-lead solder is higher than lead-free solder. Flex cracking is the result of tensile stresses inside the capacitor body exceeding the fracture strength of the ceramic. However, there are residual compressive stresses inside the capacitor body after the solder assembly cool down process, which mitigate the tensile stresses generated by PCB bending. These residual compressive stresses are higher for MLCCs assembled with lead-free solder than for MLCCs assembled with tin-lead solder. Therefore, greater PCB deflection is required for MLCCs assembled with lead-free solder for the tensile stresses to reach the ceramic fracture strength, in order to overcome the higher residual compressive stress. If bending produces a net tensile stress greater than the fracture strength of the dielectric, a crack will initiate at the bottom of the capacitor at the edge of the end termination.

MLCCs with C0G dielectric had the lowest susceptibility to flex cracking. No failures of C0G capacitors were detected within the range of deflections investigated. This result is attributed to the higher fracture toughness of C0G compared to X7R. Unfortunately, MLCCs with C0G dielectric (EIA Class I) have several drawbacks including higher price and narrow capacitance range. For example, 1812 size capacitors with C0G dielectric are almost twice as expensive as those with X7R dielectric. In addition, the maximum capacitance values for which C0G MLCCs are available are

much lower than those for Class II and III dielectrics, since the dielectric constant of C0G dielectric is significantly lower.

Comparison of flex test results for 1812 and 0805 size MLCCs showed that larger MLCCs are more susceptible to flex cracking. It is therefore highly recommended to use smaller size MLCCs in situations where similar capacitance and rated voltage MLCCs are available, to decrease flex cracking failures, cost and real estate.

Comparison of flex test results of 0805 size standard-termination MLCCs assembled with convective reflow soldering and wave soldering showed similar results. The analysis of flex test results showed that the 95% confidence intervals for MLCCs assembled with reflow and wave soldering overlap.

MLCCs with flexible terminations exhibited much more resistance to flex cracking in comparison to standard-termination MLCCs assembled with both lead-free and tin-lead solders. Flexible-termination MLCCs assembled with lead-free solder did not show any failures up to the level of strain used for testing standard-termination MLCCs. Flexible-termination MLCCs assembled with tin-lead solder showed maximum two failures out of 48 samples tested. Flex cracks in failed flexible-termination MLCCs were found to be at the interface between solder joint and end-termination or in the polymer layer of the end-termination, causing them to fail in open mode in field applications. In contrast, in failed standard-termination MLCCs flex cracks were inside the capacitor body, allowing them to fail in short mode in field applications. For standard-termination MLCCs with open mode design, flex cracks, which start from an end termination at a cute angle only cross electrodes originating from the same termination and don't cause shorting between opposing electrodes.

In order to study the effects of isothermal aging on flex cracking susceptibility of MLCCs, they were aged at high temperature and then tested in a four point bend configuration. Experiments were performed to compare the flex cracking susceptibility of standard- and flexible-termination MLCCs assembled with lead-free solder (Sn3.0Ag0.5Cu) and eutectic tin-lead solder (Sn37Pb), tested without aging or after aging at 100°C or 150°C for 200 hours.

Isothermal aging had much less effect on flex cracking susceptibility of MLCCs assembled with tin-lead solder in comparison with those assembled with lead-free solder. Aging of MLCCs at elevated temperature causes the solder alloy to creep and reduces the amount of residual compressive stress in MLCCs, especially in the case of lead-free solder when aging is performed at higher temperatures (e.g., 150°C). As a result of the reduction of compressive stresses, a higher cumulative percent failure was obtained during flex testing of MLCCs assembled with lead-free solder and aged at 150°C in comparison to un-aged samples. Stress relaxation of the solder, produced by aging the lead-free and tin-lead assemblies for 200 hours at 150°C, partially reduced the difference in flex cracking between the two assemblies, as one would expect from a reduction in the residual compressive stresses.

It is concluded from flex test results of aged MLCCs that even though assembly with lead-free solder reduces the susceptibility to flex cracking, applications for which PCBs may be stored or used at high temperatures for an extended time may increase the risk of MLCC flex-cracking such that the advantages of assembly with lead-free solder are largely negated.

Table 18 summarizes the effect of different parameters on the flex cracking of MLCCs, based on finding of this study. It includes the effect of end-termination, dielectric type, capacitor size, solder material, and solder assembly process. For each parameter different types, which were studied in this work, were compared. In the last column of Table 18, limitations for the type that exhibited more reliable results in flex testing were listed. This table can help in choosing a more reliable MLCC against flex cracking issue by considering different factors and limitations.

Table 18. Summary of the effect of different parameters on flex cracking susceptibility of MLCCs.

Parameter	**Types studied**	**Comparison of susceptibility to flex cracking**	**Limitations**
End-termination	Flexible termination vs. standard termination	Flexible termination more reliable than standard termination	Flexible-termination MLCCs: 1) Higher failures in THB for PME flexible-termination MLCCs 2) Higher cost 3) Limited availability and limited manufacturers (new technology)
Dielectric	C0G (Class I: based on neodymium titanium oxide) vs. X7R (Class II: based on barium titanate)	C0G more reliable than X7R	MLCCs with C0G dielectric: 1) Not available in high capacitance value (smaller dielectric constant for C0G) 2) Higher cost
Capacitor size	0805 vs. 1812	Smaller size more reliable than larger size	Small size MLCCs: 1) Not available in high capacitance value 2) Not available in high rated voltage
Solder material	Lead-free (Sn3.0Ag0.5Cu) vs. eutectic tin-lead (Sn37Pb)	MLCCs assembled with lead-free solder more reliable than MLCCs assembled with tin-lead solder	MLCCs assembled with lead-free solder: Increased susceptibility to flex cracking due to aging at high temperature (150°C) (still less susceptible to flex cracking than MLCCs assembled with tin-lead solder)
Solder assembly process	Convective reflow soldering vs. wave soldering	Similar results between convective reflow soldering and wave soldering	Wave soldering: Thermal shock crack for large size MLCCs

3 Temperature-humidity-bias testing of multilayer ceramic capacitors with standard and flexible terminations

In this section, effects of temperature-humidity-bias (THB) on electrical parameters of multilayer ceramic capacitors with both flexible and standard termination are investigated. There is no published data available of temperature-humidity-bias testing for the new technology flexible-termination MLCCs. Users of this new technology have the concern that long term exposure to moisture cause failure or electrical degradation in flexible-termination MLCCs. In addition, temperature-humidity-bias effects on MLCCs made of precious metal electrode (Ag-Pd) are compared with MLCCs made of base metal electrodes (Ni).

MLCCs can be either precious metal electrode (PME) capacitors or base metal electrode (BME) capacitors. In PME capacitors, electrodes are made of silver-palladium and in BME capacitors, electrodes are made of nickel. MLCCs made of precious metal electrodes (Ag-Pd) are prone to silver migration failure. Silver migration failure of MLCCs is divided into three steps. Step one is the formation of a microscopic path between internal electrodes. This path can be a crack or void which occurs during manufacturing, assembly, or in the application field during life of the ceramic capacitors. Step two involves penetration or existence of moisture and contaminants, such as chlorine ions, into the path. The final step is the silver migration of the electrode materials along the path by an electrochemical process. As a consequence of this, the insulation resistance of the ceramic capacitor decreases and causes the capacitor to fail.

3.1 Experimental procedure

In order to study effects of temperature-humidity-bias on electrical parameters of multilayer ceramic capacitors, PCBs were designed and built using FR4 material. On each PCB, 24 capacitors were assembled by convective reflow soldering using Sn3.0Ag0.5Cu lead-free solder. MLCCs with both standard terminations and flexible terminations were considered in our experimental design. Table 19 shows sample matrix of MLCCs used in temperature-humidity-bias testing. Four MLCC types were considered, two of them are flexible-termination MLCCs and two of them are standard-termination MLCCs. For both end-termination types, MLCCs with precious metal electrodes (PME) made of silver-palladium and MLCCs with base metal electrodes (BME) made of nickel were considered. Manufacturers of MLCCs used in THB testing are AVX, Syfer, and Vishay. All MLCCs are made of X7R dielectric (EIA class II [6]), which main dielectric material is barium titanate ($BaTiO_3$) and all of them are 1812 size.

Table 19. MLCCs with flexible and standard terminations used in temperature-humidity-bias testing.

Capacitor #	End-termination type	Electrode type	Manufacturer	Capacitance (μF)	Dissipation factor
1	Flexible	PME	Syfer	0.1	0.025
2	Flexible	BME	AVX	0.22	0.025
3	Standard	BME	AVX	0.1	0.025
4	Standard	PME	Vishay	0.1	0.025

Figure 40 shows the flow chart of the experimental procedure. The experimental procedure has three main steps, which are conducted in a consecutive manner: 1) temperature cycling, 2) temperature-humidity-bias testing, and 3) baking. MLCCs were first preconditioned with 20 temperature cycles from -55°C to 125°C. Preconditioning included temperature cycling with two different ramp rates, normal temperature cycling with ramp rate of 5°C/minute, and rapid temperature cycling with ramp rate of 50°C/minute. For both kinds of temperature cycling, dwell time was 15 minutes at high and low temperature. In second step, MLCCs were exposed to constant temperature-humidity-bias for 1240 hours. Table 20 shows conditions of temperature-humidity-bias testing of MLCCs. Two environmental conditions were considered, temperature and humidity together (85°C/85% RH) and dry heat (85°C). For each capacitor type, three levels of D.C. voltage bias were considered during testing, rated voltage (50 V), low voltage (1.5 V), and no voltage (0 V). Table 20 also shows test sample size for each condition per each capacitor type that is given in Table 19. Finally, for those set of MLCCs, which were tested in 85°C/85% RH, after exposure to temperature-humidity-bias, they were baked at 85°C for 24 hours.

Table 20. Conditions and sample size for temperature-humidity-bias testing of MLCCs.

Environmental condition	Preconditioning	Applied D.C. voltage bias during testing	Number of samples for each capacitor type given in Table 19
85°C/85% RH (1240 hours)	Normal temperature cycling (Ramp rate 5°C/min.)	Rated voltage (50 V)	10
		Low voltage (1.5 V)	10
		No voltage (0 V)	4
	Rapid temperature cycling (Ramp rate 50°C/min.)	Rated voltage (50 V)	10
		Low voltage (1.5 V)	10
		No voltage (0 V)	4
85°C (1240 hours)	Normal temperature cycling (Ramp rate 5°C/min.)	Rated voltage (50 V)	10
		Low voltage (1.5 V)	10
		No voltage (0 V)	4

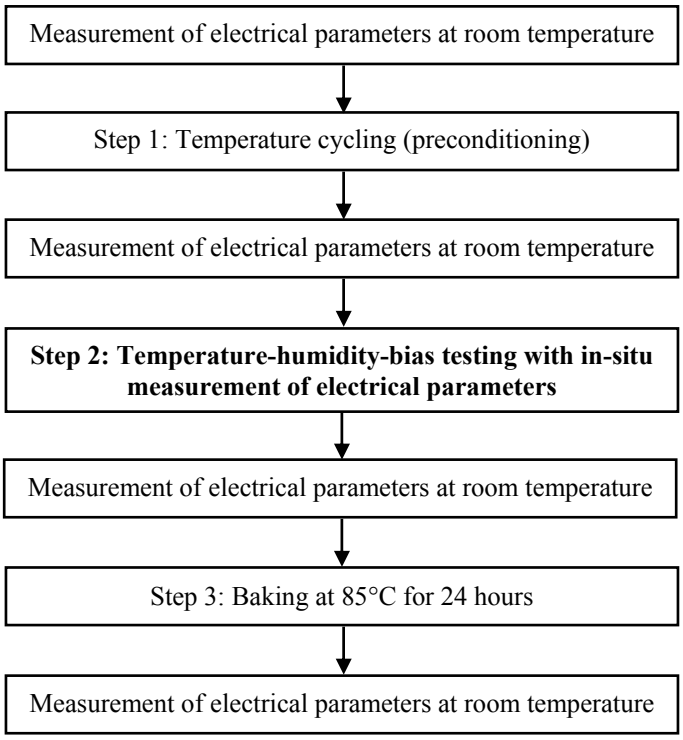

Figure 40. Flow chart of experimental procedure.

Three electrical parameters of capacitors, including, insulation resistance (I.R.), capacitance (C), and dissipation factor (D.F.) were monitored in-situ during THB testing. In addition, as shown in the flow chart of Figure 40, electrical parameters of capacitors were monitored at room temperature before and after each step. Figure 41 shows electrical circuit used for biasing capacitors during THB testing and measurement of electrical parameters of MLCCs. An LCR meter was used to measure capacitance and dissipation factor. They were measured at frequency of 1 KHz and AC voltage of 1 Vrms, according to manufacturer's datasheet of tested MLCCs. A high resistance meter was used to measure insulation resistance. Insulation resistance for all MLCCs was measured at rated voltage (50 V) after charge time of two minutes, according to

manufacturer's datasheet [71]. In this setup, 96 capacitors were tested together and electrical parameters for each capacitor were monitored once in 200 minutes. In order to limit leakage current in case of capacitor shorting during THB testing, resistors with value of 1 MΩ were used in series with each capacitor. A Labview program was developed to control LCR meter, high resistance meter, and switches for measurement of electrical parameters.

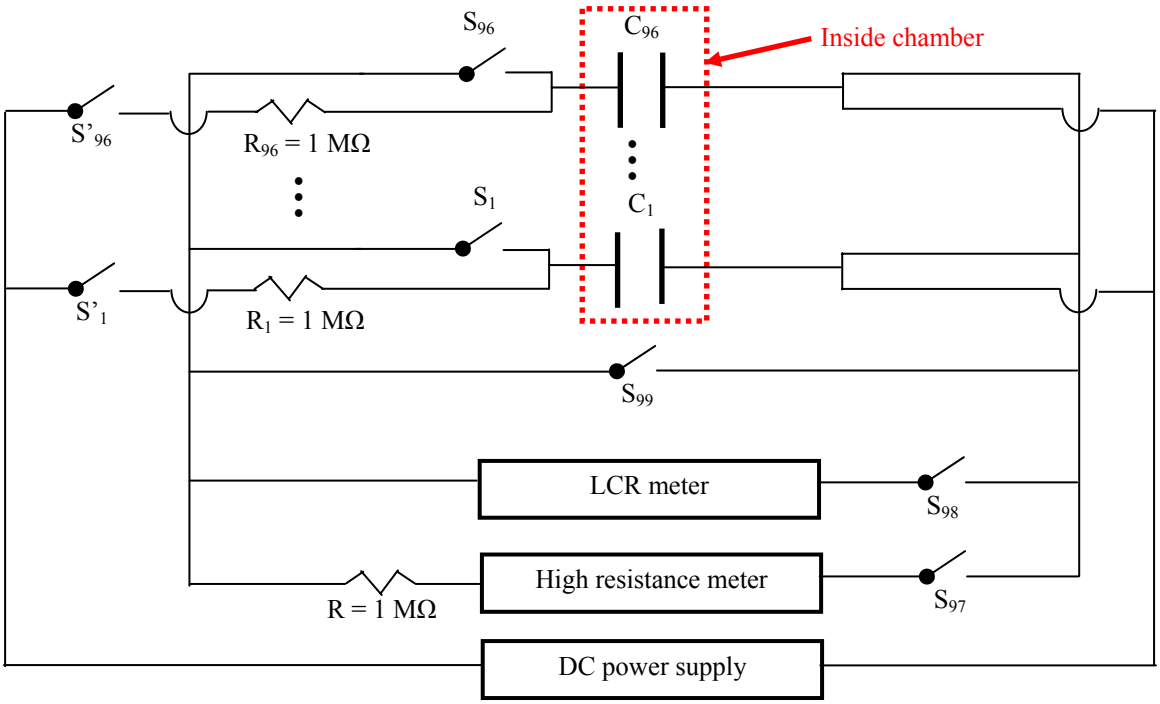

Figure 41. Electrical circuit used for biasing and measurement of electrical parameters of MLCCs during temperature-humidity-bias testing.

3.2 Experimental results

In this section, results of electrical parameters measurements during THB testing are presented. Three electrical parameters of MLCCs, including, insulation resistance (I.R.), capacitance (C), and dissipation factor (D.F.) were monitored in-situ during THB testing.

By defining the failure criterion for each of these electrical parameters, number of failures for each condition per each capacitor type is determined.

3.2.1 Experimental results of THB testing (85°C/85% RH) of MLCCs preconditioned with normal temperature cycling

In this section, results of electrical parameters measurements during testing in 85°C/85% RH for MLCCs preconditioned with normal temperature cycling with ramp rate of 5°C/min are presented. Figure 42 shows an example of the in-situ insulation resistance measurements of a flexible-termination MLCC with precious metal electrodes during testing in 85°C/85% RH and 50 V bias preconditioned with normal temperature cycling. The failure criterion for insulation resistance (I.R.) was defined as an I.R. drop to less than 10^7 Ω during THB testing and having at least 5 occurrences of I.R. value less than 10^7 Ω. For this MLCC, insulation resistance after 850 hours of testing in 85°C/85% RH drops to a value close to 1 MΩ, which is the value of the series resistor used in experimental circuit and does not recover after dropping to close to 1 MΩ.

Figure 43 shows the in-situ measurements of the capacitance for the same MLCC, which its I.R. value shown in Figure 42. The failure criterion for capacitance (C) was defined as the absolute value of capacitance change during THB testing relative to initial measurements to be greater than 10% and having at least 5 occurrences during testing. For this MLCC, an increase in capacitance value at 850 hours, which showed I.R. drop to a value close to 1 MΩ, is observed and after this instabilities can be observed in capacitance value. However, the changes in capacitance where within ±10% of the initial value and it is not considered as a failure in capacitance.

Figure 44 shows the in-situ measurements of the dissipation factor for the same MLCC, which its I.R. value shown in Figure 42. The failure criterion for dissipation factor (D.F.) was defined as D.F. increase to greater than two times the nominal value and having at least 5 occurrences during testing. The nominal value for dissipation factor according to manufacturer's datasheet for all capacitors used in this study was 0.025. For this MLCC, an increase in dissipation factor value at 850 hours, which showed I.R. drop, was observed and later it showed intermittent values higher than failure criterion (0.05) and was considered as failure in dissipation factor.

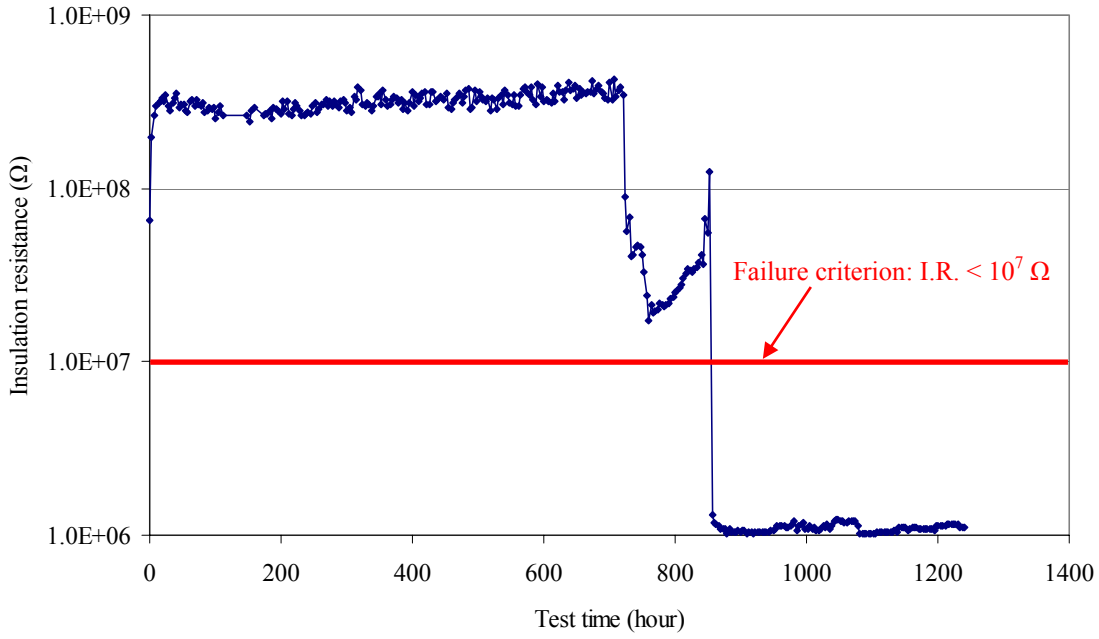

Figure 42. Insulation resistance of a flexible-termination MLCC with precious metal electrodes during testing in 85°C/85% RH biased at 50 V preconditioned with normal temperature cycling.

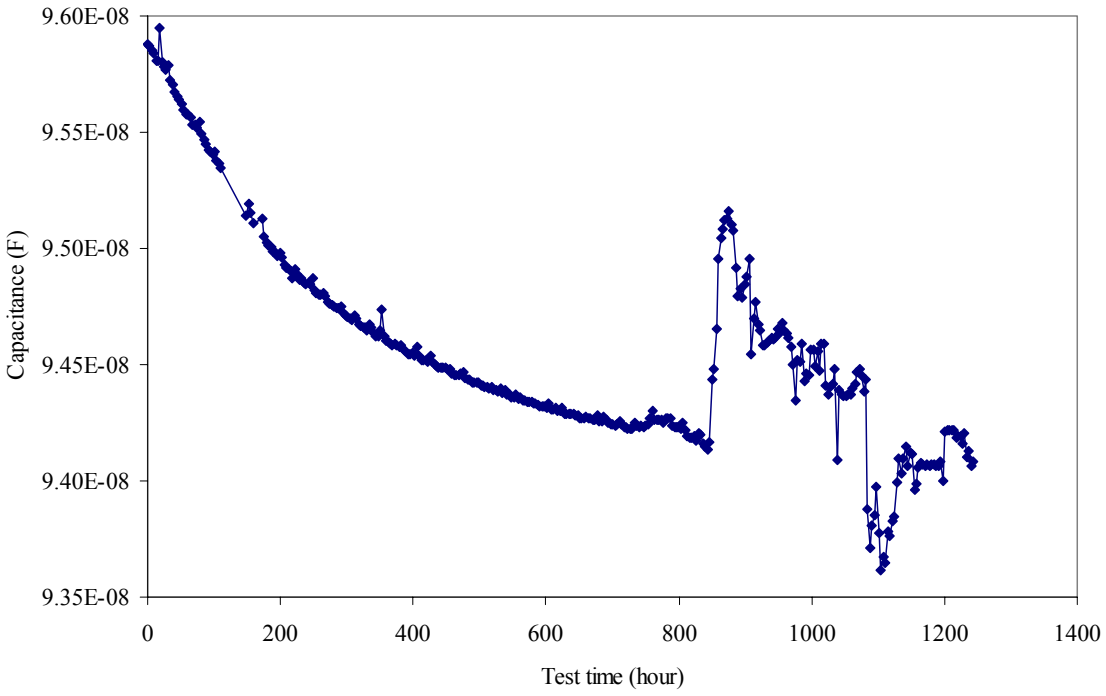

Figure 43. Capacitance of a flexible-termination MLCC with precious metal electrodes during testing in 85°C/85% RH biased at 50 V preconditioned with normal temperature cycling.

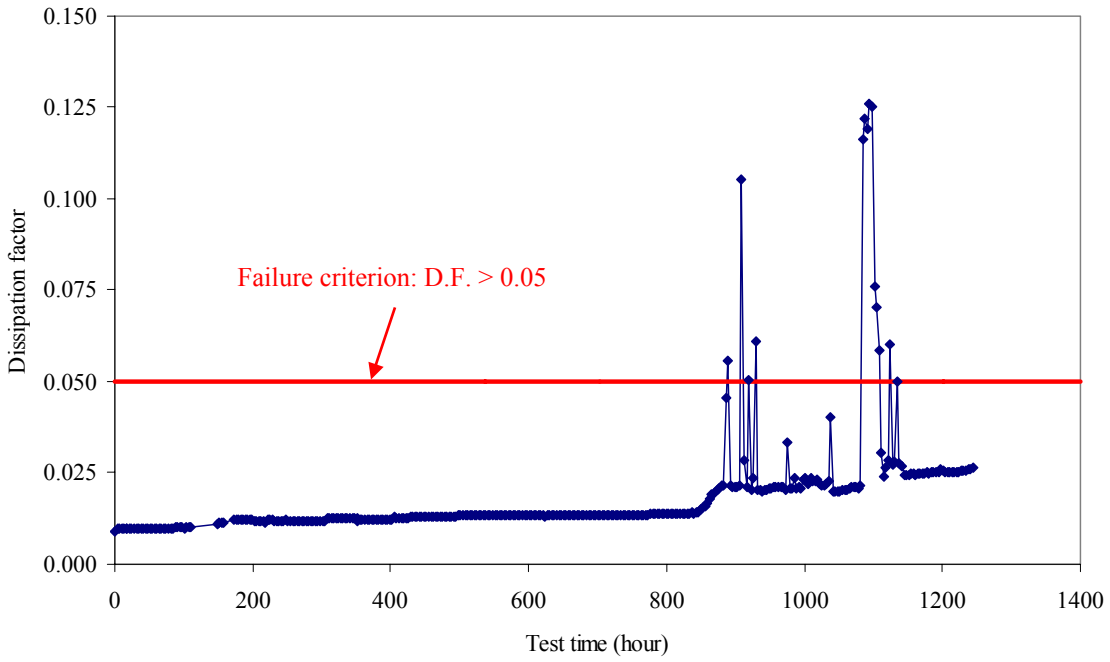

Figure 44. Dissipation factor of a flexible-termination MLCC with precious metal electrodes during testing in 85°C/85% RH biased at 50 V preconditioned with normal temperature cycling.

Figure 45 shows the in-situ insulation resistance measurements of a standard-termination MLCC with precious metal electrodes during testing in 85°C/85% RH with normal temperature cycling preconditioning and no voltage bias applied during testing. For this MLCC, insulation resistance shows a lot of intermittent failures and I.R. drops to less than failure criterion value (10^7 Ω). However, measurement at room temperature after 85°C/85% RH testing showed that I.R. value was recovered and it is not a permanent failure.

For all MLCCs, during in-situ measurement of insulation resistance, rated DC voltage (50 V) was applied for 120 seconds per each measurement. The rated DC voltage was

applied for measurement of insulation of those MLCCs with no DC voltage bias too. During 1240 hours of testing in 85°C/85% RH condition, about 360 measurements of insulation resistance for each capacitor was conducted. Therefore, for these MLCCs with no bias, totally 12 hours rated DC bias was applied.

Figure 46 shows the in-situ capacitance measurement and Figure 47 shows the in-situ dissipation factor for the same MLCC, which its I.R. value shown in Figure 45. Although this capacitor shows failure in insulation resistance, it did not fail in capacitance and dissipation factor values. Capacitance of this capacitor shows aging over time but still remains within the specifications.

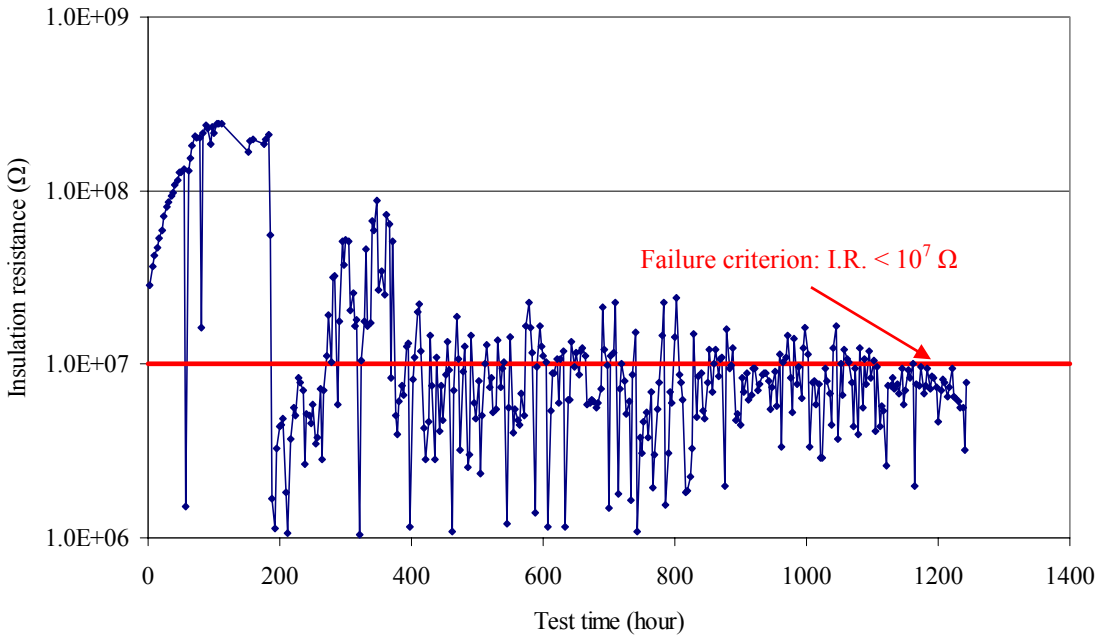

Figure 45. Insulation resistance of a standard-termination MLCC with precious metal electrodes during testing in 85°C/85% RH with no bias preconditioned with normal temperature cycling.

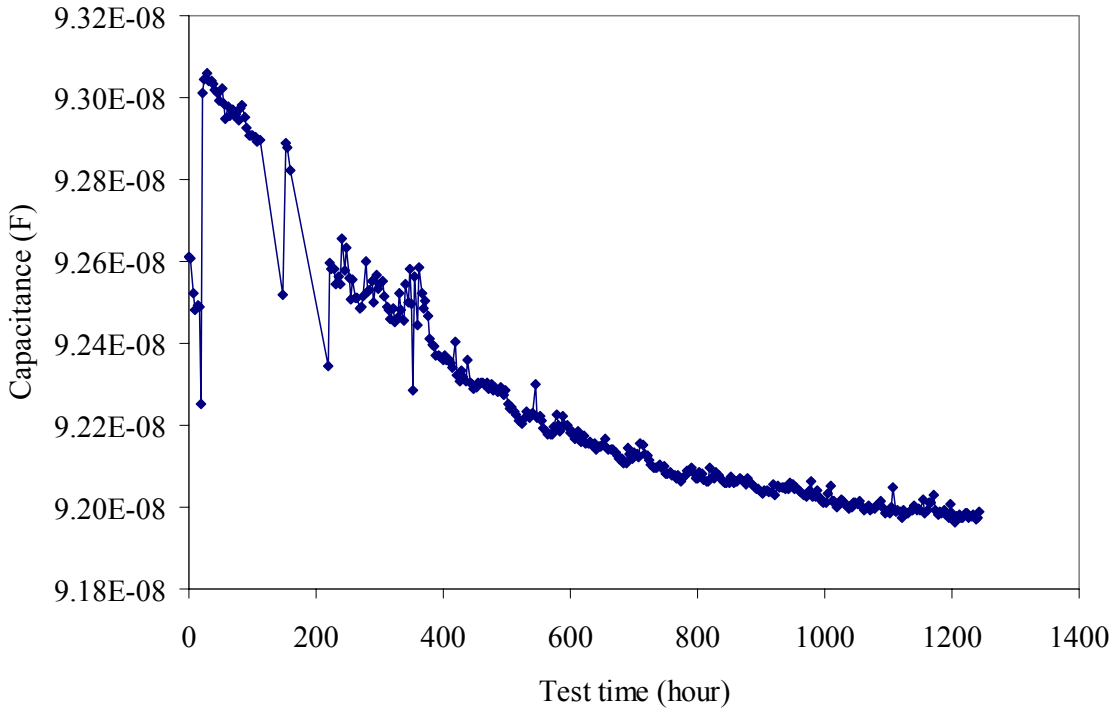

Figure 46. Capacitance of a standard-termination MLCC with precious metal electrodes during testing in 85°C/85% RH with no bias preconditioned with normal temperature cycling.

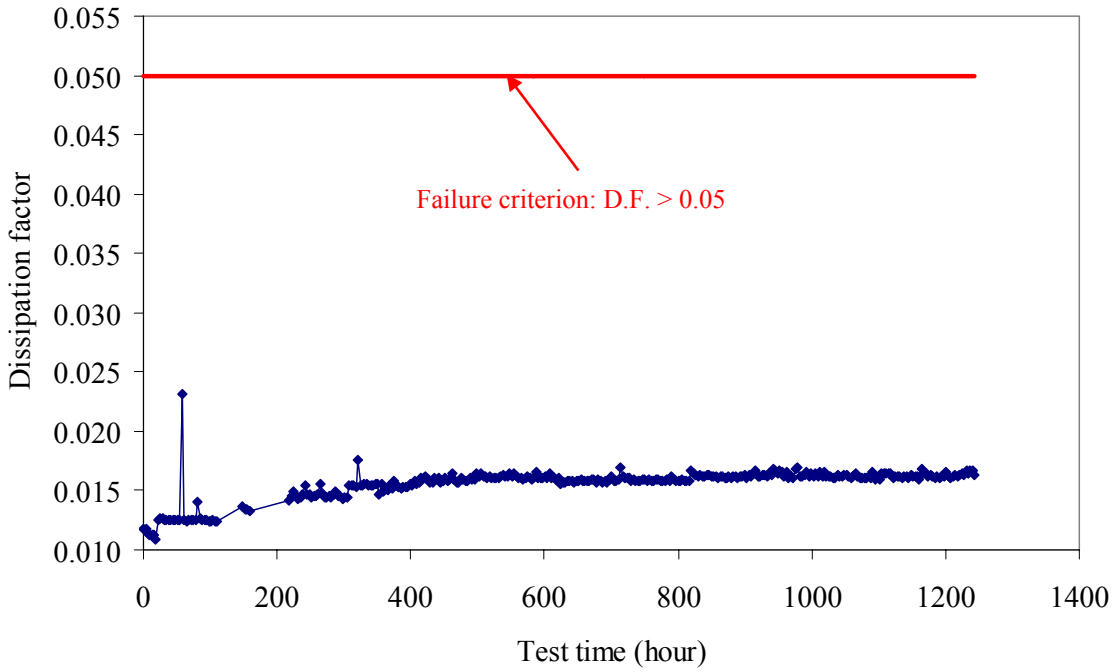

Figure 47. Dissipation factor of a standard-termination MLCC with precious metal electrodes during testing in 85°C/85% RH with no bias preconditioned with normal temperature cycling.

Figure 48 shows insulation resistance values of a flexible-termination MLCC with base metal electrodes during testing in 85°C/85% RH biased at 50 V preconditioned with normal temperature cycling. It is observed that insulation resistance of this capacitor does not drop during 1240 hours testing in 85°C/85% RH biased at 50 V and it is stable. In contrast to the MLCCs with precious metal electrodes, none of the MLCCs with base metal electrodes failed during testing in 85°C/85% RH.

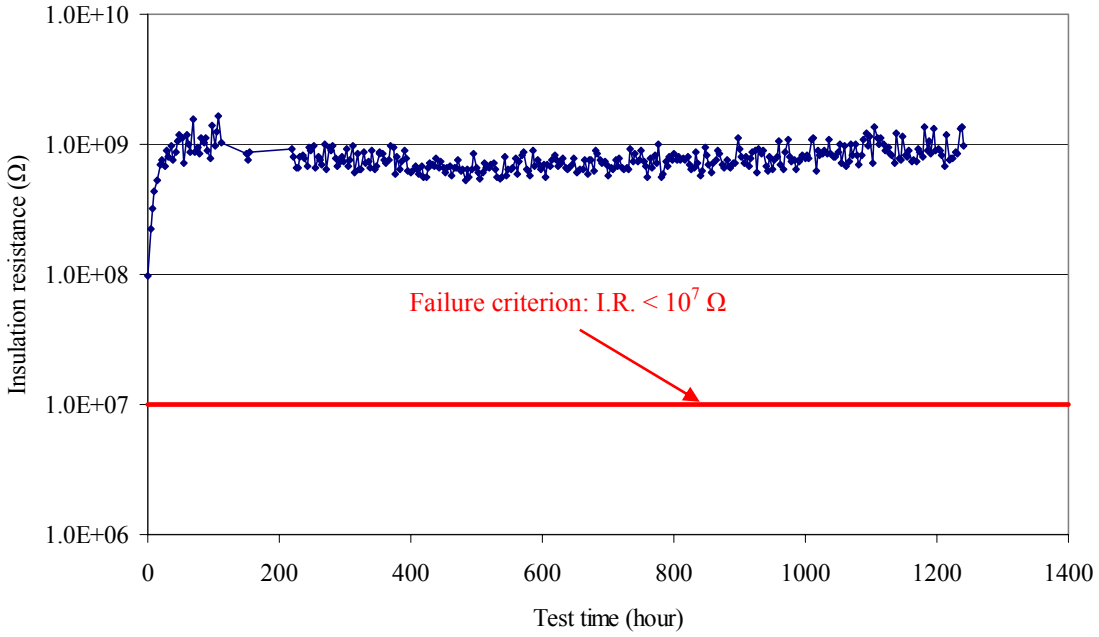

Figure 48. Insulation resistance of a flexible-termination MLCC with base metal electrodes during testing in 85°C/85% RH biased at 50 V preconditioned with normal temperature cycling.

Table 21 shows number of failures in MLCCs in 85°C/85% RH testing preconditioned with normal temperature cycling. All failures were found to be in MLCCs with precious metal electrodes made of silver-palladium and MLCCs with base metal electrodes made of nickel did not exhibit any failure. Flexible-termination MLCCs with precious metal electrodes biased showed the highest failure ratio among all tested MLCCs and 6 out of 10 samples failed during 85°C/85% RH testing based on in-situ measurements of the insulation resistance.

Table 22 shows the time-to-failure for failed MLCCs in 85°C/85% RH testing preconditioned with normal temperature cycling. The time-to-failure for each electrical

parameter (insulation resistance, capacitance, and dissipation factor) is given separately. It is shown in Table 22 that some capacitors which failed in insulation resistance, they did not fail in capacitance and dissipation factor. However, all capacitors which exhibited failure in capacitance or dissipation factor, also exhibited failure in insulation resistance.

Although in-situ measurements during 85°C/85%RH testing of MLCCs preconditioned with normal temperature cycling indicated failures in insulation resistance of 10 MLCCs out of 96 samples, measurements at room temperature after 85°C/85%RH test completion showed only four MLCCs had I.R. less than 10^7 Ω. All of these MLCCs, which had I.R. less than 10^7 Ω at room temperature after testing, were flexible-termination MLCCs with precious metal electrodes biased at 50 V during testing. Measurements at room temperature after baking for 24 hours at 85°C showed that only the same four MLCCs had I.R. less than 10^7 Ω.

Table 21. Number of failures in MLCCs in 85°C/85% RH testing preconditioned with normal temperature cycling. Cells that are empty mean that no failure occurred.

Manufacturer	End-termination	Electrode type	Bias (V)	No. of samples	No. of insulation resistance failures	No. of capacitance failures	No. of dissipation factor failures
Syfer	Flexible	PME	50	10	5	1	3
			1.5	10			
			0	4	1		
AVX	Flexible	BME	50	10			
			1.5	10			
			0	4			
AVX	Standard	BME	50	10			
			1.5	10			
			0	4			
Vishay	Standard	PME	50	10			
			1.5	10			
			0	4	4		
			Sum	**96**	**10**	**1**	**3**

Table 22.Time-to-failure for MLCCs in 85°C/85% RH testing preconditioned with normal temperature cycling. Cells that are empty mean that no failure occurred.

Manuf.	End-termination	Electrode type	Bias (V)	No. of samples	Time-to-failure of insulation resistance	Time-to-failure of capacitance	Time-to-failure of dissipation factor
Syfer	Flexible	PME	50	10	218	714	298
					318		
					856		856
					856		889
					962		
Syfer	Flexible	PME	0	4	21		
Vishay	Standard	PME	0	4	58		
					258		
					501		
					853		

3.2.2 Experimental results of THB testing (85°C/85% RH) of MLCCs preconditioned with rapid temperature cycling

In this section, results of electrical parameters measurements during testing in 85°C/85% RH for MLCCs preconditioned with rapid temperature cycling with ramp rate of 50°C/min are presented. Figure 49 shows an example of the in-situ insulation resistance measurements of a flexible-termination MLCC with precious metal electrodes during testing in 85°C/85% RH and 50 V bias preconditioned with rapid temperature cycling. For this MLCC, insulation resistance after 230 hours of testing in 85°C/85% RH drops to a value close to 1 MΩ, which is the value of the series resistor used in experimental circuit and does not recover after dropping to close to 1 MΩ. Based on the

definition of the failure criterion for insulation resistance (I.R. < 10^7 Ω), this capacitor was failed in insulation resistance.

Figure 50 shows the in-situ measurements of the capacitance for the same MLCC, which its I.R. value shown in Figure 49. The failure criterion for capacitance (C) was defined as the absolute value of capacitance change during THB testing relative to initial measurements to be greater than 10% and having at least 5 occurrences during testing. For this MLCC, an increase in capacitance value at 230 hours, which showed I.R. drop to a value close to 1 MΩ, is observed and after this instabilities can be observed in capacitance value. However, the changes in capacitance where within ±10% of the initial value and it is not considered as a failure in capacitance.

Figure 51 shows the in-situ measurements of the dissipation factor for the same MLCC, which its I.R. value shown in Figure 49. The failure criterion for dissipation factor (D.F.) was defined as D.F. increase to greater than two times the nominal value and having at least 5 occurrences during testing. For this MLCC, an increase in dissipation factor value at around 230 hours, which showed I.R. drop, was observed. Later it shows intermittent values higher than failure criterion (0.05) and finally the dissipation factor value was increased to higher than failure criterion value. This capacitor was considered as a failure in dissipation factor based on definition of failure criterion for dissipation factor.

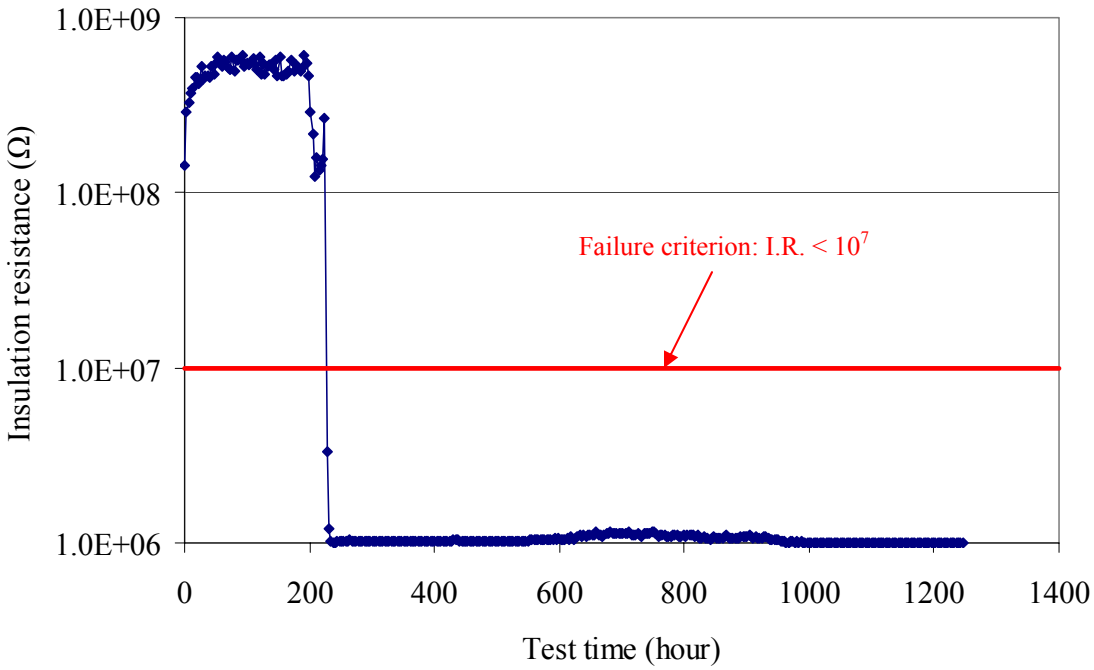

Figure 49. Insulation resistance of a flexible-termination MLCC with precious metal electrodes during testing in 85°C/85% RH biased at 50 V preconditioned with rapid temperature cycling.

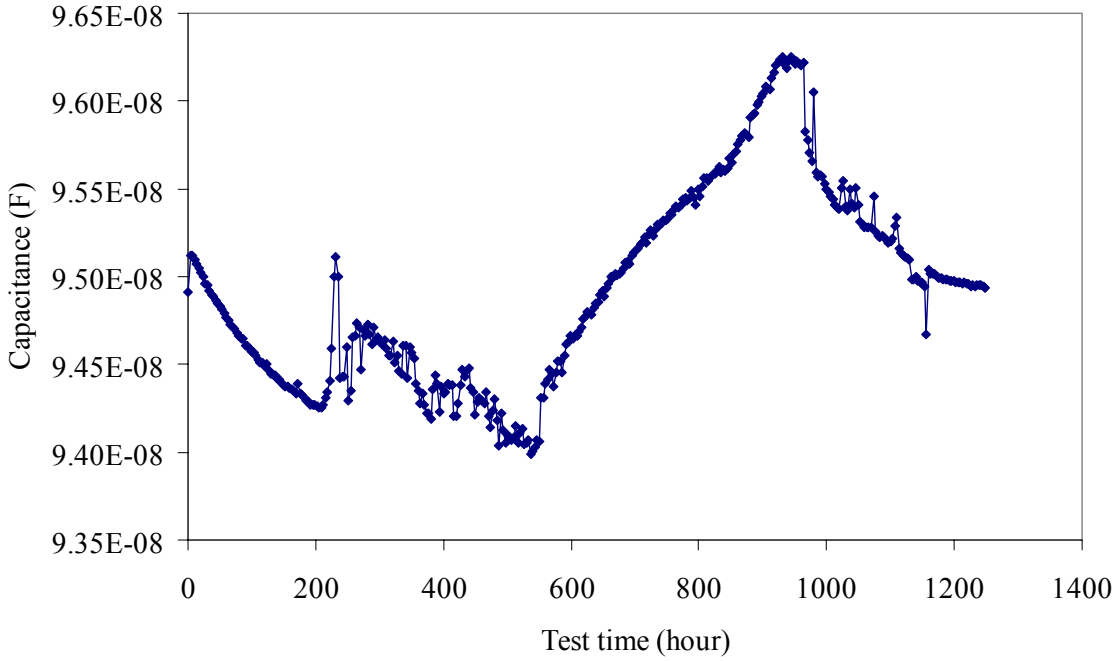

Figure 50. Capacitance of a flexible-termination MLCC with precious metal electrodes during testing in 85°C/85% RH biased at 50 V preconditioned with rapid temperature cycling.

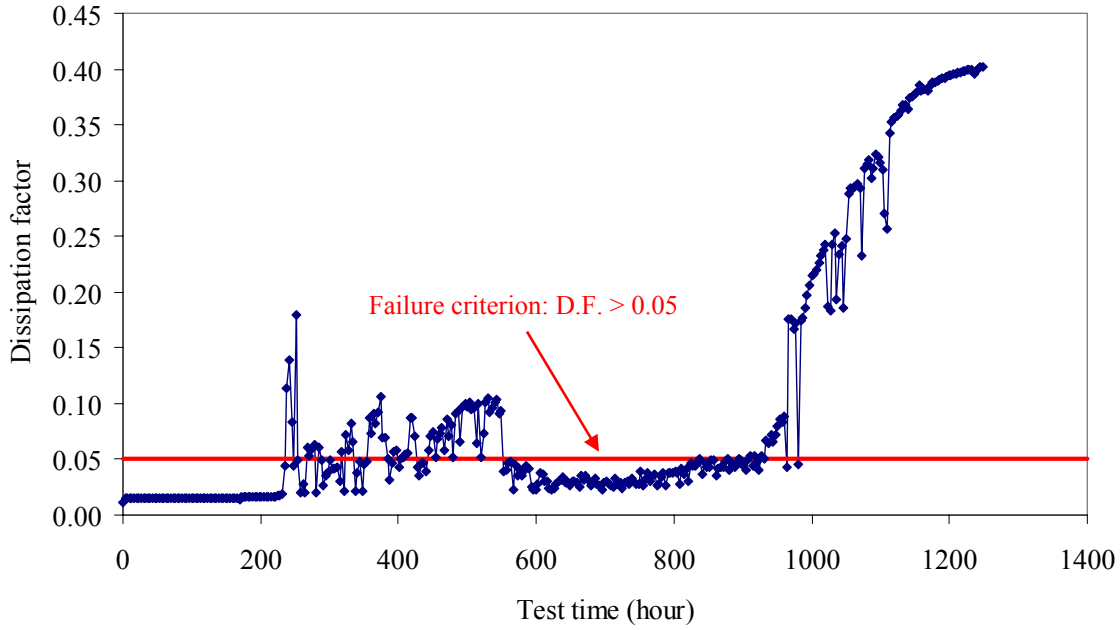

Figure 51. Dissipation factor of a flexible-termination MLCC with precious metal electrodes during testing in 85°C/85% RH biased at 50 V preconditioned with rapid temperature cycling.

Table 23 shows number of failures in MLCCs in 85°C/85% RH testing preconditioned with rapid temperature cycling. All failures were found to be in MLCCs with precious metal electrodes and MLCCs with base metal electrodes did not exhibit any failure. These results are consistent with what it was obtained for MLCCs tested in 85°C/85% RH preconditioned with normal temperature cycling. Flexible-termination MLCCs with precious metal electrodes exhibited three failures out of 24 samples during 85°C/85% RH testing based on in-situ measurements of the insulation resistance. Standard-termination MLCCs with precious metal electrodes with no bias showed two failures out of four samples tested. Only two MLCCs out of 96 samples total exhibited

failure in dissipation factor and none of the MLCCs exhibited failure in capacitance values.

Table 24 shows the time-to-failure for failed MLCCs in 85°C/85% RH testing preconditioned with rapid temperature cycling. The time-to-failure for each electrical parameter (insulation resistance, capacitance, and dissipation factor) is given separately. It is shown in Table 22 that some capacitors which failed in insulation resistance, they did not fail in capacitance or dissipation factor. However, all capacitors which exhibited failure in dissipation factor, also exhibited failure in insulation resistance.

Although in-situ measurements during 85°C/85%RH testing of MLCCs preconditioned with rapid temperature cycling indicated failures in insulation resistance of 5 MLCCs out of 96 samples, measurements at room temperature after 85°C/85%RH test completion showed only three MLCCs had I.R. less than 10^7 Ω. All of these MLCCs, which had I.R. less than 10^7 Ω at room temperature after testing, were flexible-termination MLCCs with precious metal electrodes, two of them biased at 50 V and one of them biased at 1.5 V during testing. Measurements at room temperature after baking for 24 hours at 85°C showed that only the same three MLCCs had I.R. less than 10^7 Ω and baking at 85°C did not recover these failed MLCCs. These results are similar with what it was obtained for MLCCs tested in 85°C/85% RH preconditioned with normal temperature cycling.

Table 23. Number of failures in MLCCs in 85°C/85% RH testing preconditioned with rapid temperature cycling. Cells that are empty mean that no failure occurred.

Manufacturer	End-termination	Electrode type	Bias (V)	No. of samples	No. of insulation resistance failures	No. of capacitance failures	No. of dissipation factor failures
Syfer	Flexible	PME	50	10	2		1
			1.5	10	1		
			0	4			
AVX	Flexible	BME	50	10			
			1.5	10			
			0	4			
AVX	Standard	BME	50	10			
			1.5	10			
			0	4			
Vishay	Standard	PME	50	10			
			1.5	10			
			0	4	2		1
			Sum	96	5	0	2

Table 24.Time-to-failure for MLCCs in 85°C/85% RH testing preconditioned with rapid temperature cycling. Cells that are empty mean that no failure occurred.

Manufacturer	End-termination	Electrode type	Bias (V)	No. of samples	Time-to-failure of insulation resistance	Time-to-failure of capacitance	Time-to-failure of dissipation factor
Syfer	Flexible	PME	50	10	228		238
					1179		
Syfer	Flexible	PME	1.5	10	1123		
Vishay	Standard	PME	0	4	112		
					139		205

3.2.3 Experimental results of dry heat testing (85°C) of MLCCs preconditioned with normal temperature cycling

Accelerated testing of MLCCs in dry heat environment (85°C) for the similar MLCCs, which were tested in temperature-humidity environment (85°C/85% RH) was conducted to separate the effects of moisture on MLCCs failures. MLCCs were preconditioned with normal temperature cycling and then they were tested at 85°C for 1240 hours, the same duration that were tested in 85°C/85% RH condition.

Electrical parameters (insulation resistance, capacitance, and dissipation factor) were measured in-situ during testing. MLCCs exhibited no failure in all three electrical parameters during testing at 85°C, in contrast to MLCCs, which were tested in temperature-humidity environment (85°C/85% RH). It is concluded that the presence of the moisture is necessary in order to have failure in precious metal electrode MLCCs. All failures during testing at temperature-humidity (85°C/85% RH) under voltage bias were in MLCCs with precious metal electrodes (Ag-Pd), with no failures in MLCCs with base metal electrodes (Ni). Silver migration was hypothesized to be the failure mechanism of MLCCs in THB testing, since none of the base metal electrode MLCCs exhibited failure.

Figure 52 shows the capacitance of a flexible-termination MLCC with precious metal electrodes during testing in 85°C biased at 50 V preconditioned with normal temperature cycling. It shows that the capacitance decreased with test time and it is due to aging, which is a known phenomenon for Class II ceramic dielectric. However, the capacitance value still remains within ±10% of the initial value of the capacitance, which was defined as the failure criterion for capacitance in this study. Therefore, this capacitor does not exhibit a failure in capacitance. In fact, as it was mentioned earlier, none of the standard-

and flexible-termination MLCCs tested in dry heat condition exhibited failure for duration of 1240 hours of testing.

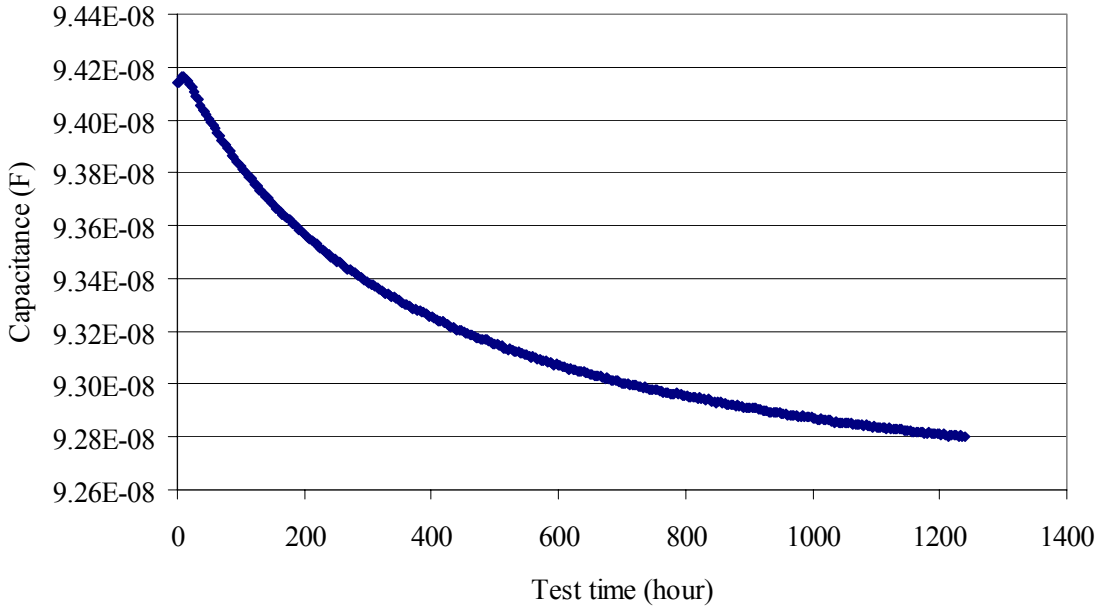

Figure 52. Capacitance of a flexible-termination MLCC with precious metal electrodes during testing in 85°C biased at 50 V preconditioned with normal temperature cycling.

3.3 Compositional and constructional analysis of THB-tested MLCCs

Compositional analysis for dielectric, electrodes, and end-terminations of MLCCs used in THB testing was conducted. MLCCs were cross-sectioned and by using environmental scanning electron microscopy (E-SEM) combined energy dispersive X-ray spectroscopy (EDX) materials and structure of MLCCs were identified.

Four MLCC types were considered in THB testing, two of them are flexible-termination MLCCs and two of them are standard-termination MLCCs. For both end-

termination types, MLCCs with precious metal electrodes (PME) made of silver-palladium and MLCCs with base metal electrodes (BME) made of nickel were considered. Flexible-termination MLCCs manufactured by AVX are made of nickel electrodes (BME) and flexible-termination MLCCs manufactured by Syfer are made of silver-palladium electrodes (PME). Standard-termination MLCCs manufactured by AVX are made of nickel electrodes and standard-termination MLCCs manufactured by Vishay are made of silver-palladium electrodes. All MLCCs used in THB testing are made of X7R dielectric (EIA class II [6]), which main dielectric material is barium titanate ($BaTiO_3$). Table 17 in previous section summarizes compositional analysis of MLCCs with standard and flexible terminations.

Figure 53 shows the EDX mapping of the end-termination for an 1812 size flexible-termination MLCC manufactured by AVX. MLCCs with flexible terminations from AVX are comprised of a conductive polymer in their end-termination. The conductive polymer used in the end-termination is a silver-loaded epoxy. Epoxy is a thermoset material that cures through the addition of heat to a stronger form by a cross-linking process. Thermoplastic materials melt to a liquid form when heated and are not suitable to be used in the end-termination of MLCCs. The conductive epoxy coats a copper termination, and is then plated with nickel and tin. Therefore, the copper layer acts as a barrier layer between silver-loaded epoxy and the capacitor body and prevents electrochemical migration of silver into the capacitor body. In addition, internal electrodes in flexible-termination MLCCs manufactured by AVX are made of nickel. Therefore, for flexible-termination MLCCs from AVX the chance of reduction in

insulation resistance and potentially shorting of internal electrodes due to silver migration failure is very low.

Syfer produces MLCCs with flexible terminations and precious metal electrodes. Figure 54 shows the EDX mapping of the end-termination of a flexible-termination MLCC manufactured by Syfer. Flexible-termination MLCCs from Syfer contain silver loaded epoxy in end terminations plated with nickel and tin. In contrast to the end-termination structure of the flexible-termination MLCCs from AVX, no copper layer exist between the epoxy layer and the capacitor body in the end-termination of the flexible-termination MLCCs from Syfer and the silver-loaded epoxy is directly attached to the capacitor body. The internal electrodes of the flexible-termination MLCCs from Syfer are made of silver-palladium, while flexible-termination MLCCs from AVX are made of nickel electrodes. The construction of the flexible-termination MLCCs from Syfer presents a potential risk of silver migration under bias and humidity, due to presence of silver in the internal electrodes and end-terminations.

Ceramic materials used as a dielectric in MLCCs are hydrophilic materials. Hydrophilicity is a physical property of a molecule that can transiently bond with water (H_2O) through hydrogen bonding. A hydrophilic molecule or portion of a molecule is one that is typically charge-polarized and capable of hydrogen bonding, enabling it to dissolve more readily in water than in oil or other hydrophobic solvents. Hydrophilic and hydrophobic molecules are also known as polar molecules and nonpolar molecules, respectively. Hydrophobe in chemistry refers to the physical property of a molecule that is repelled from a mass of water. Hydrophobic molecules tend to be nonpolar and thus prefer other neutral molecules and nonpolar solvents. Water on hydrophobic surfaces will

exhibit a high contact angle. Examples of hydrophobic molecules include the alkanes, oils, fats, and greasy substances in general. Hydrophobes are not electrically polarized [72] [73].

Since the ceramic dielectric is a hydrophilic material, if there is any crack or defect in the ceramic body of the capacitor exposed to outside surface of capacitor could be a path for moisture and contaminant penetration. The penetration of moisture between internal electrodes of the capacitor causes insulation resistance to be decreased. In PME capacitors, which are made of silver-palladium electrodes, penetration of moisture and contaminants, and application of DC voltage bias could lead to silver migration between internal electrodes and reduction in insulation resistance or electrical shorting of capacitor.

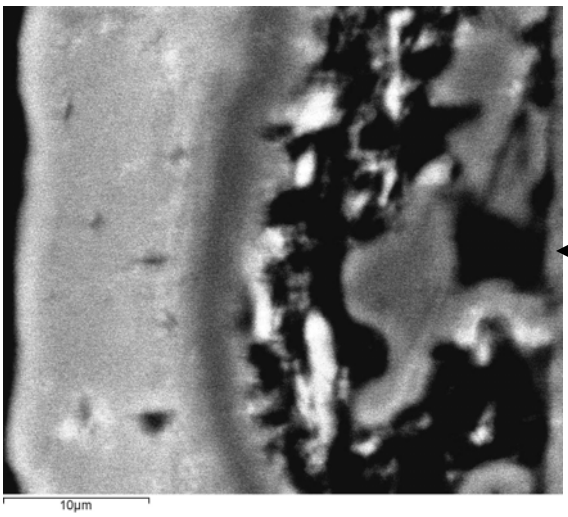

E-SEM picture of the end-termination of a flexible-termination MLCC

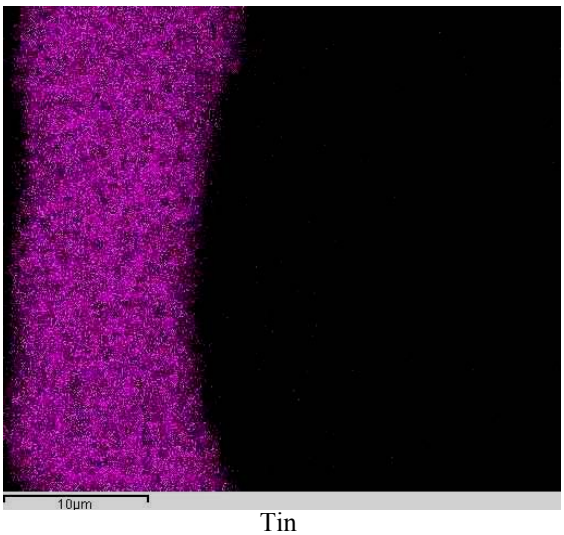

Tin

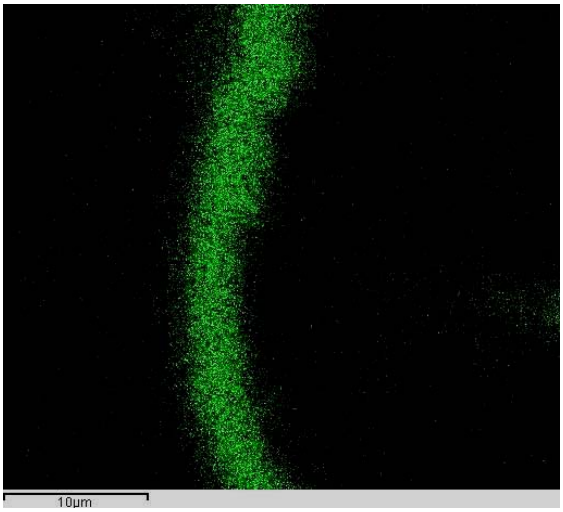

Nickel

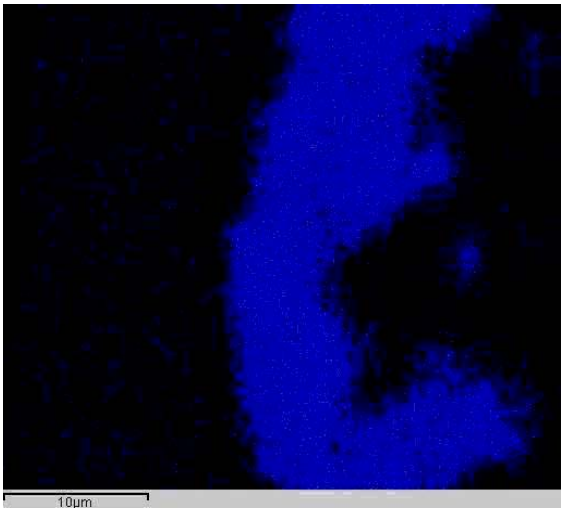

Silver

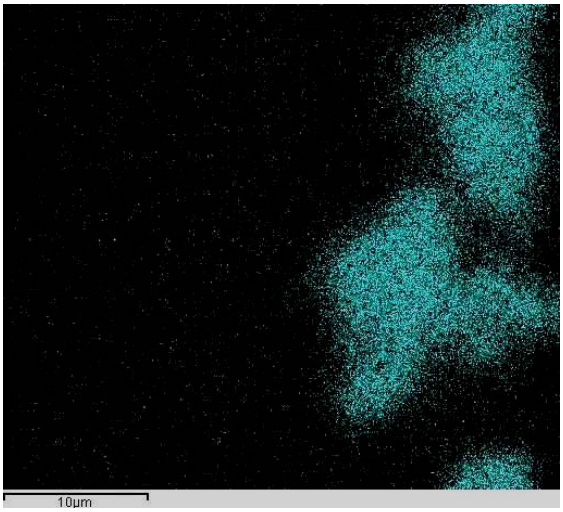

Copper

Figure 53. EDX mapping of the end-termination of a flexible-termination MLCC

manufactured by AVX.

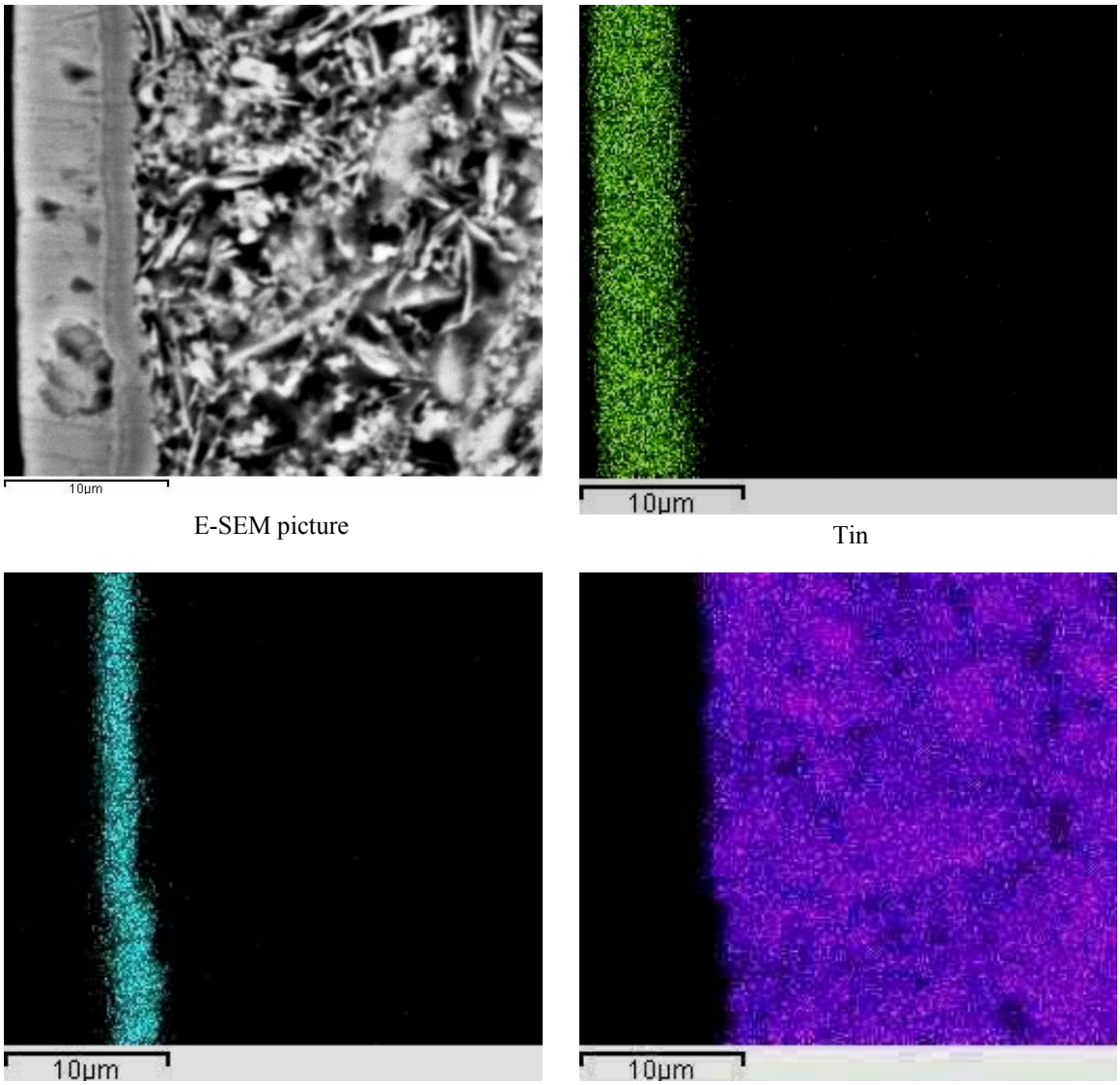

E-SEM picture

Tin

Nickel

Silver

Figure 54. EDX mapping of the end-termination of a flexible-termination MLCC manufactured by Syfer.

3.4 Conclusions and summary

In this study, effects of temperature-humidity-bias (THB) on electrical parameters of multilayer ceramic capacitors with both flexible and standard terminations were investigated. There is no published data available for temperature-humidity-bias testing of the new technology flexible-termination MLCCs. Users of this new technology have the concern that long term exposure to moisture cause failure or electrical degradation in flexible-termination MLCCs. In addition, temperature-humidity-bias effects on electrical parameters of MLCCs made of precious metal electrode (Ag-Pd) are compared with MLCCs made of base metal electrodes (Ni).

Some of the flexible-termination MLCCs are made of precious metal electrodes (silver-palladium) and contain silver-filled epoxy in their end terminations. This construction presents a potential risk of silver migration under bias and high humidity conditions. Accelerated environmental stress tests were conducted to compare electrical degradation of flexible-termination MLCCs due to environmental stresses and bias with standard-termination MLCCs.

Sensitivity of flexible-termination MLCCs to temperature, humidity, and bias were compared and explained in comparison with standard-termination MLCCs tested in two environmental stress conditions: temperature-humidity (85°C/85% RH) and dry temperature (85°C). The effects of different DC voltages (low voltage, rated voltage, and no voltage), electrode materials (BME *vs*. PME), and preconditioning (normal temperature cycling *vs*. rapid temperature cycling) were determined for flexible-and standard-termination MLCCs. Failures of MLCCs in temperature-humidity-bias testing

were explained and related to the structure, materials of the tested MLCCs and environmental conditions.

All failures during testing at temperature-humidity (85°C/85% RH) under different voltage biases were in MLCCs with precious metal electrodes (Ag-Pd), with no failures in MLCCs with base metal electrodes (Ni). MLCCs preconditioned with normal temperature cycling showed similar results with MLCCs preconditioned with rapid temperature cycling. Silver migration was hypothesized to be the failure mechanism of MLCCs in THB testing, since none of the base metal electrode MLCCs exhibited failure. Accelerated testing of similar MLCCs at dry heat condition (85°C) for the same duration that were tested in temperature-humidity (85°C/85% RH) conditions exhibited no failure in all electrical parameters. It is concluded that the presence of the moisture is necessary in order to have failure in precious metal electrode MLCCs.

Silver migration failure of MLCCs is divided into three steps. Step one is the formation of a microscopic path between internal electrodes. This path can be a crack or void which occurs during manufacturing, assembly, or in the application field during life of the ceramic capacitors. Step two involves penetration of moisture into the path. The final step is the silver migration of electrode materials along the path by an electrochemical process. As a consequence of this, the leakage current of the ceramic capacitor increases and causes the capacitor to fail.

By using energy dispersive X-ray spectroscopy (EDX) combined with E-SEM, compositional and structural analysis of tested MLCCs was conducted. The EDX mapping of the end-termination for flexible-termination MLCCs manufactured by AVX exhibited that the conductive polymer used in the end-termination is a silver-loaded

polymer. The conductive polymer coats a copper termination, and is then plated with nickel and tin. Therefore, the copper layer acts as a barrier layer between silver-loaded epoxy and the capacitor body and prevents electrochemical migration of silver into the capacitor body. In addition, internal electrodes in flexible-termination MLCCs manufactured by AVX are made of nickel. Therefore, for flexible-termination MLCCs from AVX the chance of reduction in insulation resistance and potentially shorting of internal electrodes due to silver migration failure is very low, as it was found in the experiments.

EDX mapping showed that the internal electrodes of the flexible-termination MLCCs from Syfer are made of silver-palladium. Flexible-termination MLCCs from Syfer contain silver loaded epoxy in end terminations plated with nickel and tin. In contrast to the end-termination structure of the flexible-termination MLCCs from AVX, no copper layer exist between the epoxy layer and the capacitor body in the end-termination of the flexible-termination MLCCs from Syfer and the silver-loaded epoxy is directly attached to the capacitor body. The construction of the flexible-termination MLCCs from Syfer presents a potential risk of silver migration under bias and humidity, due to presence of silver in the internal electrodes and end-terminations. In the experiments in temperature-humidity-bias conditions, flexible-termination MLCCs with precious metal electrodes showed the highest failure ratio among all tested MLCCs. Only flexible-termination MLCCs with precious metal electrodes, showed failure at room temperature after THB testing and they did not recover even after baking them at high temperature (85°C) for one day. This confirms that a permanent leakage path inside the capacitor must exist and

it is consistent with the hypothesis of silver migration as failure mechanism of PME MLCCs.

In manufacturers' qualification testing of MLCCs in temperature-humidity-bias conditions and previous work on testing of MLCCs in THB conditions, electrical parameters of MLCCs has not been measured in-situ during THB testing. They usually measured electrical parameters periodically during testing at room temperature or only before and after completion of the THB testing. In this situation, intermittent failures that occur during testing are not captured and the failed MLCCs, which are recovered at room temperature-humidity conditions, are not captured as failures too. In-situ measurement of different electrical parameters (capacitance, dissipation factor, and insulation resistance) of MLCCs during THB testing was implemented in the present study. This helps to capture intermittent failures of MLCCs during testing and finding effects of temperature-humidity-bias on each electrical parameter separately. It was shown that an MLCC exhibited out of specification value for one of the electrical parameters, while other electrical parameters are still within the specification limits.

4 Contributions

In this study the effect of different parameters on the flex cracking susceptibility of multilayer ceramic capacitors assembled on PCBs was characterized and explained. The flex cracking susceptibility of MLCCs assembled with lead-free solder (Sn3.0Ag0.5Cu) was identified and compared with those assembled with eutectic tin-lead solder (Sn37Pb) by considering MLCCs with two different sizes (1812 and 0805), two commonly used dielectric types (C0G and X7R), and different manufacturers. Flex cracking of MLCCs assembled with convective reflow soldering was compared with MLCCs assembled with wave soldering. In addition, flex cracking of the new technology of flexible-termination MLCCs assembled with tin-lead and lead-free solders was characterized and compared with standard-termination MLCCs.

Experimental results showed that MLCCs assembled with lead-free solder are less susceptible to flex cracking compared to MLCCs assembled with eutectic tin-lead solder. The present work is the first study to explain why MLCCs assembled with lead-free solder are less susceptible to flex cracking compared to MLCCs assembled with eutectic tin-lead solder. In order to find out the reasons for this difference, three factors including, solder fillet geometry, compressive residual stress inside the capacitor after reflow cool-down process, and solder material mechanical properties were considered.

The solder fillet geometrical parameters for MLCCs assembled with tin-lead and lead-free solders were measured and compared. The differences in solder fillet geometrical parameters for tin-lead and lead-free solders were not statistically significant. Therefore, solder fillet geometry is not a main contributor in the difference between flex cracking susceptibility of MLCCs assembled with lead-free and tin-lead solders.

Cooling of a capacitor after solder reflow assembly places the capacitor under compressive stress. Because for a higher-melting solder, cooling of assembled capacitors places capacitors under greater compressive stress, a capacitor assembled with a higher-melting solder should require more bending stress to crack. Since the solidus temperature for Sn3.0Ag0.5Cu lead-free solder (about 217°C) is higher than that for eutectic tin-lead solder (183°C), lead-free solder places more residual compressive stresses on a capacitor after assembly than tin-lead solder. Therefore, capacitors assembled with lead-free solder should require more applied bending stress to crack than those assembled with tin-lead solder.

The present work is the first study, which investigated the effects of isothermal aging on flex cracking susceptibility of MLCCs. Experiments were performed to compare the flex cracking susceptibility of standard- and flexible-termination MLCCs assembled with lead-free solder (Sn3.0Ag0.5Cu) and eutectic tin-lead solder (Sn37Pb), tested without aging or after aging at 100°C or 150°C for 200 hours. MLCCs were aged at high temperature and then tested in a four point bend configuration. Isothermal aging had much less effect on flex cracking susceptibility of MLCCs assembled with tin-lead solder in comparison with those assembled with lead-free solder. Aging of MLCCs at elevated temperature causes the solder alloy to creep and reduces the amount of residual compressive stress in MLCCs, especially in the case of lead-free solder when aging is performed at higher temperatures (e.g., 150°C). As a result of the reduction of compressive stresses, a higher cumulative percent failure was obtained during flex testing of MLCCs assembled with lead-free solder and aged at 150°C in comparison to un-aged samples.

Finite element analysis (FEA) was conducted of ceramic capacitors under PCB flexure in a four-point bend configuration. Comparison of the FEA results of MLCCs assembled with lead-free and tin-lead solder showed that the maximum stress inside the capacitor for an MLCC assembled with tin-lead solder is higher than lead-free solder. Flex cracking is the result of tensile stresses inside the capacitor body exceeding the fracture strength of the ceramic. However, there are residual compressive stresses inside the capacitor body after the solder assembly cool down process, which mitigate the tensile stresses generated by PCB bending. These residual compressive stresses are higher for MLCCs assembled with lead-free solder than for MLCCs assembled with tin-lead solder. Therefore, greater PCB deflection is required for MLCCs assembled with lead-free solder for the tensile stresses to reach the ceramic fracture strength, in order to overcome the higher residual compressive stress.

Standard-termination MLCCs assembled with convective reflow soldering and wave soldering showed similar results in flex testing. The analysis of flex test results showed that the 95% confidence intervals for MLCCs assembled with reflow and wave soldering overlap.

MLCCs with flexible terminations exhibited much more resistance to flex cracking in comparison to standard-termination MLCCs assembled with both lead-free and tin-lead solders due to existence of a soft polymer buffer layer in the end-terminations. Flexible-termination MLCCs assembled with lead-free solder did not show any failures up to the level of strain used for testing standard-termination MLCCs.

Flex cracks in failed flexible-termination MLCCs were found to be at the interface between solder joint and end-termination or in the polymer layer of the end-termination,

causing them to fail in open mode in field applications. In contrast, in failed standard-termination MLCCs flex cracks were inside the capacitor body, allowing them to fail in short mode in field applications. For standard-termination MLCCs with open mode design, flex cracks, which start from an end termination at a cute angle only cross electrodes originating from the same termination and don't cause shorting between opposing electrodes.

The flexible-termination MLCCs produced by some manufacturers (e.g., Syfer) are made of precious metal electrodes (silver-palladium) and contain silver-filled epoxy in their end terminations. This construction presents a potential risk of silver migration under bias and high humidity conditions. There is no published data available of temperature-humidity-bias testing for the new technology flexible-termination MLCCs. Users of this new technology have the concern that long term exposure to moisture cause failure or electrical degradation in flexible-termination MLCCs. Accelerated environmental stress tests were conducted to compare electrical degradation of flexible-termination MLCCs due to environmental stresses and bias with standard-termination MLCCs.

Sensitivity of flexible-termination MLCCs to temperature, humidity, and bias were compared and explained in comparison with standard-termination MLCCs tested in two environmental stress conditions: temperature-humidity (85°C/85% RH) and dry temperature (85°C). The effects of different DC voltages (low voltage, rated voltage, and no voltage), electrode materials (BME *vs*. PME), and preconditioning (normal temperature cycling *vs*. rapid temperature cycling) were determined for flexible- and

standard-termination MLCCs. Failures of MLCCs in temperature-humidity-bias testing were explained and related to their structure, materials and environmental conditions.

All failures during testing in temperature-humidity conditions (85°C/85% RH) under different voltage biases were in MLCCs with precious metal electrodes (Ag-Pd), with no failures in MLCCs with base metal electrodes (Ni). It was hypothesized that silver migration to be the failure mechanism of MLCCs in THB testing, since none of the base metal electrode MLCCs exhibited failure. In addition, accelerated testing of similar MLCCs at dry heat condition (85°C) for the same duration that were tested in temperature-humidity (85°C/85% RH) conditions exhibited no failure in all electrical parameters. It is concluded that the presence of the moisture is necessary in order to have failure in precious metal electrode MLCCs.

By using energy dispersive X-ray spectroscopy (EDX) combined with E-SEM, compositional and structural analysis of tested MLCCs was conducted. The EDX mapping of the end-termination for flexible-termination MLCCs manufactured by AVX exhibited that the conductive polymer used in the end-termination is a silver-loaded polymer. The conductive polymer coats a copper termination, and is then plated with nickel and tin. Therefore, the copper layer acts as a barrier layer between silver-loaded epoxy and the capacitor body and prevents electrochemical migration of silver into the capacitor body. In addition, internal electrodes in flexible-termination MLCCs manufactured by AVX are made of nickel. Therefore, for flexible-termination MLCCs from AVX the chance of reduction in insulation resistance and potentially shorting of internal electrodes due to silver migration failure is very low, as it was found in the experiments.

EDX mapping showed that the internal electrodes of the flexible-termination MLCCs from Syfer are made of silver-palladium. Flexible-termination MLCCs from Syfer contain silver loaded epoxy in end terminations plated with nickel and tin. In contrast to the end-termination structure of the flexible-termination MLCCs from AVX, no copper layer exist between the epoxy layer and the capacitor body in the end-termination of the flexible-termination MLCCs from Syfer and the silver-loaded epoxy is directly attached to the capacitor body. The construction of the flexible-termination MLCCs from Syfer presents a potential risk of silver migration under bias and humidity, due to presence of silver in the internal electrodes and end-terminations. In the experiments in temperature-humidity-bias conditions, flexible-termination MLCCs with precious metal electrodes biased at 50 V showed the highest failure ratio among all tested MLCCs. Only flexible-termination MLCCs with precious metal electrodes, showed failure at room temperature after THB testing and they did not recover even after baking them at high temperature (85°C) for one day. This confirms that a permanent leakage path inside the capacitor must exist and it is consistent with the hypothesis of silver migration as the failure mechanism of PME MLCCs.

In manufacturers' qualification testing of MLCCs in temperature-humidity-bias conditions, electrical parameters of MLCCs has not been measured in-situ during THB testing. They usually measured electrical parameters periodically during testing at room temperature or only before and after completion of the THB testing. In this situation, intermittent failures that occur during testing are not captured and the failed MLCCs, which are recovered at room temperature-humidity conditions, are not captured as failures too. In-situ measurement of different electrical parameters (capacitance,

dissipation factor, and insulation resistance) of MLCCs during THB testing was implemented in the present study. This helps to capture intermittent failures of MLCCs during testing and finding effects of temperature-humidity-bias on each electrical parameter separately. It was shown that an MLCC exhibited out of specification value for one of the electrical parameters, while other electrical parameters are still within the specification limits.

5 Publications

[1] Keimasi, M., Azarian, M. H., and Pecht, M., “Isothermal aging effects on flex cracking of multilayer ceramic capacitors with standard and flexible terminations,” Accepted for publication in Microelectronics Reliability, 15 December 2006.

[2] Keimasi, M., Azarian, M. H., and Pecht, M., “Flex cracking of multilayer ceramic capacitors assembled with lead-free and tin-lead solders,” Submitted for publication in IEEE Transactions on Device and Materials Reliability and reviewed.

[3] Keimasi, M., Ganesan, S., and Pecht, M., “Low temperature electrical measurements of silicon bipolar monolithic microwave integrated circuit (MMIC) amplifier,” Microelectronics Reliability, Vol. 46/2-4, pp. 326-334, 2006.

[4] Azarian, M. H., Keimasi, M., and Pecht, M., “Moisture sensitivity levels for plastic encapsulated surface mount capacitors,” Ready to Submit to IEEE Transactions on Components and Packaging Technologies.

[5] Keimasi, M., Azarian, M. H., and Pecht, M., "Temperature-humidity-bias testing of multilayer ceramic capacitors with standard and flexible terminations,” was written for publication in a journal.

[6] Keimasi, M., Azarian, M. H., and Pecht, M., “Comparison of flex cracking of multilayer ceramic capacitors assembled with lead-free and eutectic tin-lead solders,” Capacitor and Resistor Technology Symposium, Orlando, Florida, USA, pp. 15-25, April 3-6, 2006.

[7] Azarian, M. H., Keimasi, M., and Pecht, M., “Non-destructive techniques for detection of defects in multilayer ceramic capacitors,” Components for Military &

Space Electronics Conference, Los Angeles, California, USA, pp. 125-130, February 6-9, 2006.

[8] Azarian, M. H., Keimasi, M., and Pecht, M., "Effects of lead-free solder on flex cracking of multilayer ceramic capacitors with flexible and standard terminations," Components for Military & Space Electronics Conference, Los Angeles, California, USA, pp. 244-251, February 6-9, 2006.

[9] Mishra, R., Keimasi, M., and Diganta, D., "The temperature ratings of electronic parts", Electronics cooling magazine, Vol. 10, No. 1, pp. 20-29, February 2004.

[10] Keimasi, M., Azarian, M. H., and Pecht, M., "How to choose a reliable multilayer ceramic capacitor," Ready to submit to a magazine.

6 References

[1] Zogbi, D. M., "Shortages reveal sweet spot in global capacitor markets," TTI, Inc., 1 March 2004, http://www.ttiinc.com, visited on 12 July, 2006.

[2] Zogbi, D., "Fastest growing ceramic capacitor manufacturers: 2003-2004," TTI, Inc., 6 December 2004, http://www.ttiinc.com (Last visited on 19 October, 2005).

[3] Zennicek, T., Zednicek, S., Sita, Z., McCracken, C., Millman, W., and Gill, J., "Technology of niobium oxide capacitor," Advancing Microelectronics, pp. 6-10, May/June 2004.

[4] Kemet Electronics Corporation, "Ceramic chip capacitors," http://www.kemet.com, visited on 23 May 2004.

[5] Prymak, J. D., and Berganthal, J., "Capacitance monitoring while flex testing," IEEE Transactions on Components, Packaging, and Manufacturing Technology, Part A, Vol. 18, No. 1, pp. 180-186, March 1995.

[6] EIA Standard, "Ceramic dielectric capacitors classes I, II, III and IV – part I: characteristics and requirements," EIA-198-1-F, November 2002.

[7] Harper, C. A., Passive electronic component handbook, Second Edition, McGraw-Hill, USA, 1997.

[8] Kishi, H., Mizuno, Y., and Chazono, H., "Base-metal electrode-multilayer ceramic capacitors: past, present and future perspectives," Japanese Journal of Applied Physics, Vol. 42, pp. 1-15, 2003.

[9] Kahn, M., "Multilayer ceramic capacitors – materials and manufacture," AVX Corporation, Technical information, http://www.avxcorp.com, visited on 5 February 2005.

[10] Koripella, C. R., "Mechanical behavior of ceramic capacitors," IEEE Transactions on Components, Hybrids, and Manufacturing Technology, Vol. 14, No. 4, pp. 718-724, December 1991.

[11] Koripella, C. R., "Mechanical properties of ceramic capacitors," Kemet Tech Topics, Vol. 1, No. 5, Kemet Electronics Corporation, September 1991.

[12] Kemet Electronics Corporation, "Electrode materials for multilayer ceramic capacitors," Kemet Tech Topics, Vol. 2, No. 6, July 1992.

[13] Gormally, P. M., "High volume manufacturing of ceramic chip capacitors, wet vs. dry fabrication," Vishay Vitramon®.

[14] Kemet Electronics Corporation, "Wet vs. dry: multilayer ceramic capacitor manufacturing processes," Kemet Tech Topics, Vol. 1, No. 4, August 1991.

[15] Syfer Technology Limited, "FlexiCapTM termination. Application Note," Reference number: AN0001 - FlexiCapTM, Issue 3, www.syfer.com, visited on 15 June 2006.

[16] Nicker, D., "Bend it, shape it, don't break it," Passive Component Industry, Paumanok Publications, Inc., pp. 18-21, March/April 2003.

[17] Thales, research & technology, "Electronic components: ceramic capacitors polymer terminations," TRT/DHE/RD, March 2004.

[18] Stewart, M., "AVX MLCC Flexiterm: guarding against capacitor crack failures," AVX Corporation, Technical Information, http://www.avxcorp.com, visited on November 2005.

[19] Stewart, M., "A soft termination MLCC solution to guard against capacitor crack failures," CARTS 2005, Palm Springs, California, USA, pp. 219-224, March 2005.

[20] Kemet Electronics Corporation, "Ceramic open mode capacitors," www.kemet.com, visited on 15 April 2005.

[21] Sato, K., Ogata, Y., Ohno, K., and Ikeo, H., “Mechanism of ceramic capacitor leakage failures due to low DC stress,” Proceedings of the 18th International Reliability Physics Symposium, pp. 205-212, 1980.

[22] Freiman, S. W., and Pohanka, R. C., “Review of mechanically related failures of ceramic capacitors and capacitor materials,” Journal of American Ceramic Society, Vol. 72, No. 12, pp. 2258-2263, 1989.

[23] Zhan, S., Azarian, M. H., Pecht, M. G., “Surface insulation resistance of conformally coated printed circuit boards processed with no-clean flux,” IEEE Transactions on Electronics Packaging Manufacturing, Vol. 29, No. 3, pp. 217-223, July 2006.

[24] Electrochemical migration: electrically induced failures in printed wiring assemblies, IPC Standard, IPC-TR-476A, Northbrook, Illinois, May 1997.

[25] Berganthal, J., “Ceramic chip capacitors “flex cracks”: understanding & solutions,” Kemet Electronics Corporation, Document No.: F-2111, January 1998.

[26] Prymak, J. D., “Flex testing II,” Kemet Tech Topics, Vol. 4, No. 6, Kemet Electronics Corporation, October 1994.

[27] Prymak, J. D., “Flex or bend testing,” Kemet Tech Topics, Vol. 3, No. 7, Kemet Electronics Corporation, September 1993.

[28] Al-Saffar, R., Freer, R., Tribick, I., and Ward, P., “Flexure strength of multilayer ceramic capacitors,” British Ceramic Transactions, Vol. 98, No. 5, pp. 241-245, 1999.

[29] Maxwell, J., "Board flexure comparison between surface mount multi-layer ceramic and film capacitors," CARTS 1999, Illinois, March 1999.

[30] Syfer Technology Limited, "Mechanical cracking of chip capacitors," http://www.Syfer.com, visited on March 2005.

[31] Nies, C., and Maxwell, J., "Important factors in board flexure testing of surface mount capacitors," CARTS, Asia, Singapore, pp. 75-82, 1991.

[32] Long, B., Prevallet, M., and Prymak, J., "Effects of lead-free solders on flex performance," CARTS 2005, Palm Springs, CA, pp. 97-101, March 2005.

[33] Blattau, N., Barker, D., and Hillman, C., "Lead free solder and flex cracking failures in ceramic capacitors," CARTS 2004, 24th Capacitor and Resistor Technology Symposium, San Antonio, Texas, pp. 101-105, March 29 - April 1, 2004.

[34] Blattau, N., Barker, D., and Hillman, C., "Design guidelines for preventing flex cracking failures in ceramic capacitors," CARTS 2003, 23rd Capacitor and Resistor Technology Symposium, Scottsdale, Arizona, pp. 155-162, March 31 - April 3, 2003.

[35] Blattau, N., and Hillman, C., "Has the electronics industry missed the boat on Pb-free? Failures in ceramic capacitors with Pb-free solder interconnects," IPC/JEDEC 5th International Lead Free Conference on Electronic Components and Assemblies, San Jose, CA, March 18-19, 2004.

[36] Hillman, C., Blattau, N., and Barker, D., "Design guidelines for avoiding flex cracking in ceramic capacitors," Global SMT and Packaging, Volume 3, No. 1, pp. 18-21, January/February 2003.

[37] Franken, K., Maier, H. R., Prume, K., and Waser, R., "Finite-element analysis of ceramic multilayer capacitors: failure probability caused by wave soldering and bending loads," Journal of American Ceramic Society, Volume 83, No. 6, pp. 1433-1440, June 2000.

[38] Freiman, S. W., and Gonzalez, A. C., "Electrical failures due to cracks in multilayer ceramic capacitors," In Advances in Ceramics, Vol. 19, Multilayer ceramic devices. Edited by Blum, J. B., and Cannon, W. R., American Ceramic Society, Westerville, OH, pp. 191-201, 1986.

[39] Ling, H. C., and Jackson, A. M., "Correlation of silver migration with temperature-humidity-bias (THB) failures in multilayer ceramic capacitors," IEEE Transactions on Components, Hybrids, and Manufacturing Technology, Vol. 12, No. 1, pp. 130-137, March 1989.

[40] Munikoti, R., and Dhar, D., "Low-voltage failures in multilayer ceramic capacitors: a new accelerated stress screen," IEEE Transactions on Components, Hybrids, and Manufacturing Technology, Vol. 11, No. 4, pp. 346-350, December 1988.

[41] Munikoti, R., and Dhar, D., "Highly accelerated life testing (HALT) for multilayer ceramic capacitor qualification," IEEE Transactions on Components, Hybrids, and Manufacturing Technology, Vol. 11, No. 4, pp. 342-345, December 1988.

[42] Rawal, B. S., and Chan, N. H., "Conduction and failure mechanisms in barium titanate based ceramics under highly accelerated conditions," AVX Corporation, Technical Information, http://www.avxcorp.com, visited on November 2005.

[43] Chen, W. P., Jiang, X. P., Wang, Y., Peng, Z., and Chan, H. L. W., "Water-induced degradation of barium titanate ceramics studied by electrochemical hydrogen charging," Journal of American Ceramic Society, Vol. 86, No. 4, pp. 735-737, 2003.

[44] Donahoe, D., Pecht, M., Lloyd, I., and Ganesan, S., "Moisture induced degradation of multilayer ceramic capacitors," Microelectronics Reliability, Vol. 46, pp. 400-408, 2006.

[45] Donahoe, D. N., Hillman, C. D., and Pecht, M. G., "Failures in base metal electrode (BME) capacitors," 23rd Capacitor and Resistor Technology Symposium, pp. 129-133, March/April 2003.

[46] Donahoe, D., "Moisture in multilayer ceramic capacitors," PhD Thesis, University of Maryland – College Park, Mechanical Engineering Department, Maryland, USA, 2005.

[47] Condra, L. W., Johnson, G. M., Pecht, M. G., and Christou, A., "Evaluation of manufacturing variables in the reliability of surface mount capacitors," IEEE Transactions on Components, Hybrids, and Manufacturing Technology, Vol. 15, No. 4, pp. 542-552, August 1992.

[48] Weiler, J. C., "Hybrid moisture problems," WESCON/96, pp. 110-113, October 1996.

[49] Chittick, R. C., and Bush, E. L., "Capacitor reliability – the role of the methanol test," Electronic Engineering, pp. 65-67, May 1985.

[50] Chittick, R. C., Gray, E., Alexander, J. H., Drake, M. P., and Bush, E. L., "Nondestructive screening for low voltage failure in multilayer ceramic capacitors,"

IEEE Transactions on Components, Hybrids, and Manufacturing Technology, Vol. CHMT-6, No. 4, pp. 510-516, December 1983.

[51] Erdahl, D. S., and Ume, I. C., "Online-offline laser ultrasonic quality inspection tool for multilayer ceramic capacitors – Part 1," IEEE Transaction on Advanced Packaging, Vol. 27, No. 4, pp. 647-653, November 2004.

[52] Ousten, Y., Mejdi, S., Fenech, A., Deletage, J. Y., Bechou, L., Perichaud, M. G., and Danto, Y., "The use of impedance spectroscopy, SEM and SAM imaging for early detection of failure in SMT assemblies," Microelectronics reliability, Vol. 38, pp. 1539-1545, 1998.

[53] Ousten, Y., Carbonne, B., Xiong, N., and Danto, Y., "Evaluation of ceramic chip capacitors using acoustic microscopy and electrical impedance analysis," CARTS Europe 1990, pp. 138-142, 1990.

[54] Bechou, L., Mejdi, S. Ousten, Y. and Danto, Y., "Non-destructive detection and localization of defects in multilayer ceramic capacitors using electromechanical resonances," Quality Reliability Engineering International, Vol. 12, pp. 43-53, 1996.

[55] Boser, O., "Electromechanical resonances in ceramic capacitors and evaluation of the piezoelectric materials' properties," Advanced Ceramic Materials, Vol. 2, No. 2, pp. 167-172, 1987.

[56] Love, G. R., and Ewell, G. J., "Acoustic microscopy of ceramic capacitors," IEEE Transactions on Components, Hybrids, and Manufacturing Technology, Vol. CHMT-1, No. 3, pp. 251-257, September 1978.

[57] Chan, N. H., and Rawal, B. S., “An electrically excited acoustic emission test technique for screening multilayer ceramic capacitors,” IEEE Transactions on Components, Hybrids, and Manufacturing Technology, Vol. 11, No. 4, pp. 358-362, December 1988.

[58] Spiiggs, R. S., and Cronshagen, A. H., “Nondestructive X-ray inspection of ceramic chip capacitors for delaminations,” International Reliability Physics Symposium, pp. 157-163, 1976.

[59] "Directive 2002/95/EC of the European Parliament and of the Council 27 January 2003 on the Restriction of the Use of Certain Hazardous Substances in Electrical and Electronic Equipment," Official Journal of the European Union, Vol. 37, pp. 19-23, February 13, 2003.

[60] "Directive 2002/96/EC of the European Parliament and of the Council 27 January 2003 on Waste Electrical and Electronic Equipment," Official Journal of the European Union, Vol. 37, pp. 24-38, February 13, 2003.

[61] Ganesan, S., Pecht, M., Lead-free electronics, John Wiley & Sons, Inc., USA.

[62] Monotonic bend characterization of board level interconnect, IPC/JEDEC Standard, IPC/JEDEC-9702, June 2004.

[63] Siewert, T., Liu, S., Smith, D. R., and Madeni, J. C., “Database for solder properties with emphasis on new lead-free solders,” National Institute of Standards and Technology & Colorado School of Mines, Release 4.0, Colorado, USA, February 2002.

[64] Dasgupta, A., Oyan, C., Barker, D., and Pecht, M., "Solder creep-fatigue analysis by an energy-partitioning approach," Transactions of the ASME, Vol. 114, pp. 152-160, June 1992.

[65] Wiese, S., Rzepka, S., and Meusel, E., "Time-independent plastic behavior of solders and its effect on FEM simulations for electronic packages," 8th International Symposium on Advanced Packaging Materials, pp. 104-111, 3-6 March 2002.

[66] Wereszczak, A. A., Breder, K., Ferber, M. K., Bridge, R. J., Riester, L., Kirkland, T. P., "Failure probability prediction of dielectric ceramics in multilayer capacitors," pp. 73-83 in Ceramic Transactions, Vol. 97, Multilayer Electronic Ceramic Devices. Edited by Jean, J. H., Jean, T. K., Nair, K. M., and Niwa, K., American Ceramic Society, Westerville, OH, 1999.

[67] White, G. S., Nguyan, C., and Rawal, B., "Young's modulus and thermal diffusivity measurements of barium titanate based dielectric ceramics," AVX Corporation, Technical Information, http://www.avxcorp.com, visited on November 2005.

[68] Maxwell, J., "Surface mount soldering techniques and thermal shock in multilayer ceramic capacitors," AVX Corporation, Technical Information, www.avxcorp.com, visited on October 2006.

[69] Hunt, C., and Dusek, M., "The measurement of creep rates and stress relaxation for micro sized lead-free solder joints," National Physical Laboratory Report, DEPC MPR 021, United Kingdom, April 2005.

[70] Zhang, Q., “Isothermal mechanical and thermo-mechanical durability characterization of selected Pb-free solders,” Ph.D. Thesis, University of Maryland, College Park, USA, 2004.

[71] “Datasheet of multilayer ceramic capacitors with X7R dielectric,” AVX Corporation, http://www.avxcorp.com, visited on August 2006.

[72] Goss, K. U., and Schwarzenbach, R. P., "Rules of thumb for assessing equilibrium partitioning of organic compounds: successes and pitfalls,” Journal of Chemical Education, Vol. 80, No. 4, pp. 450-455, April 2003.

[73] Ben-Naim, A., Hydrophobic interactions, Plenum Press, New York, 1980.